UCSF
UC San Francisco Electronic Theses and Dissertations

Title

ESX-1: A novel alternative secretion system in Mycobacterium tuberculosis that mediates the host-pathogen interaction

Permalink

https://escholarship.org/uc/item/5tn7q45c

Author

Stanley, Sarah A

Publication Date

2006

Peer reviewed|Thesis/dissertation

eScholarship.org Powered by the California Digital Library
University of California

ESX-1: A novel alternative secretion system in *M. tuberculosis* that mediates the host-pathogen interaction

by

Sarah A. Stanley

DISSERTATION

Submitted in partial satisfaction of the requirements for the degree of

DOCTOR OF PHILOSOPHY

in

Biomedical Sciences

in the

GRADUATE DIVISION

of the

UNIVERSITY OF CALIFORNIA, SAN FRANCISCO

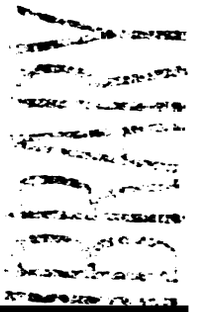

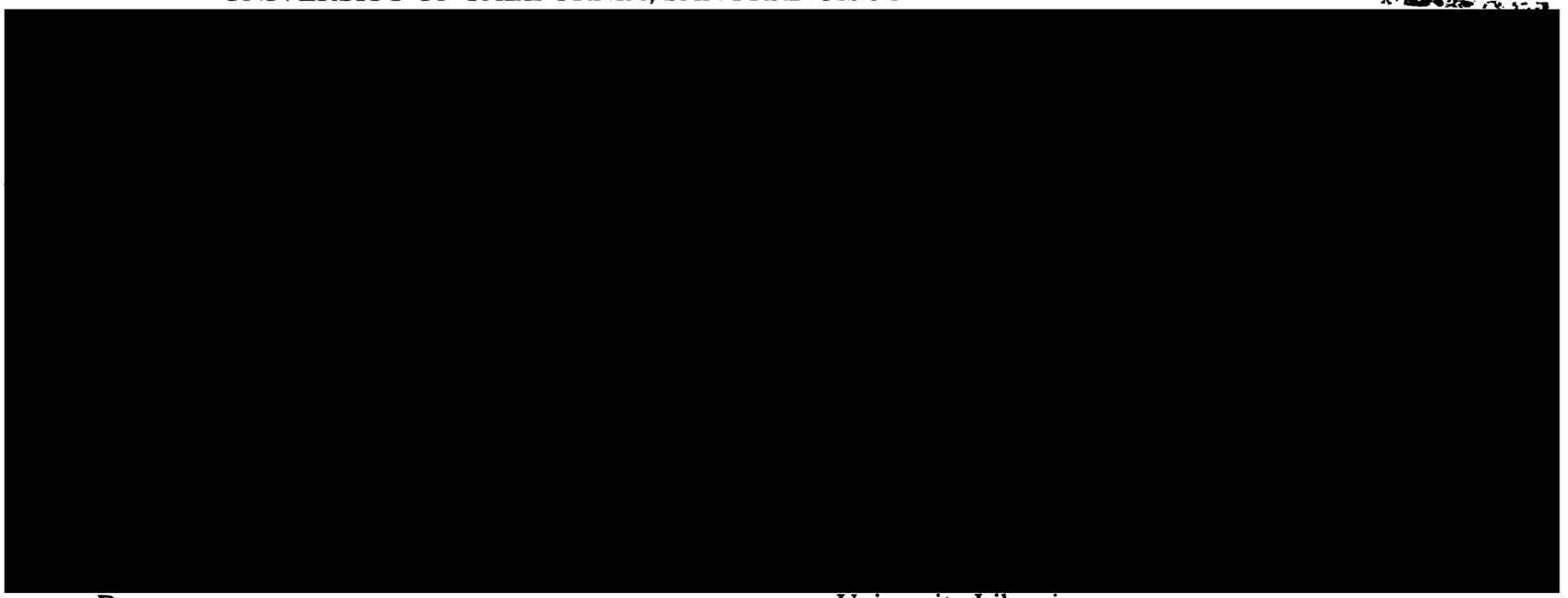

Date University Librarian

Degree Conferred:.....

for my father

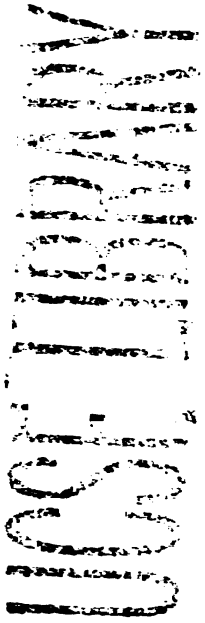

ACKNOWLEDGMENTS

My first thanks are for Jeff, for being a brilliant and inspirational scientist and mentor. All the members of the Cox lab have been supportive through the years, but I am especially grateful to Madhulika Jain, Sridharan Raghavan, Jason Macgurn, and Scott Converse who were my co-first years in the Cox lab. Having Madhulika and Sridharan to talk to, and Jason to make me laugh kept me sane, and their intelligence and scientific brilliance were indispensable to my development as a scientist. My family has been incredibly, amazingly loving and supportive, and I would like to thank my mother and sister Sharon for bearing with me as I struggled through this process. Without them I don't know where I would be. I owe the biggest thanks to my father, who was my first inspiration and the reason that I am a scientist. Dave has been with me through the end of this process, and I will always be grateful for his love and support. Not only has he renewed my faith in science and humanity, but he also makes my days better and brighter. I owe a lot to so many people at UCSF, including Rich Locksley and Eric Brown, my amazing thesis committee. I would also like to thank Anita Sil for her advice over the years. Finally, I owe a big thanks to Dan Portnoy of UC Berkeley for his advice and support.

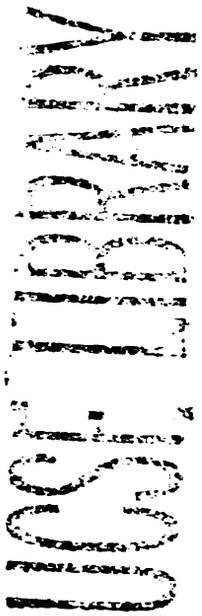

Chapter 2 of this thesis contains previously published material:

Stanley, S.A., Raghavan, S., Hwang, W.W., and Cox, J.S. (2003) Acute infection and macrophagae subversion by *Mycobacterium tuberculosis* require a specialized secretion system. *Proceedings of the National Academy of Sciences* 100(22), 13001-13006.

ABSTRACT

ESX-1: A novel alternative secretion system in *M. tuberculosis* that mediates the host-pathogen interaction

Sarah A. Stanley

Mycobacterium tuberculosis is one of the world's most successful pathogens, infecting approximately one-third of humanity. This remarkable bacterium has infected human beings for millennia, and has evolved mechanisms for the manipulation of host biology to create an optimal environment for bacterial survival and growth. Here we describe the identification and characterization of ESX-1, the first alternative secretion system identified in *M. tuberculosis*, and show its fundamental importance for virulence. We have identified three genes, *Rv3870, Rv3871,* and *Rv3877,* that encode components of the ESX-1 secretion system, which functions to secrete ESAT-6 and CFP-10, proteins with dual functions as immunodominant antigens and virulence factors. Components and substrates of ESX-1 are required for full virulence of *M. tuberculosis* in both mice and macrophages. The ESX-1 secretion system functions to subvert host cell biology, and is required for the suppression of Interleukin-12 (IL-12) and Tumor Necrosis Factor-α (TNF-α). ESX-1 is also required for the induction, both *in vivo* and *in vitro,* of type I Interferons (IFNs), cytokines usually associated with an anti-viral immune response. We show that the induction of type I IFNs may be a pathogenic strategy that enhances virulence of *M. tuberculosis*. We also examine the role of the ESAT-6 and CFP-10 in the protective immune response to *M. tuberculosis*. We find that restoration of a functional ESX-1 system to the live attenuated vaccine strain mycobacterium Bacille Calmette-

Guerin results in an increase in immunogenicity of this strain, which may lead to the development of more a more effective vaccine. These studies identify ESX-1 mediated secretion of ESAT-6 and CFP-10 to one of the most important pathways identified in *M. tuberculosis*, both for virulence of the organism and for induction of the protective immune response to infection, and begin to describe the mechanisms by which ESX-1 secretion regulates host biology and the outcome of infection.

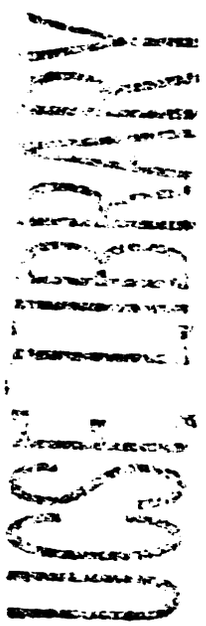

TABLE OF CONTENTS

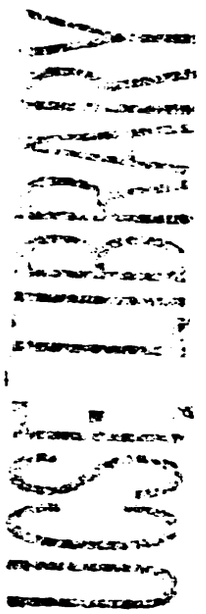

LIST OF FIGURES AND TABLES

Chapter 2

Chapter 3

Chapter 4

Appendix A

Appendix B

Chapter 1

Introduction

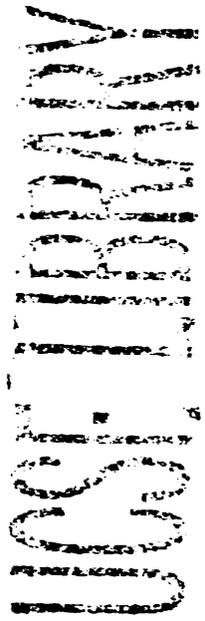

The interface of a bacterial pathogen with its host cell constitutes an ongoing, dynamic, and complex interaction in which bacteria must overcome host immunity to establish infection. Bacteria such as *M. tuberculosis,* which can persist in infected hosts for long periods of time, are particularly adept at tuning host biology to create an environment for optimal bacterial growth and persistence. *M. tuberculosis* infects host macrophages, cells which are specialized for the phagocytosis and destruction of invading micro-organisms. As macrophages also play a role in the direction of subsequent immune responses to infection, the parasitization of macrophages affords *M. tuberculosis* a unique opportunity for the manipulation of the host immune system. The immune response to *M. tuberculosis* is well characterized, and much is known about the host pathways required for control of infection. The extent to which *M. tuberculosis* elicits and exploits host immunity for its own benefit is not understood, however, and the molecular mechanisms of the host-pathogen interaction are poorly characterized.

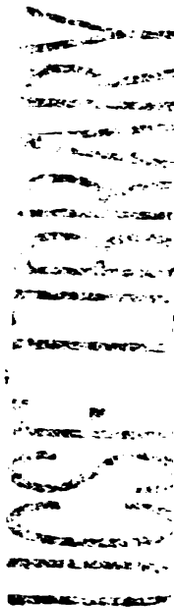

Upon phagocytosis of a bacterial pathogen by a macrophage, numerous host response pathways are initiated. One of the primary lines of defense is the maturation of the phagosome to a phago-lysosome. The lysosome is an inhospitable environment for micro-organisms due to the low pH and activity of degradative enzymes. Additionally, organisms within the phagosome are subjected to targeted oxidative stress through the activity of enzymes such as inducible nitric oxide synthase (iNOS), which leads to the production of NO and other reactive nitrogen intermediates (RNIs), and phox, which leads to the production of reactive oxygen intermediates (ROIs) (Nathan and Shiloh 2000). RNIs play a prime role in the control of mycobacterial infection, while ROIs have

only a minor role (MacMicking, North et al. 1997; Cooper, Segal et al. 2000). Macrophages also secrete chemokines and cytokines with autocrine and paracrine functions in the activation and mobilization of immune cells. Interleukin-12 (IL-12) is a cytokine produced by macrophages with a critical role in the control of mycobacterial infection (Cooper, Magram et al. 1997). The primary role of IL-12 is to elicit the production of Interferon-γ (IFN-γ) from effector T-cells. IFN-γ is primarily responsible for the induction of iNOS by macrophages, and accelerates phagosome maturation (Via, Fratti et al. 1998). Macrophages also secrete Tumor Necrosis Factor-α (TNF-α), which is required for granuloma formation during mycobacterial infection and also acts on macrophages to prime production of iNOS (Flynn, Goldstein et al. 1995). Many mechanisms for the subversion and/or evasion of these immune responses by *M. tuberculosis* have been described. *M. tuberculosis* actively blocks the production of IL-12 by macrophages, possibly leading to a decrease in the production of IFN-γ (Giacomini, Iona et al. 2001; Nau, Richmond et al. 2002). *M. tuberculosis* is also able to evade the effects of IFN-γ by blocking IFN-γ induced signaling (Banaiee, Kincaid et al. 2006). Finally, *M. tuberculosis* also arrests phagosome maturation (Armstrong and Hart 1975; Sturgill-Koszycki, Schaible et al. 1996; Russell 1998), thereby avoiding the toxic environment of the phagoslysosome, and possibly decreasing antigen presentation via the MHC II pathway. The bacterial effectors required for immune evasion as well as the specific host pathways involved have yet to be identified.

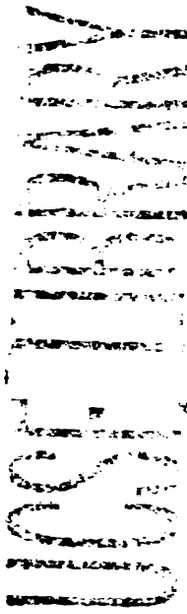

One of the most important paradigms in bacterial pathogenesis is the use of alternative secretion systems for the secretion of virulence factors that manipulate host immunity.

Prior to the initiation of the work described in this thesis, however, no alternative secretion systems had been described in *M. tuberculosis*, in part because of the absence of the genetic and molecular tools required for the analysis of such systems. With the completion of the genome sequencing project in 1998 (Cole, Brosch et al. 1998), and the coincident advent of technologies for the genetic manipulation of *M. tuberculosis*, the field was armed with the tools to begin probing the genetic and molecular determinants of pathogenesis and virulence. The first screen for genes required for growth *in vivo*, performed by Cox et. al., adopted the signature-tag mutagenesis (STM) scheme to screen pools of 48 random transposon mutants for individuals that were unable to replicate within the lungs of mice during the first three weeks of infection. This screen identified approximately 65 genes necessary for growth in the lungs, and uncovered many novel virulence pathways (J. Cox, unpublished data).

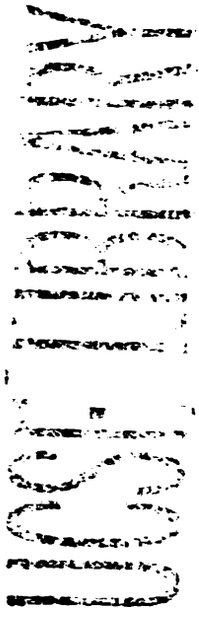

A group of mutants identified in the STM screen allowed us to define the first alternative secretion system in *M. tuberculosis*. Mutants of this class had transposon insertions in genes located at the RD1 (Region of Difference-1) locus of *M. tuberculosis*. The RD1 locus is present in virulent mycobacterial species but absent in the live attenuated vaccine strain mycobacterium BCG (Behr, Wilson et al. 1999). The RD1 locus contains the genes *esxA* and *esxB*, encoding ESAT-6 and CFP-10, small proteins that are secreted during growth *in vitro* (Andersen, Andersen et al. 1995; Berthet, Rasmussen et al. 1998), but lack characteristic signals that would target them to the Sec system of secretion. The function of ESAT-6 and CFP-10 was unknown, however they were known to be major immunodominant antigens during infection (Andersen, Andersen et al. 1995). We and

other groups speculated that the genes at the RD1 locus encoded a novel secretion system required for the secretion of ESAT-6 and CFP-10. In particular, genes flanking *esxA/B* include two AAA-ATPases of the SpoIII/FtsK family of ATPases (*Rv3870 and Rv3871)*, and a twelve transmembrane domain protein (*Rv3877).* SpoIIIE/FtsK family ATPases are known to transduce chemical energy into force, and have important roles in the translocation of various macromolecules (Vale 2000).

In this study, we provide the first experimental evidence that individual genes at the RD1 locus are required for secretion of ESAT-6/CFP-10. We show that the genes *Rv3870, Rv3871,* and *Rv3877* encode components of a secretion apparatus, subsequently named ESX-1, that work together to export ESAT-6 and CFP-10. The ESX-1 secretion machine is one of the most importance determinants of virulence of *M. tuberculosis*, as we have found that mutants of this class are avirulent during *M. tuberculosis* infection of mice. This attenuation is also observed at the level of the infection of macrophages infected *ex vivo*. The major focus of this work is the attempt to identify the mechanisms by which the ESX-1 secretion system contributes to virulence. We found that ESX-1 mediated secretion of virulence factors has profound effects on the host response to *M. tuberculosis*. ESX-1 mediated secretion regulates gene expression in infected macrophages, and is required for the suppression of IL-12 and TNF-α production during infection. ESX-1 is also required for the induction of genes involved in apoptosis, including daxx and TRAIL, and may be involved in the induction of apoptosis of infected macrophages. We also found that the ESX-1 secretion system has a profound effect on gene regulation in mouse tissues *in vivo,* and is required for the induction of a type I IFN

response, both *in vivo* and *in vitro,* thereby revealing the production of type I IFN to be a novel virulence pathway for *M. tuberculosis* infection.

A second focus of this study concerns the role of ESAT-6 and CFP-10 as immunodominant antigens, and the importance of these antigens for a protective immune response to *M. tuberculosis* infection. BCG, which lacks ESAT-6 and CFP-10 is widely regarded as an ineffective vaccine. We reasoned that the loss of ESAT-6 and CFP-10 resulted in a decrease in immunogenicity which hampers the effectiveness of the protective immune response engendered by BCG. To test this hypothesis, we restored ESAT-6/CFP-10 secretion to BCG, and analyzed the virulence and immunogenicity of the resulting recombinant strain. We found that the immune response to the recombinant strain was characterized by an enhanced T-cell response. An increase in virulence was also observed, highlighting the importance of these proteins as virulence factors.

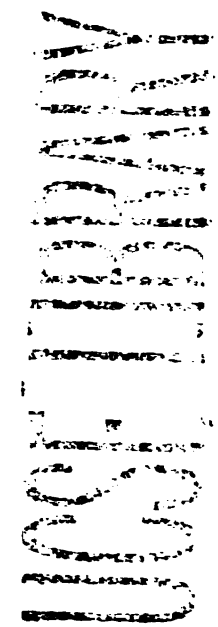

Chapter 2

Acute infection and macrophage subversion by *Mycobacterium tuberculosis* requires a novel specialized secretion system

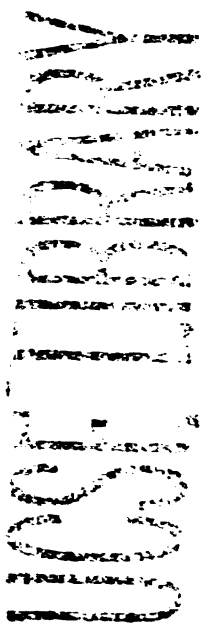

Abstract.

Although many bacterial pathogens utilize specialized secretion systems for virulence, no such systems have been described for *Mycobacterium tuberculosis*, a major pathogen of humans that proliferates in host macrophages. In a screen to identify genes required for virulence of *M. tuberculosis*, we have discovered three components and two substrates of the first Sec-independent secretion pathway described in *M. tuberculosis*, which we designate the Snm pathway. Here we demonstrate that the novel proteins Snm1, Snm2, and Snm4 are required for the secretion of ESAT-6 and CFP-10, small proteins previously identified as major T cell antigens. Snm2, a member of the AAA ATPase family, interacts with substrates and with Snm1, another AAA ATPase. We show that *M. tuberculosis* mutants lacking either the Snm system or these substrates exhibit defects in bacterial growth during the acute phase of a mouse infection and are attenuated for virulence. Strikingly, *snm* mutants fail to replicate in cultured macrophages and fail to inhibit macrophage inflammatory responses, two well-established activities of wild-type *M. tuberculosis* bacilli. Thus, the Snm secretion pathway works to subvert normal macrophage responses and is a major determinant of *M. tuberculosis* virulence.

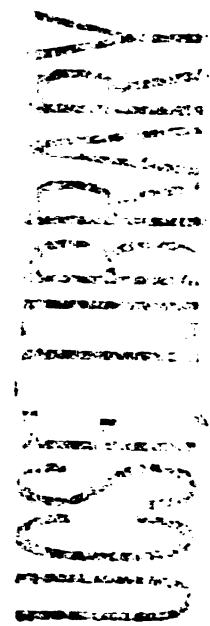

Introduction.

The etiologic agent of human tuberculosis, Mycobacterium tuberculosis, infects one third of the world's population and can survive within an infected individual for decades (McKinney, Jacobs et al. 1998; Dye, Scheele et al. 1999). During infection, *M. tuberculosis* resides primarily within macrophages, myeloid cells whose function is to phagocytose and destroy invading microorganisms. Numerous experiments employing *in*

vitro infection of macrophages have demonstrated that live *M. tuberculosis* cells assert a profound inhibitory influence on their cellular host. One well-studied example of *M. tuberculosis*-mediated manipulation of macrophage function is the bacterium's ability to alter macrophage signaling required for the production of immunostimulatory cytokines and effector molecules (Falcone, Bassey et al. 1994; Beltan, Horgen et al. 2000). For example, *M. tuberculosis* actively suppresses the transcriptional induction of the p40 subunit of interleukin-12 (IL-12), a cytokine critical for control of mycobacterial infection (Giacomini, Iona et al. 2001; Nau, Richmond et al. 2002). The production of the pro-inflammatory cytokine TNF-α and the antimicrobial effector nitric oxide (NO) are also critical for controlling *M. tuberculosis* infection. Interestingly, avirulent mycobacterial strains elicit significantly more TNF-α and NO from infected macrophages than *M. tuberculosis*, suggesting that suppression of these responses is important for virulence (Beltan, Horgen et al. 2000).

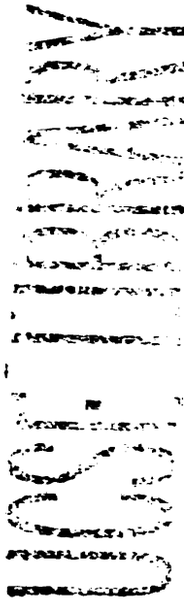

Many bacterial pathogens influence immune responses by secreting effector proteins that directly manipulate host cell function (Lee and Schneewind 2001). While most secreted proteins are exported via the classical Sec pathway (Economou 1999), virulence factors are often secreted by specialized Sec-independent systems (Finlay and Falkow 1997). To date, no alternative secretion pathways have been described in *M. tuberculosis*. Many of the proteins secreted by *M. tuberculosis* bacilli during growth in culture have been identified, some of which lack identifiable N-terminal signal sequences that would target them to the Sec pathway (Sonnenberg and Belisle 1997). However, the reliability of these

approaches to identify secreted proteins is confounded by the high rates of cell autolysis in mycobacterial cultures (Tullius, Harth et al. 2001).

ESAT-6 and CFP-10 are two secreted proteins of unknown function originally identified as immuno-dominant antigens of *M. tuberculosis*. Several recent studies have suggested that these proteins are important for virulence. Deletion of the genes encoding ESAT-6 and CFP-10 from the virulent *M. bovis* strain results in a diminution of virulence (Wards, de Lisle et al. 2000). Furthermore, all strains of the attenuated vaccine strains of Bacille Calmette-Guerin (BCG) have deletions encompassing the *esat-6* locus, also known as the RD1 region (Mahairas, Sabo et al. 1996). Importantly, deletion of RD1 from *M. tuberculosis* attenuates the organism and, conversely, incorporation of the RD1 region from *M. tuberculosis* into BCG restores ESAT-6 and CFP-10 expression and increases virulence and immunogenicity (Pym, Brodin et al. 2002; Lewis, Liao et al. 2003; Pym, Brodin et al. 2003). Interestingly, ESAT-6 and CFP-10 lack characteristic signal sequences that would target them to the Sec system of secretion and are secreted by an unknown mechanism.

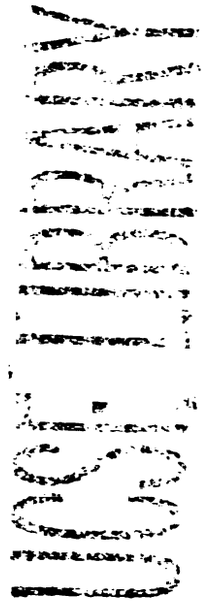

Analyses of the *M. tuberculosis* genome have suggested that genes neighbouring the *esat-6-cfp-10* operon may be important for ESAT-6 and CFP-10 secretion (see Fig. 1A) (Tekaia, Gordon et al. 1999; Gey Van Pittius, Gamieldien et al. 2001; Pallen 2002). This speculation is strengthened by the observation that 4 out of 10 homologues of the *esat-6-cfp-10* operon scattered within the *M. tuberculosis* genome are also flanked by homologues of these neighboring genes. These genes encode a variety of proteins

including two AAA ATPases (*Rv3870* and *Rv3871*) and a 12-transmembrane domain protein (*Rv3877*). However, experimental evidence for the role of these proteins in ESAT-6 and CFP-10 secretion is lacking.

Here we describe the identification of avirulent mutants of *M. tuberculosis* with lesions in *Rv3870, Rv3871,* and *Rv3877.* We show that these genes encode components of a novel secretion system that work together to export ESAT-6 and CFP-10. These mutants fail to inhibit macrophage cytokine responses and are attenuated in mice and macrophages. Our studies describe the first alternative secretion system identified in *M. tuberculosis* and show that this pathway is a major determinant of *M. tuberculosis* virulence.

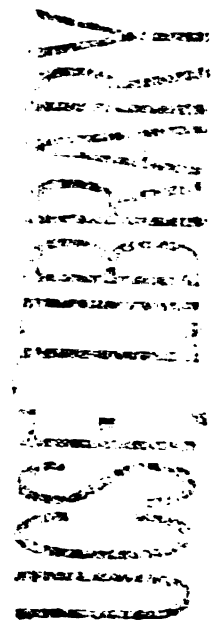

Results.

Isolation of Attenuated M. tuberculosis STM Mutants Defective for ESAT-6/CFP-10 Secretion. Using a previously described signature-tagged mutagenesis (STM) methodology in which mice are infected with pools of 48 randomly-generated transposon mutants (Cox, Chen et al. 1999), we identified four attenuated mutants, each containing a single transposon insertion within the RD1 region of the *M. tuberculosis* genome. Although this locus has been implicated in virulence, the individual genes within the region have not been studied (Fig. 1A). We found that the transposons had inserted within the unknown genes *Rv3870, Rv3871* (two separate isolates), and *Rv3877*, which flank the *esat-6* and *cfp-10* genes in the genome of *M. tuberculosis* (Fig. 1A). For reasons described below, we have renamed these genes *snm1*, *snm2,* and *snm4* (for secretion in mycobacteria). Each of the four mutants was well represented in its inoculum pool at the

time of infection but was drastically under-represented in pools from the lungs of two infected mice after three weeks of infection (Fig. 1B). Thus, the proximity of the *snm* genes to one another in the genome and the severity of the growth defects of these four mutants suggest strongly that these genes function together to promote *M. tuberculosis* growth during the early stages of infection.

To test the hypothesis that Snm1, Snm2, and Snm4 are each required for ESAT-6 and CFP-10 secretion, we examined cell supernatants from exponentially growing *M. tuberculosis* cultures. Using antibodies specific for ESAT-6 and CFP-10, we detected both proteins in the cell supernatant fraction from wild-type cultures as well as in extracts from cell pellets (Fig. 1C, lanes 1 and 2). To verify that the presence of ESAT-6 and CFP-10 in the cell supernatant was not due to cell lysis, we probed the blots with antibodies specific for GroEL, an intracellular chaperone. As expected, GroEL was found exclusively in cell pellets. Remarkably, the mutations in each of the *snm* genes blocked ESAT-6 and CFP-10 secretion into the cell culture supernatant, as neither protein was detected in cell supernatants from the mutants (Fig. 1C, lanes 3-8). Importantly, ESAT-6 and CFP-10 were still detected in cell pellets of the mutants, demonstrating that synthesis of the proteins was not abrogated by the mutations. The decreased level of ESAT-6 and CFP-10 detected in the pellet of the *snm1* mutant was not observed in subsequent experiments. The secretion defect in *snm4* mutant cells was complemented to nearly wild-type levels by introduction of a single copy of the wild-type gene into the genome (lanes 13-15). Furthermore, the block in ESAT-6 and CFP-10 secretion was not due to a general defect in total protein export as SDS-PAGE analysis of supernatants from both

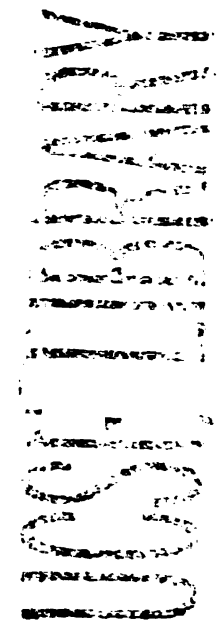

wild-type and *snm4* mutant cell cultures revealed nearly identical protein profiles except for one of three prominent bands in the low molecular weight range (Fig. 1D). The protein profiles of cell supernatants from the *snm1* and *snm2* mutants appeared identical to that from the *snm4* mutant (data not shown).

Components and Substrates of the Snm Secretory Pathway Interact. The observation that each of the three Snm proteins is required for ESAT-6 and CFP-10 secretion suggested that these proteins work together in the same pathway. This notion was strengthened by the results of a yeast two-hybrid screen in which we identified both ESAT-6 and Snm2 in a search for M. tuberculosis proteins that interacted with CFP-10. No other interactors were identified in this screen, suggesting that CFP-10 makes specific contacts with both proteins. To verify these results and to identify other Snm interactions, we constructed both "bait" and "prey" vectors to test for interactions between ESAT-6, CFP-10, Snm2, and the soluble C-terminal domain of Snm1 (Fig. 2). Snm4 was not compatible for yeast two-hybrid analysis as it is predicted to contain mostly transmembrane domains. As expected, an interaction between CFP-10 and ESAT-6 was detected, confirming biochemical evidence that these proteins interact (Renshaw, Panagiotidou et al. 2002). In addition to the CFP-10 and Snm2 interaction, we also identified interactions between Snm2 and Snm1. Thus, we were able to construct a simple interaction map connecting all four of these proteins, consistent with the model in Fig. 7. In particular, Snm2 appears to be a central player as it interacts with both the CFP-10 substrate as well as Snm1, a component likely anchored in the cytoplasmic membrane in vivo. Deletion analysis showed that the C-terminal domain of Snm2, which includes the second AAA ATPase domain, is sufficient to interact with CFP-10, whereas full-length Snm2 is required for

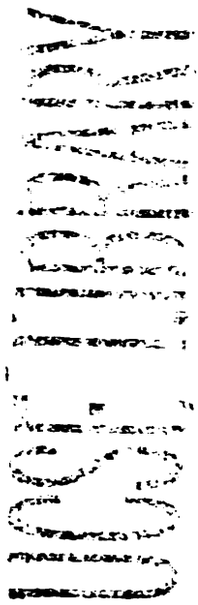

Snm1 binding (Fig. 2). Taken together, these data support our genetic data that the *snm* genes encode for components of a novel secretion pathway that functions to directly secrete ESAT-6 and CFP-10 from M. tuberculosis cells.

The Snm Secretory Pathway is Required for Virulence. The identification of the three *snm* genes in our STM screen suggested that the Snm pathway is critical for *M. tuberculosis* growth *in vivo*. To determine if the *snm* mutants were defective for growth *in vivo* when infected as a clonal population, we injected C57BL/6 mice with 1 x 10^6 colony forming units (CFU) of either the wild-type Erdman strain or the *snm4* mutant strain. Wild-type cells replicated extensively in the lungs during the first ten days of infection, leading to a 100-fold increase in c.f.u. (Fig. 3A). In contrast, *snm4* mutant cells were defective for growth during the first ten days after infection, resulting in only ten-fold growth at this time point. Interestingly, replication of the mutant progressed after ten days of infection, reaching near wild-type levels 15 days after infection. Due to variations in seeding of the lungs, the difference in growth between wild-type and *snm4* mutant cells is most clearly seen when the data are normalized to bacterial burdens immediately after infection (Fig. 3B). Histopathological examination of tissues 10 d after infection revealed that the *snm4* mutant strain induced a less robust inflammatory immune response than wild-type cells, a finding consistent with a decreased bacterial burden at this time point (Fig. 5). Furthermore, the maximal *in vivo* growth rates of the mutant cells (doubling time (t_d) = 1.84 d for *snm4*) were significantly slower than wild-type bacilli (t_d = 1.03 d). Accordingly, the growth defect of *snm4* mutant cells resulted in a lower total fold increase in c.f.u. in the lung by three weeks. Attenuated growth was also observed in the

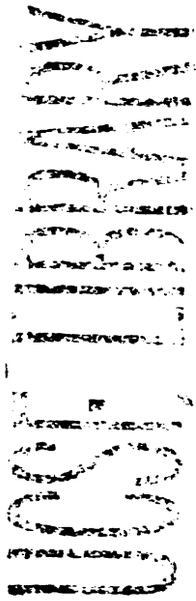

spleen at early time points (Fig. 3C). Defects in growth observed *in vivo* were not a result of an intrinsic growth defect as growth rates of wild-type and mutant cells in liquid culture were identical (wild-type t_d = 0.93 d, *snm4* t_d = 0.91 d). The *in vivo* growth defects of the *snm4* mutant were rescued by expression of the *snm4* gene as the complemented strain was able to replicate at nearly wild-type levels (Fig. 3A,C). Importantly, *snm1* and *snm2* mutant cells displayed *in vivo* growth phenotypes identical to the *snm4* mutant, demonstrating that all three genes are required for normal growth kinetics during infection (data not shown).

To determine whether *esat-6* and *cfp-10* are required for growth *in vivo*, we made precise deletions of each gene from the genome by replacing each open reading frame with the hygromycin resistance marker. As shown in Fig. 1C (lanes 9-12), extracts prepared from either mutant strain lack ESAT-6 and CFP-10. Because *cfp-10* is the upstream gene in an operon with *esat-6* (Berthet, Rasmussen et al. 1998), transcriptional attenuation due to polarity can explain the absence of ESAT-6 in the Δ*cfp-10* mutant. However, the observation that CFP-10 protein is undetectable in the Δ*esat-6* mutant suggests that ESAT-6 is required for stable CFP-10 accumulation. In support of this notion, Renshaw et al. have demonstrated that ESAT-6 and CFP-10 only adopt fully folded states when present together (Renshaw, Panagiotidou et al. 2002). Although the role of the individual proteins in virulence is therefore difficult to test, we sought to determine whether ESAT-6 and/or CFP-10 is required for replication *in vivo*. Like *snm* mutant cells, Δ*esat-6* mutant cells grow more slowly than wild-type cells during infection and fail to attain high levels during the later stages of infection (Fig. 3A, B). The phenotype of the Δ*esat-6* mutant is

unlikely to be the result of a polar effect on *snm4* as there is a strong terminator downstream of the *esat-6/cfp-10* operon. The slight increase in growth rate of *snm4* mutant cells compared to Δ*esat-6* mutant cells could be due to partial complementation resulting from the release of intracellular ESAT-6 and CFP-10 from lysed cells. Overall, the similarity of the *in vivo* growth curves of the two mutants indicates that the growth defect of *snm* mutants results from the failure to secrete ESAT-6 and/or CFP-10. However, we cannot rule out the possibility that other substrates secreted by the Snm pathway may also be important during infection.

To determine if *snm4* is required for virulence of *M. tuberculosis,* BALB/c mice were infected with 1 x 10^6 c.f.u. of *snm4* mutant cells or the complemented strain. All of the mice infected with the complemented strain succumbed to infection by 112 days after infection, with a mean survival time of 90 days (Fig. 3E). These kinetics are very similar to those reported in the literature for infection with the wild-type Erdman strain under the same conditions (McKinney, Honer zu Bentrup et al. 2000). In contrast, none of the mice infected with *snm4* mutant cells succumbed to infection during the course of the experiment (140 d). Measurement of bacterial burden on day 100 after infection revealed no significant difference in the total number of bacteria in the lungs (5.6 ± 1.0 x 10^6 for wild-type and 6.2 ± 1.7 x 10^6 for *snm4*). Therefore, despite the fact that *snm4* mutant cells eventually attain wild-type levels in the tissues, they are strikingly less virulent than wild-type *M. tuberculosis* cells. Although it is not well understood, decreased virulence does not always correlate with a decrease in *M. tuberculosis* burden (North, Ryan et al. 1999). Whether the modest growth defect of the *snm4* mutant early after infection causes the

decrease in virulence at later stages of infection, or whether Snm4 acts during both phases of infection, is impossible to determine at this time. However, our results demonstrate that the Snm pathway is required not only for normal growth kinetics *in vivo* but also for overall virulence of *M. tuberculosis*.

Snm Pathway Alters Innate Responses of Macrophages. Macrophages infected with avirulent mycobacterial species produce greater amounts of cytokines and reactive nitrogen species than macrophages infected with virulent *M. tuberculosis*. Thus, it has been postulated that *M. tuberculosis* has evolved mechanisms for suppressing macrophage responses. To determine whether Snm components and substrates are required to dampen cytokine responses, we measured the amount of pro-inflammatory cytokines elicited by wild-type, *snm4*, and Δ*esat-6* mutant cells 24 h post-infection by ELISA. As has been shown for infection with human monocytes (Giacomini, Iona et al. 2001; Nau, Richmond et al. 2002), murine macrophages infected with heat-killed *M. tuberculosis* cells elicit substantially more IL-12 p40 than macrophages infected with live bacilli (Fig. 4A). Like heat-killed bacteria, live *snm4* mutant cells elicited high amounts of IL-12 p40 secretion, yet the bacilli were viable at this time point (Fig. 4F). Importantly, Δ*esat-6* mutant cells also induced high levels of IL-12 p40. Although it has been suggested that IL-12 suppression by *M. tuberculosis* results from increased induction of the anti-inflammatory cytokine IL-10 (Giacomini, Iona et al. 2001), no IL-10 was detected in any of the infections (data not shown). TNF-α induction was also enhanced in macrophages infected with both *snm4* and Δ*esat-6* mutant cells (Fig. 4B). As expected, the differences in IL-12 cytokine levels were reflected in differences in IL-12

mRNA levels (Fig. 4C). While this pattern of transcriptional activation generally holds true for TNF-α, heat-killed bacilli elicited large amounts of TNF-α cytokine release yet TNF-α mRNA was induced only partially and was similar to that elicited by live cells (Fig. 4D). TNF-α expression in macrophages is controlled by multiple mechanisms, including transcriptional and posttranscriptional regulation (Gao, Xue et al. 2001). Although we do not yet understand the basis for this inconsistency, differences in posttranscriptional regulation may explain the discrepancy between TNF-α mRNA and protein at this timepoint.

Macrophage recognition of *M. tuberculosis* molecules is also sufficient to elicit nitric oxide (NO) production in resting macrophages (Thoma-Uszynski, Stenger et al. 2001). As with the cytokine response, all of the mutants elicited a higher amount of NO (as determined by measuring nitrite concentrations) than that elicited by wild-type cells 24 h post infection (Fig. 4E). Importantly, *snm1* and *snm2* mutant cells also elicited higher levels of NO, as well as IL-12 p40 and TNF-α production compared to wild-type cells (data not shown). Taken together, these results suggest that the Snm pathway and ESAT-6/CFP-10 function to inhibit macrophage signalling, thus suppressing the pro-inflammatory and effector responses normally elicited upon contact with bacteria.

The Snm pathway is required for growth in macrophages. The inability of *snm4* mutant cells to suppress macrophage activation could result from loss of a specific suppressive activity or from a decrease in viability soon after phagocytosis. To distinguish between these possibilities, we examined the ability of the *snm4* mutant to replicate within

cultured macrophages. Bone marrow derived macrophages from C57BL/6 mice were infected at an MOI of 1 with wild type or *snm4* mutant cells. As shown in Fig. 4F, viability of *snm4* cells is unaffected 24 hours after infection, indicating that the failure of *snm4* to suppress cytokine production at 24 hours does not simply result from a loss of viability. However, at later timepoints, *snm4* mutant cells fail to replicate at wild-type levels, resulting in three-fold fewer bacilli at 5 days after infection. Therefore, the Snm pathway is responsible for multiple suppressive effects on macrophages and is required for bacterial replication after phagocytosis.

Snm mutants are not defective for cell-to-cell spread. It has been reported that mutants in *M. tuberculosis* lacking the RD1 locus or individual genes at this locus are defective for cell-to cell spread. These mutants induce less lysis of macrophage monolayers during infection than wild type bacteria as measured by LDH release (Hsu, Hingley-Wilson et al. 2003). We have also found that infection of macrophages with *snm* mutants results in low levels of LDH release when compared to wild-type (data not shown). Guinn et. al. (Guinn, Hickey et al. 2004) followed infections of macrophages with wild-type and RD1 mutants by microscopy, and found that infections with RD1 mutants resulted in fewer infected macrophages by four days after infection than infections with wild-type bacteria. However, they also found that a higher proportion of macrophages infected with RD1 mutant bacteria contained >10 bacilli. They concluded that RD1 mutants are defective for lysis of infected cells and cell-to-cell spread, resulting in fewer infected cells, but greater numbers of bacteria per infected cell. We repeated these experiments as described by Guinn et. al., and also found that at late time-points a lower percentage of

macrophages were infected in *Rv3877* mutant infections than wild-type (Fig. 6A). In direct contradiction to Guinn et. al., however, we did not see an increase in the number of infected macrophages containing >10 bacilli. In fact, we found that at later timepoints macrophages infected with the *Rv3877* mutant contained on average, fewer bacilli than those infected with wild-type (Fig. 6B). We believe that RD1/*snm* mutants are not defective for cell lysis, but are defective for growth in infected macrophages. The observed difference in LDH release and the lower percentage of infected macrophages results from the failure of RD1 mtuants to grow and therefore lyse macrophages, rather than a loss of an active lytic process.

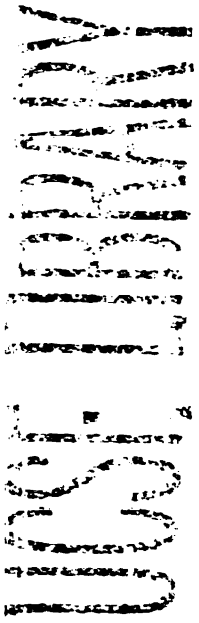

Discussion

In this study, we have identified the first Sec-independent protein secretion system in *M. tuberculosis*. We have shown that three Snm components are required for the transport of the ESAT-6 and CFP-10 substrates from the cell. The Snm secretion system is a major determinant of *M. tuberculosis* virulence as mutants lacking either components or substrates are profoundly attenuated in a mouse model of infection. The reduced virulence of *snm* mutant cells displayed during *in vivo* infection is likely due to their inability to limit macrophage responses. Although a number of studies have described the immunosuppressive effects *M. tuberculosis* cells exert on infected macrophages, this is the first demonstration of mycobacterial gene products required for manipulating macrophage activation during infection.

Snm4 mutants fail to limit both cytokine and effector responses early after infection of cultured macrophages, and ultimately fail to replicate after phagocytosis. We hypothesize that the Snm system also functions to inhibit initial macrophage responses to infection *in vivo*, leading to reduced amounts of direct antimicrobial effectors such as nitric oxide and reduced levels of cytokines required for communication with other cells of the immune system. The phenotype of *snm4* mutants is specific and not simply a consequence of attenuation as other mutants isolated from the STM screen are able to suppress macrophage responses (our unpublished observations). Consistent with our macrophage results, the Snm secretion system is required for normal growth kinetics during the early stages of infection with *M. tuberculosis*. While the defective growth of *snm4* mutants in cultured macrophages is likely a result of elevated nitric oxide production, the attenuated growth observed *in vivo* could result from the elevated levels of both effector molecules and cytokines.

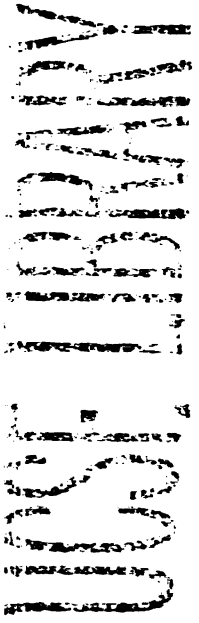

Despite an early growth delay *in vivo*, *snm4* mutants ultimately reach bacterial numbers similar to wild-type in the lungs and other tissues. Interestingly, this modest difference in growth stands in contrast to the marked attenuation of the *snm4* mutant in our virulence studies. Others have reported that there is not a strict correlation between mycobacterial burden and virulence in a time-to-death assay (North, Ryan et al. 1999). Indeed, mutants have recently been studied that have no apparent growth or persistence defects but are attenuated for virulence (Kaushal, Schroeder et al. 2002; Steyn, Collins et al. 2002). Because a decrease in virulence is not always accompanied by a decrease in c.f.u. in the lungs, it is difficult to know whether the decrease in virulence of the *snm4* mutant is

related to the early growth defect. There are at least two possibilities. First, the Snm pathway is required only during the initial two weeks of infection but the delayed growth of *snm4* mutant cells influences subsequent immune responses such that the animal is better able to cope with chronic infection. Alternatively, the virulence defect of *snm4* mutant cells may be the result of the Snm system functioning during the chronic stage of infection. Although it will be interesting to determine if the growth and virulence defects are separable, the tools required to experimentally regulate *M. tuberculosis* gene expression during infection do not currently exist.

Our data indicate that the Snm proteins interact to form a pathway to promote ESAT-6 and CFP-10 secretion and release into the extracellular milieu. While we cannot rule out an indirect role for the Snm proteins in substrate secretion, the specific two-hybrid interactions and operon organization strongly suggest a direct role in secretion. Our results are consistent with a model in which *snm1, snm2* and *snm4* encode part of a previously unrecognized secretion apparatus that allows for the export of ESAT-6 and CFP-10 (Fig. 7). Primary sequence analysis has placed Snm1 and Snm2 within the SpoIIIE/FtsK subfamily of AAA ATPases (Gey Van Pittius, Gamieldien et al. 2001; Pallen 2002). Because members of this family transduce chemical energy into force (Vale 2000), it is possible that Snm1 and Snm2 may push ESAT-6 and CFP-10 through a channel that includes Snm4. This activity would be analogous to other AAA ATPases, such as Cdc48 in eukaryotic cells and FtsH in *E. coli*, that interact with and translocate protein substrates across cellular membranes. Alternatively, the role of Snm1 and Snm2 may be akin to that of signal recognition particle (SRP) and its membrane-bound receptor

(SR) in the general secretion pathway, where GTP binding and hydrolysis by cytoplasmic (SRP/Snm2) and membrane bound proteins (SR/Snm1) endow fidelity and linearity to the pathway rather than drive substrate translocation (Keenan, Freymann et al. 2001). However, biochemical experiments in more tractable *Mycobacterial* species will be required for a more thorough mechanistic understanding of the Snm system.

Although the evolution of prokaryotic alternative secretion pathways to interact with and directly inhibit eukaryotic cell functions is a common theme among gram-negative bacterial pathogens, equivalent systems in gram-positive pathogens have not been as clearly defined. Although direct evidence for the secretion of ESAT-6/CFP-10 or their homologues directly into host cells is lacking, the Snm pathway likely represents a new mode of host-pathogen interaction. The presence of *snm* and *esat-6/cfp-10* homologues in the genomes of a large number of gram-positive bacteria, including pathogens such as *Bacillus anthracis*, suggests that the Snm system represents an evolutionarily-conserved secretion pathway utilized by many different prokaryotes (Pallen 2002).

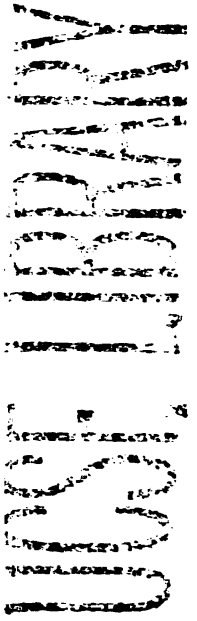

Materials and Methods.

Strains and plasmids. All strains, plasmids (Table 1) and methods for genetic manipulation of *M. tuberculosis* used in this study are listed in supporting information on the PNAS web site, www.pnas.org. *M. tuberculosis* (Erdman) and BCG (Pasteur) were cultivated as described (Cox, Chen et al. 1999). Sauton's medium was used for supernatant preparations and yeast media was purchased from Q-biogene.

Protein preparation and analysis. Concentrated culture supernatants were prepared by growing *M. tuberculosis* in Sauton's medium supplemented with 0.05% Tween-80 to mid-log phase. Cells were inoculated into Sauton's medium without Tween-80 at OD_{600}=0.05, incubated in roller bottles for 5 days, harvested by centrifugation, and supernatants concentrated. Cell lysates and supernatants were separated by SDS-PAGE using 10-20% polyacrylamide gels. Proteins were visualized by silver stain or immunobloting using Abs against Esat-6 (Hyb 76-8), CFP-10 (K8493) or GroEL (HAT5), all kind gifts of Dr. P. Andersen.

Yeast 2-hybrid. Bait and prey vectors are listed in Table 1 and primers used to amplify genes are listed in Table 2, which is published as supporting information on the PNAS web site, www.pnas.org. For directed 2-hybrid analysis, genes were amplified, sequenced, and inserted into both bait (pEG202) and prey (pjsc401) vectors. The resulting plasmids were used to transform yeast strains EGY48 and W303-1a and their expression was verified by Western blot. All possible bait-prey combinations were tested by mating and replica plating to X-gal + galactose plates (Golemis, Serebriiskii et al. 1999).

Bacterial infections. Mice were infected i.v. and samples were processed exactly as described previously (Cox, Chen et al. 1999). To normalize to inoculum size, total c.f.u. at each time point was divided by total c.f.u at day 1. Bone marrow derived macrophages were infected in triplicate wells using DMEM containing 5% horse serum and 5% fetal calf serum at an MOI of 1, incubated for 2 h, washed, and fresh medium was added.

Media was changed 36h after infection. Infected cells were lysed with 0.5% Triton X-100 and plated on 7H10 agar.

ELISAs and Nitrite Measurements. Cultured macrophage supernatants were assayed for cytokine levels using ELISA kits (BD Biosciences). Nitrite levels were measured using Griess reaction.

Quantitative PCR. 3 μg total macrophage RNA was reverse transcribed in a 20 μl reaction and diluted to 100 μl with water. 2.5 μl was used in a quantitative real-time PCR reaction with oligonucleotides specified in Table 2 (Overbergh, Valckx et al. 1999) using SYBR green as label. Results shown are from two separate infection experiments, with each PCR reaction performed in triplicate. All values reported were in the linear range of the experiment and were normalized to actin values. A relative standard curve for actin was generated from serial dilution of a pooled reference of all of the cDNA samples.

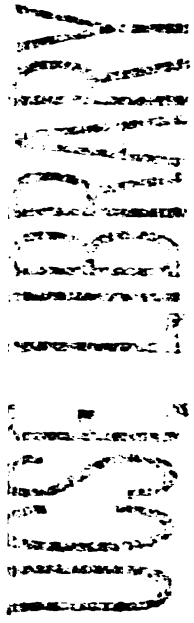

Enumeration of bacteria in macrophages. $2x10^5$ macrophages were plated on coverslips individually in 2mL of media per well of a 12-well dish. Macrophages were infected as described above. At each timepoint, coverslipse were removed, washed x3 with PBS, placed in Truant stain for 20 minutes, rinsed by dunking in 2 successive beakers of 500mL PBS, placed in decolorizing solution for 2 min, rinsed again in PBS, and mounted on glass slides with anti-fade. Cells were visualized using fluorescent microscope, and > 400 macrophages were counted for each timepoint for each strain.

Figure 1. *M. tuberculosis snm* mutants fail to secrete ESAT-6 and CFP-10.

(A) Schematic representation of the transposon insertion sites (black arrows) from three *snm* mutants within the *M. tuberculosis* genome. (B) Signature tags from mutant mycobacteria harvested from the inoculum (input) and the lungs of two mice after 3 weeks of growth were amplified, radiolabelled and hybridized to tag array filters. Tags from underrepresented mutants are shown next to control spots. (C) Western blot detection of ESAT-6, CFP-10 and GroEL from cell supernatant (S) and cell pellet lysate (P) fractions of WT and mutant cells. Loading was normalized by OD_{280} and efficiency of transfer was confirmed by Ponceau S staining of the membrane. The decreased level of ESAT-6 and CFP-10 detected in the pellet of the *snm1* mutant was not observed in subsequent experiments. (D) Silver stain of WT and mutant (*snm4*) cell culture supernatants separated by SDS-PAGE. The protein band absent in the *snm4* mutant is marked with an asterisk.

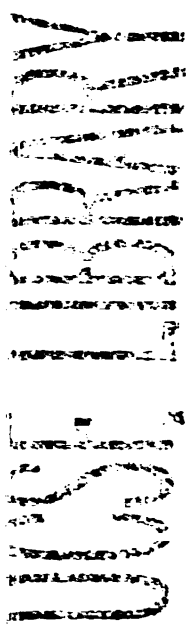

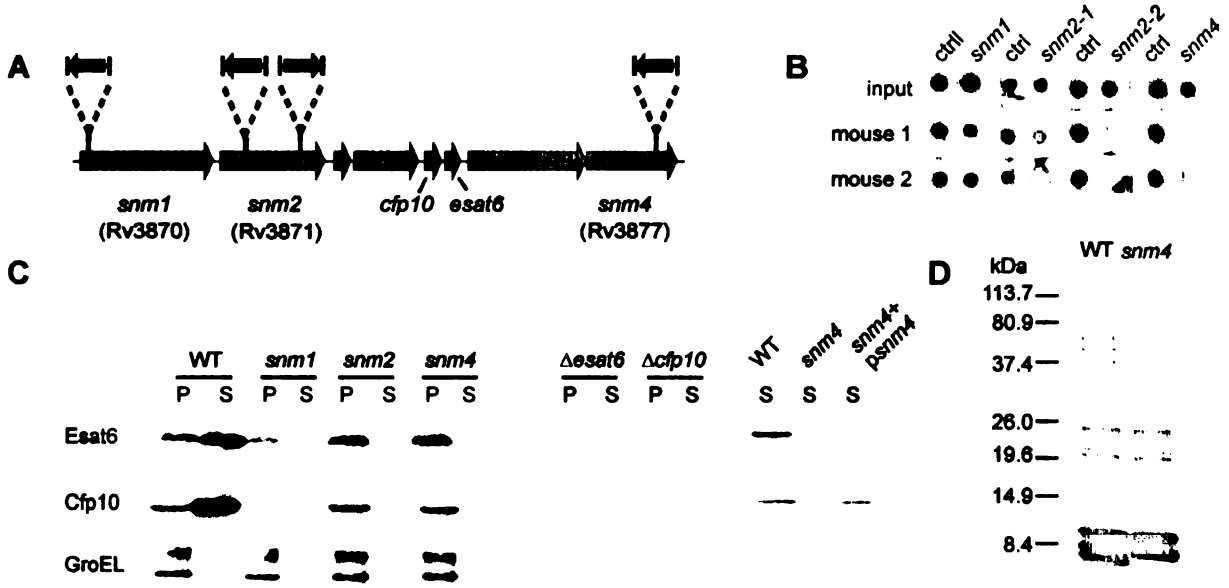
A
snm1
(Rv3870)
snm2
(Rv3871)
cfp10
esat6
snm4
(Rv3877)
B
ctrl
snm1
ctrl
snm2-1
ctrl
snm2-2
ctrl
snm4
input
mouse 1
mouse 2
C
WT
snm1
snm2
snm4
Δesat6
Δcfp10
WT
snm4
snm4+ psnm4
P S P S P S P S P S P S S S S
Esat6
Cfp10
GroEL
D
kDa
WT snm4
113.7
80.9
37.4
26.0
19.6
14.9
8.4

Figure 2. Components and substrates of the Snm secretion pathway interact.

Diploid yeast strains harboring the indicated bait and prey yeast-two hybrid constructs were replica plated to galactose + X-gal indicator plates and allowed to develop overnight at 30° C. ESAT-6, CFP-10, and Snm2 were expressed as full-length fusion proteins and the Snm1 constructs expressed the N-terminal, non-transmembrane domain portion of the protein (a.a. 252-747). Strains containing plasmids expressing only the C-terminal (Snm2-C, a.a. 248-591) or N-terminal (Snm2-N, a.a. 1-241) portions of Snm2 were also tested. Expression of all fusion proteins was confirmed by Western blotting using antibodies that recognize LexA (baits) or the HA epitope tag (preys).

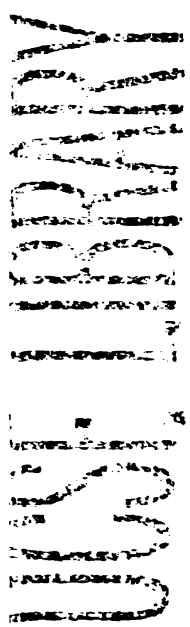

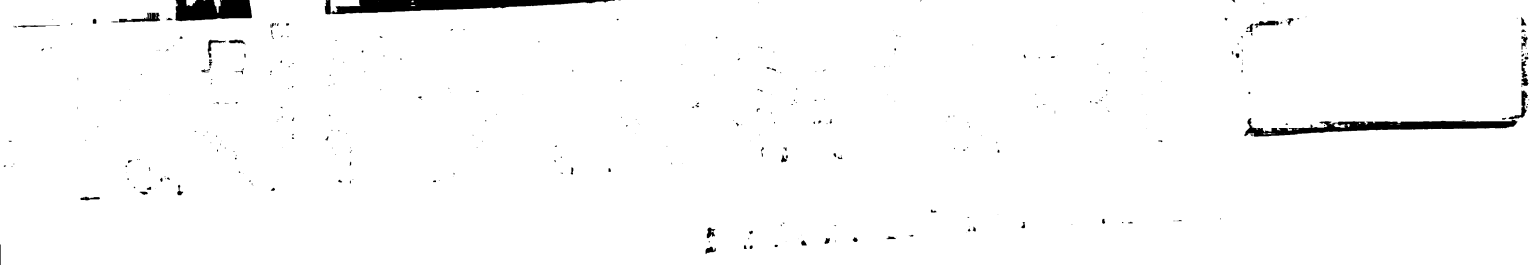

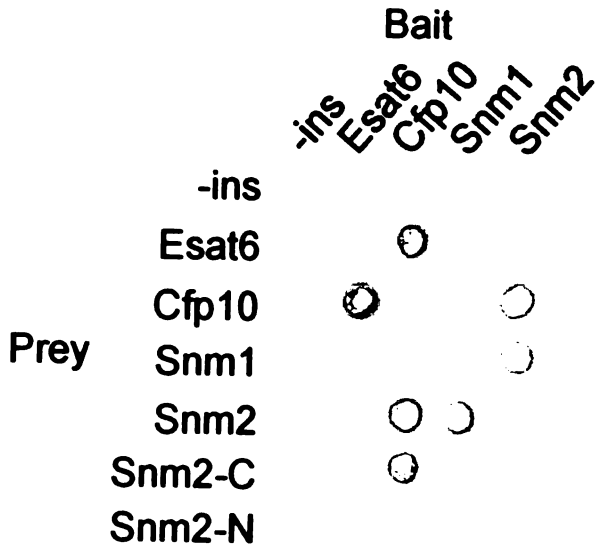
Bait
-ins
Esat6
Cfp10
Snm1
Snm2
Prey
-ins
Esat6
Cfp10
Snm1
Snm2
Snm2-C
Snm2-N

Figure 3. Snm-mediated secretion is required for *M. tuberculosis* virulence.

(A) C57BL/6 mice were injected with $1x10^6$ c.f.u. of each strain, and bacilli were harvested from lungs at 1, 5, 10, 15 and 21 days after infection. Error bars represent the SEM from two combined experiments using five mice per timepoint per experiment. (B) c.f.u. data from (A) normalized to initial inoculum (see Methods). (C) c.f.u. isolated from spleens of mice infected in (A). (D) c.f.u. data from (C) normalized to initial inoculum. (E) Survival of BALB/c mice (n = 15 per group) infected with 10^6 c.f.u. of indicated strains.

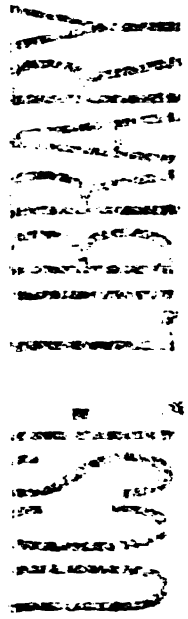

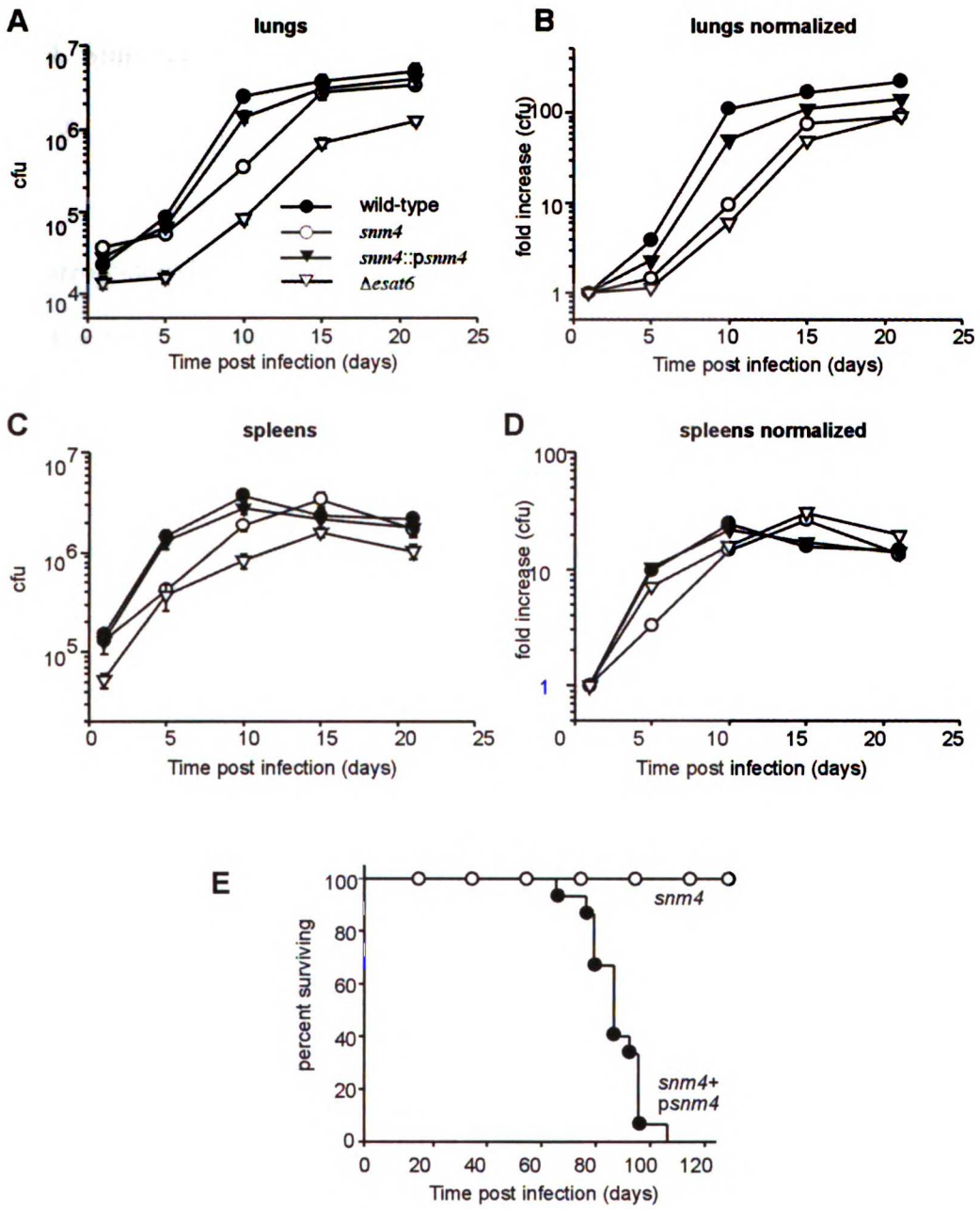
A
lungs
cfu
wild-type
snm4
snm4::psnm4
Δesat6
Time post infection (days)
B
lungs normalized
fold increase (cfu)
Time post infection (days)
C
spleens
cfu
Time post infection (days)
D
spleens normalized
fold increase (cfu)
Time post infection (days)
E
percent surviving
snm4
snm4+
psnm4
Time post infection (days)

USF LIBRARY

Figure 4. Snm pathway mutants induce enhanced macrophage inflammatory responses.

Bone marrow-derived macrophages were infected and culture supernatants were collected and the concentration of IL-12 p40 (A) and TNF-α (B) were measured by ELISA. Total RNA was harvested from macrophage monolayers and IL-12 p40 (C) and TNF-α (D) mRNA levels were measured by quantitative PCR and normalized to actin mRNA levels. Each sample was assayed in triplicate and error bars represent standard deviation from at least two experiments. (E) Nitrite concentration from culture supernatants was measured using the Griess reaction. (F) *M. tuberculosis*-infected macrophages were infected at an MOI of 1, and harvested immediately after the 2 h phagocytosis period ("0 h") and at the indicated time points and bacterial c.f.u. were determined by plating.

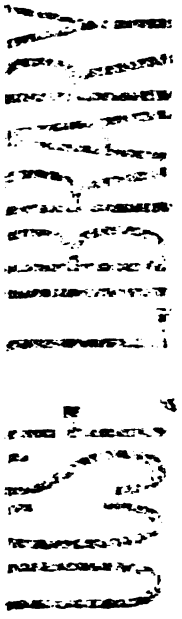

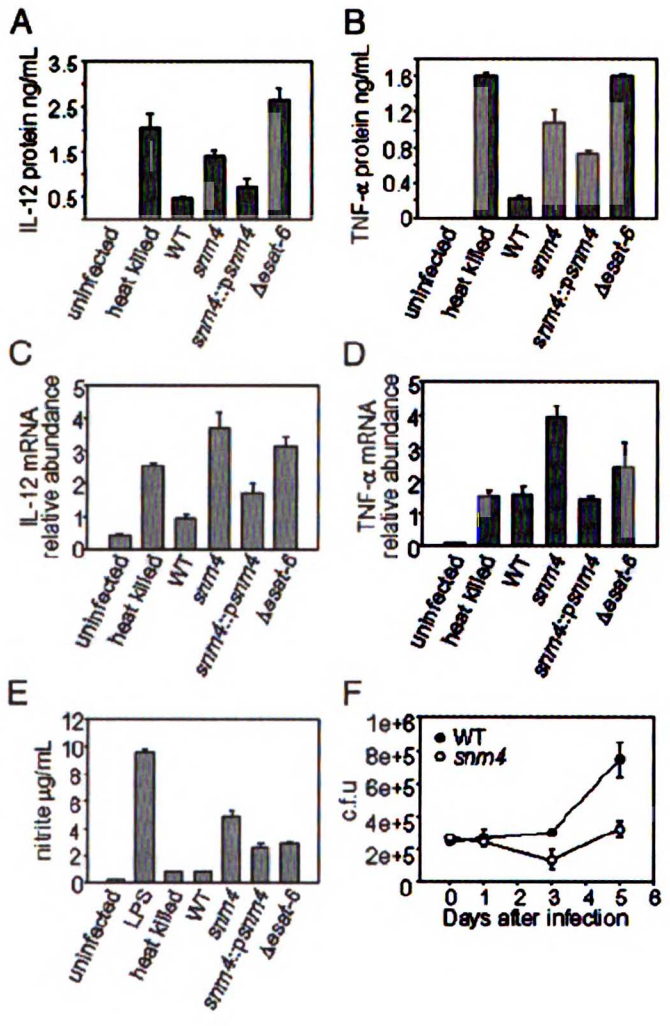

UCSF LIBRARY

Figure 5. Haemotoxylin and Eosin stained lung and spleen sections from mice infected with wild-type or *snm* mutant cells harvested 10d after infection (200x magnification).

Sections from lungs of mice after 10 days of infection with wild-type *M. tuberculosis* show a pronounced infiltrate composed primarily of macrophages and lymphocytes, centered around bronchioles and venules that extend into the interstitium. In contrast, cestions of lungs from mice infected with *snm4* mutant cells show mild inflammation and rare, poorly formed granulomas. Spleens from mice infected with wild-type cells show and expansion of the white pulp and a marked expansion of the red pulp by granulomas. In contrast, spleens from mice infected with *snm4* mutant cells show a slight expansion of both the white pulp and red pulp with only a subtle increase in macrophages in these areas. Sections are stained with haemotoxylin and eosin.

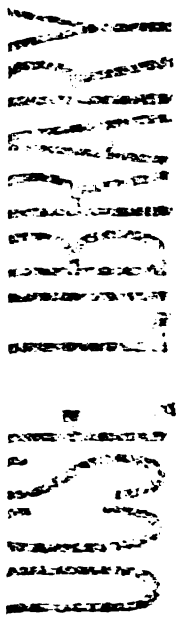

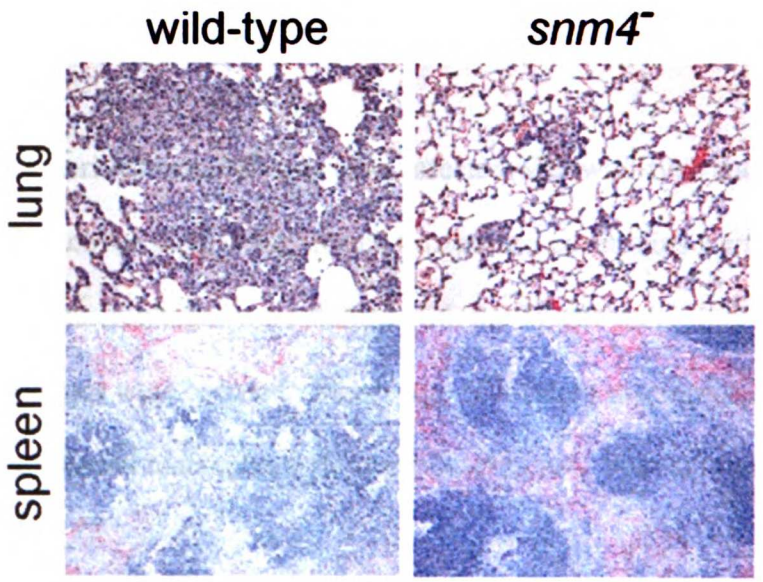

UST LIBRARY

Figure 6. Snm mutants are defective for growth, but not cell-to-cell spreading.

Bone marrow-derived macrophages were infected with wild-type and *snm4* mutant *M. tuberculosis* on cover slips. At indicated timepoints, cover slips were washed, and bacteria inside macrophages were stained with the Truant stain. Individual bacteria in >400 macrophages were counted. Percentage of infected macrophages (A) and number of bacilli per infected macrophage (B) were determined. Shown is a representative experiment of 2.

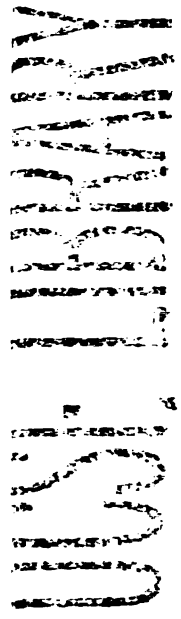

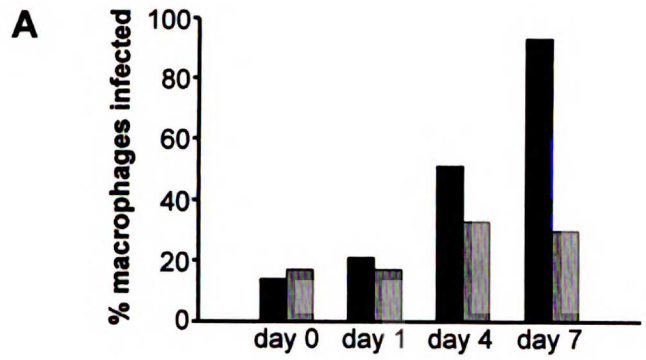
A
% macrophages infected
100
80
60
40
20
0
day 0
day 1
day 4
day 7

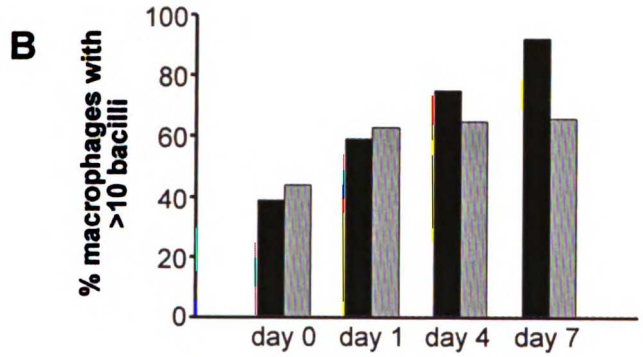
B
% macrophages with >10 bacilli
100
80
60
40
20
0
day 0
day 1
day 4
day 7

USU LIBRARY

Figure 7. Hypothetical model of Snm-mediated secretion of ESAT-6 and CFP-10.

ESAT-6 and CFP-10, depicted here as a dimer, are targeted to the membrane via Snm2 (Rv3871). The energy for translocation of ESAT-6 and CFP-10 is generated by Snm1 (Rv3870) and/or Snm2 (Rv3871), members of the SpoIIIE/FtsK family of proteins that posses AAA/ATPase domains for the transduction of chemical energy into force. ESAT-6 and CFP-10 are pushed through a pore which includes Snm4 (Rv3877), a protein with 12 predicted transmembrane domains. See text for details.

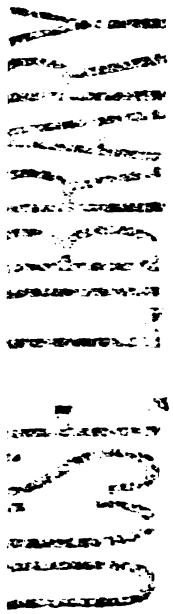

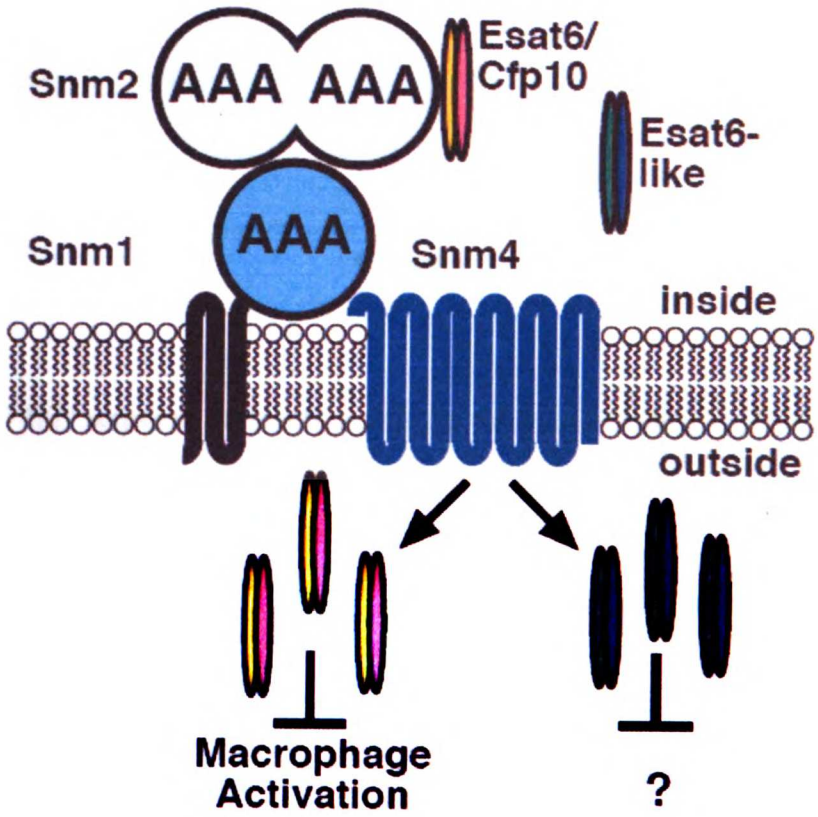

UCSF LIBRARY

Chapter 3

The type I IFN response to infection with *M. tuberculosis* requires ESX-1 mediated secretion and contributes to pathogenesis.

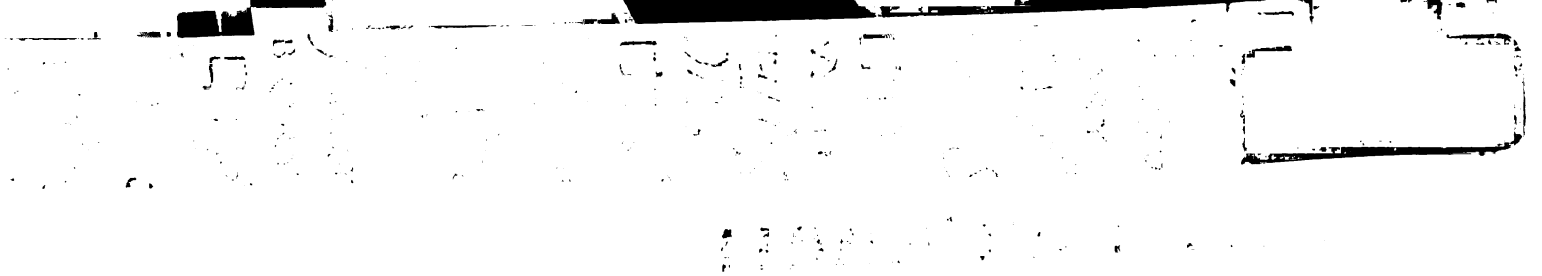

Abstract.

The ESX-1/Snm secretion system is a major determinant of *Mycobacterium tuberculosis* pathogenesis, though the pathogenic mechanisms resulting from ESX-1 mediated secretion remain unclear. By global transcriptional profiling of tissues from infected mice we identified that genes regulated by ESX-1 *in vivo* are predominantly interferon (IFN) regulated. We found that the ESX-1 secretion system is required for the production of host type I IFNs during infection *in vivo* and in macrophages *in vitro*. The macrophage signaling pathway leading to the production of type I IFN required the host kinase TANK-binding kinase 1 (TBK-1) and occurs independently of Toll-like receptor (TLR) signaling. Importantly, the induction of type I IFNs during *M. tuberculosis* infection is a pathogenic mechanism as mice lacking the type I IFN receptor were better able to control bacterial growth in the spleen, although growth in the lung was unaffected. We propose that the ESX-1 secretion system secretes effectors into the cytosol of infected macrophages, thereby triggering the type I IFN response for the manipulation of host immunity.

Introduction.

The outcome of infection by a bacterial pathogen is determined by a complex interplay of virulence factors produced by an invading microbe and the immune responses to infection mounted by the host. Immune responses are characterized by the upregulation of a multitude of cytokines, chemokines, and products with direct or indirect microbial toxicity, and are normally shaped to best protect the host from a particular invading

organism. Many pathogens have evolved strategies for evading or suppressing immune responses, as well as eliciting or misdirecting responses in a way that benefits microbial growth (Coombes, Valdez et al. 2004). *Mycobacterium tuberculosis,* the causative agent of human tuberculosis, is a highly successful pathogen of humans, in part because it has evolved multiple mechanisms for evading or suppressing the host immune response to infection. For example, *M. tuberculosis* is able to evade the effects of IFN-γ, or type II IFN (Ting, Kim et al. 1999; Fortune, Solache et al. 2004), a cytokine critical for controlling mycobacterial infections (Flynn, Chan et al. 1993). Recently, it was identified that type I IFNs, cytokines associated mainly with antiviral function, are also elicited by infection with *M. tuberculosis* (Weiden, Tanaka et al. 2000; Giacomini, Iona et al. 2001). The role of these cytokines in *M. tuberculosis* control, and whether *M. tuberculosis* actively promotes or inhibits this response has yet to be determined.

Type I IFNs are a family of cytokines consisting of multiple IFN-α's and a single IFN-β that all signal through the type I IFN receptor. Type I IFNs have well characterized roles in defense against viruses, inhibition of cell growth, control of apoptosis, and modulation of the immune response (Taki 2002). Recent work has highlighted the importance of type I IFNs during bacterial infection and there is growing interest in the significance of these cytokines in the pathogenesis and virulence of a diverse group of bacterial pathogens. *Listeria monocytogenes*, a gram-positive bacterium that has been used widely as a model for intracellular bacterial infection, has been shown to induce type I IFN production by infected macrophages (O'Riordan, Yi et al. 2002). Type I receptor knockout mice (*IFNAR1-/-)* that are unable to respond to type I IFNs are sensitive to viral

infection but are resistant to infection with *L. monocytogenes* (Auerbuch, Brockstedt et al. 2004; Carrero, Calderon et al. 2004; O'Connell, Saha et al. 2004), demonstrating that these cytokines can inhibit host defense against bacterial infection. It is hypothesized that *L. monocytogenes* provokes the production of type I IFNs as a pathogenic mechanism for the suppression of host immune responses. Although the exact mechanism of this suppression remains unclear, there is evidence to suggest that apoptosis promoted by type I IFNs in the spleen may be a necessary requirement for optimal bacterial growth (Auerbuch, Brockstedt et al. 2004; Carrero, Calderon et al. 2004; O'Connell, Saha et al. 2004). The mechanism of induction of type I IFNs by *L. monocytogenes* is dependent on bacterial entry into the cytosol (O'Riordan, Yi et al. 2002), leading to the activation of TANK-binding Kinase 1 (TBK1) (O'Connell, Vaidya et al. 2005), which in turn phosphorylates and activates the IRF-3 transcription factor, leading to the transcription of the IFN-β gene. The cytosolic receptor that *L. monocytogenes* uses to activate TBK1, as well as bacterial products required for this activation, remain unknown. *M. tuberculosis*, unlike *L. monocytogenes,* is found exclusively in membrane bound compartments, suggesting that type I IFN production proceeds through a different pathway. Lewinsohn et. al. showed that CFP-10, a protein secreted by the ESX-1 system of *M. tuberculosis,* gains access to the cytosol during infection and is presented by the MHC Class-I antigen processing pathway (Lewinsohn 2006), demonstrating the possibility that products from *M. tuberculosis* may gain access to cytosolic signaling receptors during infection.

The ESX-1/Snm alternative secretion system in *M. tuberculosis* is a major determinant of virulence (Hsu, Hingley-Wilson et al. 2003; Stanley, Raghavan et al. 2003; Guinn,

Hickey et al. 2004). Three substrates of this secretion system have been identified to date; ESAT-6, CFP-10 (Hsu, Hingley-Wilson et al. 2003; Stanley, Raghavan et al. 2003; Guinn, Hickey et al. 2004) and Rv3616c (Fortune, Jaeger et al. 2005), encoded by the genes *esxA* (*esat-6*), *esxB* (*cfp-10*), and *Rv3616c* respectively. ESAT-6 and CFP-10 form a tight 1:1 dimer that is required for the stability of both proteins (Renshaw, Panagiotidou et al. 2002; Renshaw, Lightbody et al. 2005). The *esxA* mutant therefore lacks both ESAT-6 and CFP-10 (Stanley, Raghavan et al. 2003). Because the secretion of each identified substrate is dependent upon the presence of the others, it has been proposed that these substrates may also be components of the secretion machinery (Fortune, Jaeger et al. 2005). Three cytosolic or membrane-bound components of the ESX-1 secretion machinery, encoded by the genes *Rv3870* (*snm1*), *3871* (*snm2*), and *3877*(*snm4*), have been identified to date. Strains of *M. tuberculosis* that lack components of the ESX-1 secretion system or the substrates ESAT-6 and CFP-10 are extremely attenuated for growth and virulence during infection of both mice and macrophages (Hsu, Hingley-Wilson et al. 2003; Stanley, Raghavan et al. 2003; Guinn, Hickey et al. 2004). ESX-1 mediated secretion of ESAT-6/CFP-10 is important for controlling the cytokine responses of macrophages infected with *M. tuberculosis.* In particular, mutants lacking a functional ESX-1 secretion system or ESAT-6/CFP-10 elicit higher levels of IL-12 and TNF-α from infected macrophages (Stanley, Raghavan et al. 2003). The ESX-1 secretion system is required for full virulence of *M. tuberculosis* and for subversion of normal immune responses, however the mechanism by which ESX-1 affects host biology has yet to be determined. It is possible that ESX-1 mediates secretion of ESAT-6/CFP-10 into the

cytosol of infected macrophages for interaction with cytosolic signaling pathways for the manipulation of host biology.

There is conflicting evidence regarding the role of type I IFN in *M. tuberculosis* infection. *M. tuberculosis* infection of macrophages and dendritic cells leads to induction of type I IFN in addition to a number of chemokines and cytokines important for controlling the immune response to infection. Recently it was shown that signaling through the type I IFN receptor during *M. tuberculosis* infection of macrophages was required for the production of a number of immunologically important products, including iNOS, IP-10, RANTES, and IRG1(Shi, Blumenthal et al. 2005). Additionally, it has been shown that *M. tuberculosis* may actively inhibit type I IFN signaling (Prabhakar, Qiao et al. 2003), an activity that may be related to pathogenicity. Finally, *M. tuberculosis* was shown to have a slight growth advantage in the lungs of *IFNAR1-/-* mice following aerosol infection (Cooper, Pearl et al. 2000), although growth in other organs was not examined. These data indicate a protective role for type I IFNs during infection with *M. tuberculosis*. In contrast, a hypervirulent clinical isolate of *M. tuberculosis* was found to produce significantly higher levels of type I IFN, correlated with a decrease in the production of the important cytokines IL-12 and TNF-α. Interestingly, treatment of *M. tuberculosis* infected mice with purified IFNα/β further increased bacillary loads, and decreased survival time (Manca, Tsenova et al. 2001). Exogenous addition of type I IFNs to macrophages infected with mycobacterium BCG enhanced bacterial growth (Bouchonnet, Boechat et al. 2002), providing further evidence for a detrimental role of type I IFNs during mycobacterial infection. Thus, type I IFNs have been shown to have

both beneficial and detrimental effects on host resistance during infection, and the role type I IFN during *M. tuberculosis* infection remains unclear.

Here we report our studies of the role and mechanism of induction of type I IFNs during *M. tuberculosis* infection. We have identified pathways that are required for the induction of IFNβ during infection of both mice and macrophages. *M. tuberculosis* infection of macrophages leads to an induction of IFNβ that is dependent on TBK1 signaling in macrophages, revealing a similarity in the pathways utilized by *L. monocytogenes* and *M. tuberculosis* for the induction of IFNβ. We also show that a functional ESX-1 system is required for the induction of IFNβ both *in vivo* and *in vitro*. Additionally, we found that mice lacking the type I IFN receptor are resistant to infection with *M. tuberculosis* in the spleen, indicating that the production of these cytokines is detrimental to the host. Our data indicate that the ESX-1 secretion system functions to elicit type I IFN to promote bacterial replication during infection.

Results.

Type I IFN regulated genes are induced during mouse infection in an ESX-1 dependent manner. To identify host genes regulated by ESX-1 during the early stage of mouse infection, we analyzed gene expression profiles in lungs and spleens of C57BL/6 mice infected with either wild-type or *esxA* mutant *M. tuberculosis*. Mice were infected with 10^7 CFU of *M. tuberculosis*, and total RNA was prepared from lungs and spleens harvested 24h after infection. PolyA RNA samples were amplified by *in vitro* transcription, labeled with Cy5, and subjected to competitive hybridization against a Cy3

labeled pooled reference sample. Hybridizations were carried out on MEEBO oligonucleotide arrays covering almost 22,000, or approximately 88% of mouse genes (Verdugo and Medrano 2006). Three independent biological experiments with four mice per group were repeated at least twice. Values from each infected sample were normalized to values from uninfected controls, and genes whose expression levels were greater than three-fold different from uninfected were chosen as genes regulated during infection (see materials and methods for detailed explanation of array experiments and analysis). Infection with *M. tuberculosis* resulted in gene expression level changes in 194 genes in the spleen (Fig. 1A, appendix B table 1) and 160 genes in the lung (Fig. 1B, appendix B table 2). Many of the genes induced were genes already known to be associated with infection, including cytokines, chemokines, and other immuno-responsive genes, in addition to several genes not previously associated with mycobacterial infection.

To identify host genes whose expression is dependent on a functional ESX-1 secretion system, we compared gene expression profiles of wild-type infected tissues with those infected with the *esxA* mutant. Interestingly, it appeared that a number of genes that were upregulated in response to infection with wild-type *M. tuberculosis* were not induced by the mutant. To define the genes that were dependent on *esxA* for their induction, we chose genes that had greater than two-fold lower expression levels in infections with *esxA* mutants as compared to wild-type in each of the three biological replicate experiments. We found that 39 genes were dependent on *esxA* for expression in the spleen (Fig. 2A), and 35 in the lung (Fig. 2B). Because wild-type and mutant bacterial numbers were

equivalent at 24h, the differences observed can not be a result of the growth defect of the *esxA* mutant at this early time-point. Many of the genes that were differentially induced in wild-type vs. mutant infection are genes whose induction is known to be interferon dependent. Of these genes, the majority are known to be induced by both type I (IFNβ and the IFNαs) and type II IFNs (IFN-γ). Interestingly, we observed differences in the induction of genes usually associated with an anti-viral, type I IFN mediated response, including MxA and 2',5' oligoadenylate synthase (Stark, Kerr et al. 1998), indicating that type I IFNs might be differentially induced in mutant infections compared to wild-type. Indeed, in both the spleen and lung samples we observed differential induction of the gene encoding the chemokine IP-10, which has been shown to be completely dependent on type I IFN signaling during infection with *M. tuberculosis* (Shi, Blumenthal et al. 2005). We were, however, unable to detect any type I IFN transcript, presumably because the abundance of these transcripts is below the level of detection of our microarrays.

ESX-1 is required for the induction of IFNβ in vivo. The type I IFN response is characterized by the initial induction of IFNβ, which leads to the subsequent induction of many IFNα genes (Perry, Chen et al. 2005). To determine whether the induction of interferon dependent genes in spleens and lungs of infected mice could in part result from the production of type I IFNs, we performed quantitative RT-PCR to measure IFN-β mRNA in these tissues. IFN-β induction was observed in the spleens (Fig. 3A) and lungs (Fig. 3B) of infected mice as early as 24h after infection, and was still detectable 5 days after infection (data not shown). Levels of IFNβ mRNA in lungs of mice infected with

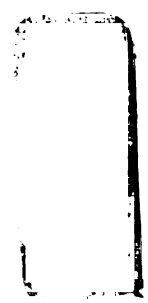

the *esxA* mutant strain were equivalent to uninfected samples, consistent with the decreased levels of induction of interferon regulated genes observed by microarray analysis. The *esxA*::esxA complemented strain partially restored IFNβ levels, reflecting the fact that this strain produces lower levels of ESAT-6/CFP-10 than the wild-type (data not shown). The induction of IFN-β *in vivo* is therefore completely dependent on ESAT-6/CFP-10.

The ESX-1 secretion system is required for the induction of IFN-β during infection of macrophages by M. tuberculosis. It has been reported that macrophages and dendritic cells infected with *M. tuberculosis* produce type I IFNs. To characterize the kinetics of induction of IFN-β by macrophages during infection with *M. tuberculosis*, we infected murine bone marrow-derived macrophages with wild-type *M. tuberculosis* and measured the levels of IFN-β mRNA at multiple timepoints after infection. Infection with *M. tuberculosis* resulted in a robust induction of IFN-β mRNA, with levels similar to those induced by lipopolysaccharide (LPS) (Fig. 4A). Infection of murine bone marrow derived macrophages (BMDM) with wild-type *M. tuberculosis* resulted in the rapid induction of IFN-β, with a peak production of mRNA at 4h after infection. The levels of IFN-β mRNA decreased by 8h post infection and a low level of IFN-β production was sustained through 24h post-infection (data not shown). These kinetics are similar to those observed in infection of bone marrow derived macrophages with *L. monocytogenes* (O'Connell, Vaidya et al. 2005). Infection of BMDMs with *M. tuberculosis* also resulted in the production of IFN-β protein, which was detectable by ELISA in the supernatants of infected cells 24h after infection (Fig. 4B). The production of type I IFN by

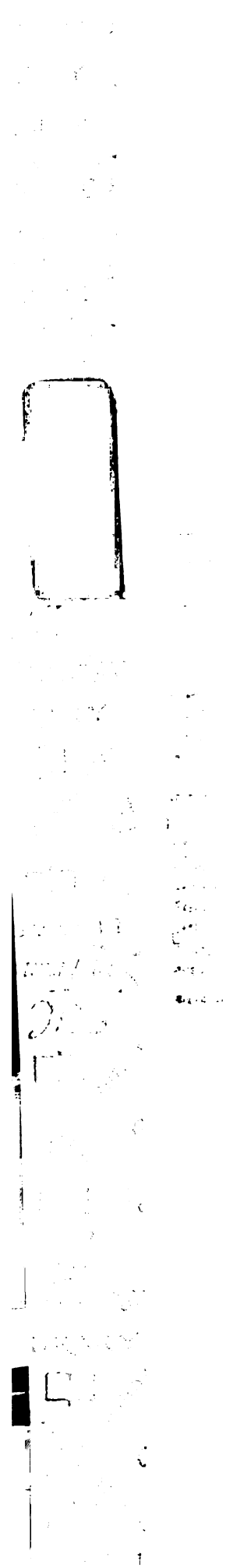

macrophages infected with *M. tuberculosis* led to phosphorylation and activation of STAT-1 with kinetics that reflect those of mRNA production (data not shown). This activation of STAT-1 was solely attributable to the production of type I IFN as the production of IFN-γ by infected macrophages was not detected at any timepoint (data not shown).

We next examined the role of the ESX-1 secretion system in the induction of IFN-β mRNA by macrophages. Importantly, the *esxA* mutant failed to induce IFN-β to any appreciable degree at any time-point examined after infection (Fig. 4C). To test whether ESAT-6/CFP-10 secretion was required for the induction of IFN-β, we infected BMDMs with *Rv3870, Rv3871,* and *Rv3877* mutants, all of which lack a functional ESX-1 secretion system and synthesize, but do not secrete ESAT-6/CFP-10 (Fig. 4D and data not shown). These mutants were also unable to elicit IFN-β production in infected macrophages. The defects were complemented by reintroduction of a single copy of the relevant gene (Fig. 4D). As expected, the observed defect in mRNA production during infection with the *esxA* mutant resulted in a decrease in cytokine production (Figure 4B).

To rule out the possibility that failure to induce IFN-β is a general property of attenuated mutants, we tested a panel of STM mutants that were identified as defective for growth *in vivo* for the ability to induce IFN-β. Although the majority of mutants tested, including *mmpL8*⁻ and *mmpL4*⁻ strain elicited IFN-β to wild-type levels (data not shown), we were surprised to find that *mmpL7*⁻ mutant bacteria were defective for induction of IFN-β (Fig. 4E). MmpL7 is required for transport of the complex lipid PDIM, which is required for

virulence. We also tested *fadD28*⁻, *fadD26*⁻, *mas*⁻, and *tesA*⁻ mutant bacteria, all of which are defective for synthesis of PDIM, and found that these strains also failed to induce IFN-β (Fig. 4E). Thus PDIM is required for the induction of IFN-β by bone marrow-derived macrophages. As these mutants have been shown to secrete ESAT-6 and CFP-10 to wild-type levels (S. Raghavan, unpublished data), PDIM mutants do not fail to induce IFN-β because they lack a functional ESX-1 secretion system. What relationship, if any, exists between these seemingly distinct virulence pathways has yet to be determined.

During infection with *L. monocytogenes,* type I IFNs exert an immunosuppressive function, characterized by suppression of the cytokines IL-12 and TNF-α (Auerbuch, Brockstedt et al. 2004). Exogenous addition of IFNα/β to mice infected with *M. tuberculosis* resulted in a decrease in levels of IL-12 and TNF-α, suggesting a similar function for type I IFNs during infection with *M. tuberculosis* (Manca, Tsenova et al. 2001). *M. tuberculosis* is known to actively suppress macrophage production of IL-12 (Nau, Richmond et al. 2002), and we have shown that ESX-1 mediated secretion of ESAT-6/CFP-10 is required for suppression of the production of IL-12 as well as TNF-α in bone marrow-derived macrophages (Stanley, Raghavan et al. 2003). Because the ESX-1 secretion system is also required for the production of IFNβ, we tested the hypothesis that IFNβ production induced by ESAT-6/CFP-10 secretion is responsible for the suppression of cytokine production also mediated by this secretion system. Bone marrow macrophages derived from mice lacking the type I IFN receptor (*IFNAR1-/-*) were infected with WT and *Rv3877* mutant *M. tuberculosis*, and levels of IL-12 and TNF-α were measured in the supernatants 24h after infection. *Rv3877* mutants elicited

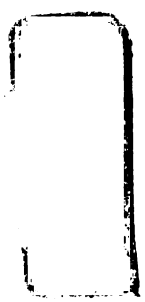

significantly higher levels of IL-12 and TNF-α than wild-type bacteria in both wild-type and *IFNAR1-/-* macrophages (Fig. 5). Therefore, IFNβ is not required for the cytokine repression mediated by the secretion of ESAT-6/CFP-10.

Infection with M. tuberculosis results in induction of IFN-β in a TLR independent manner. Activation through a subset of the TLRs is known to lead to the production of type I IFNs. TLR3 and TLR4 stimulation leads to induction of type I IFNs via a signaling pathway that requires the adapter molecule TRIF (Kawai, Takeuchi et al. 2001; Yamamoto, Sato et al. 2002). TLR7 and TLR9 also activate type I IFN, but use the adaptor MyD88 (Hemmi, Kaisho et al. 2003). Since mycobacterial products have been shown to signal through TLR4 expressed on the surface of macrophages (Means, Wang et al. 1999), we first determined whether signaling through TLR4 is required for the induction of IFN-β by *M. tuberculosis*. TLR4 deficient macrophages were infected for 4h and the production of IFN-β was assessed by qRT-PCR. Induction of IFN-β mRNA by *M. tuberculosis* remained intact in the absence of TLR4 (Fig. 6A) whereas LPS induction of IFN-β was completely blocked in these cells (data not shown). Macrophages deficient for MyD88 or TRIF were also able to activate the production of IFN-β to wild-type levels (Fig. 6C, D). Although TLR2 has not been shown to lead to the production of IFN-β, mycobacterial products, including the 19kD lipoprotein, have been shown to induce signaling through TLR2 (Sieling and Modlin 2001; Stenger and Modlin 2002). TLR2 deficient macrophages, however, had no defect in the induction of IFN-β (Fig. 6B). These data agree with recently published results indicating that the induction of IFN-β occurs independently of TLR signaling (Shi, Blumenthal et al. 2005).

Induction of IFN-β by M. tuberculosis is independent of RIP2, but requires TBK-1.

Receptors present in the cytosol of macrophages are also capable of initiating signaling that results in the induction of IFN-β (Perry, Chen et al. 2005). Although *M. tuberculosis* remains confined to the phagosome, it is possible that bacterial products gain entry to the host cell cytosol for interaction with signaling pathways, a common strategy among virulent pathogens for controlling the host-response to infection. Entry of a bacterial product from *M. tuberculosis* into the cytosol of the macrophage could result in the induction of IFN-β by interaction with a cytosolic detection pathway. The nucleotide-binding oligomerization domain containing proteins NOD1 and NOD2 have been shown to recognize and initiate responses to a variety of bacterial products encountered within the cytosol (Inohara and Nunez 2003). Recent work suggests that NOD2 may be involved in macrophage responses to *M. tuberculosis* (Ferwerda, Girardin et al. 2005). To determine whether either NOD protein is involved in the induction of IFN-β by *M. tuberculosis,* we tested macrophages deficient in RIP2, as both NOD proteins signal through RIP2 upon ligand binding (Kobayashi, Inohara et al. 2002). We observed wild-type levels of IFN-β mRNA in RIP2 deficient macrophages during infection with *M. tuberculosis* (Fig. 6E) indicating that NOD1 and NOD2 are not required for IFN-β production.

Induction of IFN-β by the cytosolic bacterial pathogen *L. monocytogenes* is also independent of NOD protein signaling, but requires TBK-1, a kinase that has been shown to be critical for induction of type I IFNs in viral infection (Sharma, tenOever et al. 2003;

Perry, Chow et al. 2004). TBK and IKKε are the main kinases responsible for phosphorylation and activation of IRF3 (Pomerantz and Baltimore 1999; Fitzgerald, McWhirter et al. 2003), which leads to the activation of IFN-β. We found that the induction of IFN-β by *M. tuberculosis* is completely dependent on TBK-1, as there is a complete lack of IFNβ mRNA production in TBK-1 deficient macrophages infected with *M. tuberculosis* (Fig. 6F). Thus, despite the different localization of these two pathogens, the signaling pathways leading to IFN-β production are as yet indistinguishable.

Mice deficient in the type I IFN receptor show increased splenic resistance to infection with M. tuberculosis. The failure of avirulent ESX-1 mutant bacteria to induce type I IFN suggests that the elicitation of these cytokines may be important for bacterial virulence. However, type I IFNs are also required for the elicitation of several immunoregulatory molecules involved in protection against infection. Thus, the role of these cytokines during infection with wild-type *M. tuberculosis* is difficult to predict. To determine the role of type I IFNs during infection with *M. tuberculosis*, C57BL/6 and congenic *IFNAR1*-/- mice were infected with 10^6 *M. tuberculosis* via the IV route, and organs were harvested for enumeration of CFUs at various timepoints after infection. No difference in resistance was observed in the lungs of infected mice under these conditions (Fig. 7A). Interestingly, however, by ten days after infection spleens from infected *IFNAR1*-/- mice were significantly smaller then those from wild-type infected mice (Fig 7B). Bacterial numbers isolated from the spleens of mice at 10d after infection were almost five fold lower in *IFNAR1*-/- mice as compared to wild-type (Fig.7C). This difference was maintained through 21d after infection, when bacterial numbers were

approximately three fold lower in the receptor deficient mice. These data indicate that signaling through the type I IFN receptor is important for full virulence of *M. tuberculosis*. The attenuation of ESX-1 mutants is therefore at least partially a result of the failure to induce IFN-β. To test this hypothesis, we infected *IFNAR1-/-* mice with wild-type and *esxA* mutant cells, and enumerated bacteria at 10d after infection, the timepoint at which attenuation of *esxA* mutants is most dramatic. The difference in bacterial numbers between wild type and the Δ*esxA* strain in C57BL/6 mice at this timepoint was approximately five fold (Fig. 7D). In *IFNAR1-/-* mice, however, the difference between wild-type and the Δ*esxA* strain was diminished (Fig. 7D), indicating that the failure to induce type I IFNs is at least partially responsible for the attenuation of the Δ*esxA* strain relative to wild-type bacteria.

Apoptosis of infected macrophages is promoted by type I IFNs. A well known function of type I IFNs is the promotion of apoptosis by various cell types. Production of type I IFNs is known to sensitize cells infected with *L. monocytogenes* to apoptosis (Stockinger, Materna et al. 2002), and the elicitation of these cytokines by *L. monocytogenes* results in apoptosis of cells in the spleen, which is thought to be required for the promotion of virulence by type I IFNs (Auerbuch, Brockstedt et al. 2004; Carrero, Calderon et al. 2004; O'Connell, Saha et al. 2004). To test whether the induction of type I IFNs by *M. tuberculosis* might lead to the induction of apoptosis in infected macrophages, we infected bone marrow-derived macrophages with wild-type *M. tuberculosis*. By 24h post infection, 20% of macrophages were apoptotic as indicated by positive TUNEL staining (Fig. 8A). To our surprise, this apoptosis was completely dependent on the ESX-1

secretion system, as macrophages infected with these mutants had levels of apoptosis similar to uninfected cells (Fig. 8A). To determine whether apoptosis elicited by wild-type *M. tuberculosis* was dependent on type I IFN signaling, we infected *IFNAR-/-* macrophages, and assessed apoptosis by TUNEL 24h after infection. The percentage of *IFNAR-/-* macrophages undergoing apoptosis was decreased by approximately 50% as compared to wild-type macrophages at the same timepoint (Fig. 8A). These data show that *M. tuberculosis* is able to induce apoptosis of macrophages in a type I IFN dependent manner.

The induction of apoptosis by *L. monocytogenes* requires type I IFN. Signaling through the type I IFN receptor during *L.monocytogenes* infection results in the induction of the mediators of apoptosis TRAIL, daxx, and PKR (O'Connell, Saha et al. 2004). To test whether these apoptotic pathways are induced by infection with *M. tuberculosis*, we infected wild-type macrophages and measured mRNA levels of daxx, PKR, and TRAIL by qRT-PCR. Levels of the three mRNA species increased upon infection, peaking by 8h post infection (Fig. 8B,C, and data not shown). Interestingly, the induction of these mRNAs was dependent on a functional ESX-1 system (Fig 8B,C, data not shown). It remains to be determined what role type I IFNs play in the increased transcriptional levels of daxx, PKR, and TRAIL observed upon infection with *M. tuberculosis.*

Discussion.

The ESX-1 secretion system and its substrates ESAT-6 and CFP-10 are known to be major virulence factors of *M. tuberculosis,* though the exact mechanism by which this

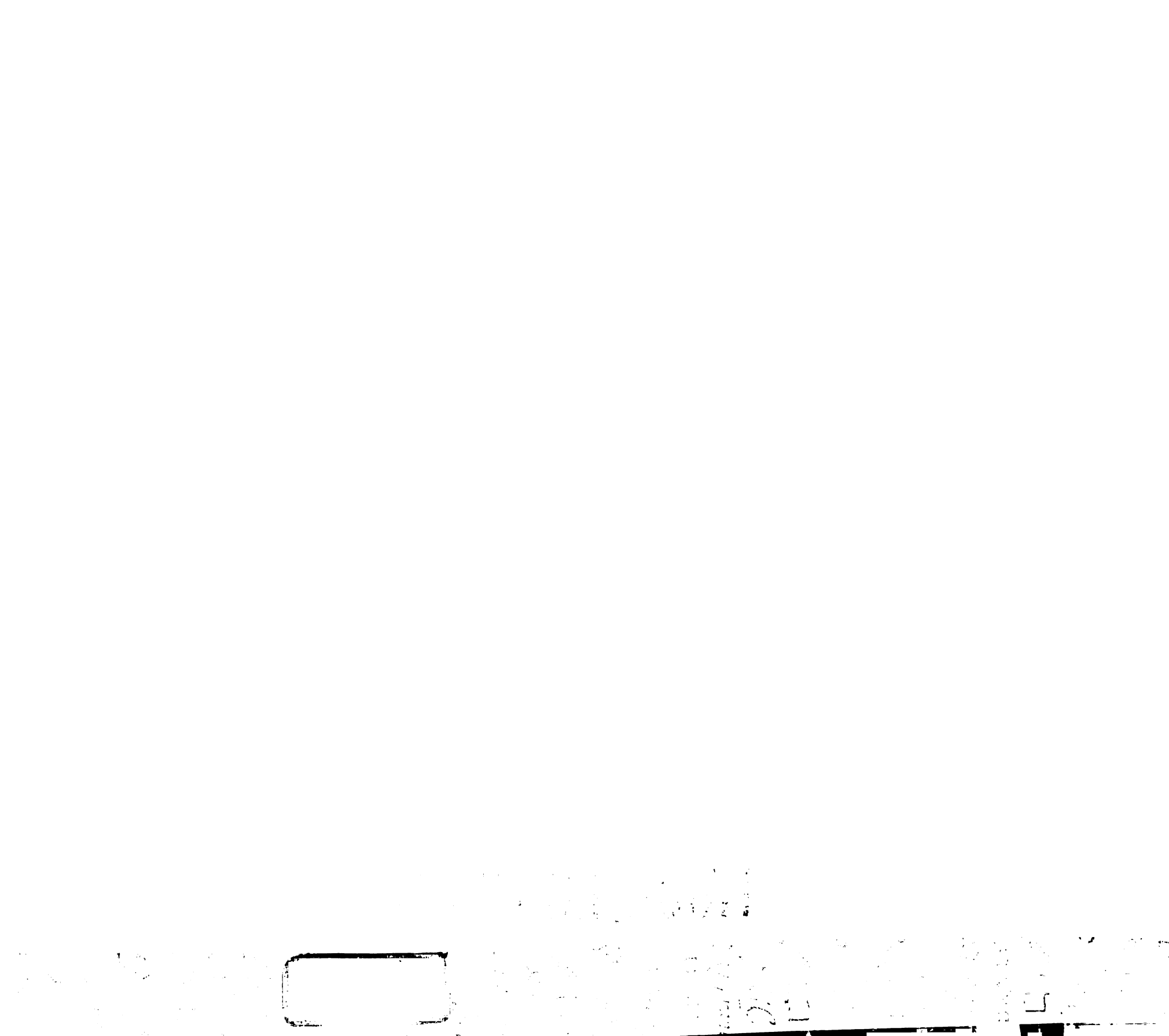

system contributes to virulence has yet to be elucidated. We have found that an *esxA* mutant of *M. tuberculosis* fails to induce the type I IFN, IFN-β, in both lungs and spleens of infected animals. Gene expression profiling experiments from tissues of infected mice suggest that the failure to induce type I IFNs by this mutant results in a defect in induction of a set of genes previously characterized as interferon dependent, including genes that are understood as being part of an antiviral type I IFN response, such as 2',5' oligoadenylate synthase, and MxA, as well as genes that are known to be induced by infection with *M. tuberculosis*, including IP-10. It is likely that the defect in IFN-β production observed *in vivo* occurs at the level of the infected macrophage, as we also found that components and substrates of the ESX-1 secretion system are required for generation of IFN-β by bone-marrow derived macrophages infected *ex vivo*.

An interesting remaining question is the mechanism by which the ESX-1 secretion system leads to the induction of IFN-β in infected macrophages. It is likely that the ESX-1 secretion system functions to secrete bacterial products into the macrophage for the induction of IFN-β, but the specific macrophage receptor which leads to the induction of this pathway has yet to be identified. *M. tuberculosis* is known to be confined to the phagosome during infection, however we and other groups (Shi, Blumenthal et al. 2005) have found the induction of IFN-β to be independent of TLRs, the only known phagosomal receptors whose activation can lead to the induction of type I IFNs. It is possible that the ESX-1 system secretes a bacterial effector into the phagosomal lumen that engages an as yet unidentified phagosomal receptor which leads to the induction of IFN-β. A more interesting possibility is that the ESX-1 system functions in a manner

similar to type III or type IV secretion systems of other pathogenic bacteria (Lee and Schneewind 2001) for delivery of bacterial effectors directly into the cytosol of infected macrophages. Recently, it was shown that CFP-10 presentation by MHC I is requires components which are specific to the cytosolic antigen processing pathway, evidence which demonstrates that CFP-10 gains access to the cytosol during infection (Lewinsohn 2006). Additional evidence that *M. tuberculosis* is capable of accessing cytosolic signaling pathways was provided by Ferwerda et. al. (Ferwerda, Girardin et al. 2005) who showed that NOD proteins are involved in the response to infection with *M. tuberculosis*. The ESX-1 secretion system, which likely controls multiple aspects of virulence, may do so by secreting effectors into the cytosol for the manipulation and/or activation of multiple host signaling pathways, including the TBK-1 pathway which leads to the induction of IFN-β. *L. monocytogenes,* a pathogenic gram positive cytosolic bacterium, enters the cytosol of infected cells as a necessary step of its life-cycle, and induces type I IFNs only upon entry into the cytosol (O'Riordan, Yi et al. 2002). It is possible that *M. tuberculosis* and *L. monocytogenes* utilize the same cytosolic pathway for the induction of type I IFNs.

Type I IFNs are required for the generation of an immune response that protects the host against viral infections. In contrast, the production of type I IFNs by *Listeria monocytogenes* is detrimental to the host, and actually promotes bacterial replication and virulence. We propose that type I IFNs may have a similar role in promoting bacterial growth during infection with *M. tuberculosis*. We observed that bacterial growth was restricted in the spleens of *INFAR1*-deficient animals, indicating the importance of these

cytokines for full virulence of *M. tuberculosis*. We found, however, that growth was unaffected in the lungs of *IFNAR1*-/- mice. Other groups have reported that type I IFNs are required for macrophage production of iNOS (Shi, Blumenthal et al. 2005), a product that is required for control of infection, suggesting that *M. tuberculosis* might have a growth advantage in *INFAR1*-deficient animals. In support of this hypothesis, Cooper et. al. (Cooper, Pearl et al. 2000) reported a slight growth advantage in the lungs of *IFNAR1*-/- mice on a B6/129 background. We did not observe a growth advantage in the lung at any timepoint examined, however. One potential reason for this discrepancy is the difference in strain background. Also, the route of infection (aerosol vs. IV) and the initial inoculum of bacteria used in the two studies were different. It is possible that type I IFNs can be both beneficial and detrimental to the host depending upon the context of infection.

The exact function of type I IFNs during infection with *M. tuberculosis* has yet to be determined. The production of large amounts of type I IFNs can lead to suppression of the production of other cytokines, including IL-12 and TNF-α (Manca, Tsenova et al. 2001; Nagai, Devergne et al. 2003), which are also critical for controlling infection. We did not observe higher levels of IL-12 or TNF-α in infected *IFNAR1*-/- bone marrow-derived macrophages, or in mice infected with the *esxA* mutant strain. Type I IFNs also play a role in diverse cellular processes such as apoptosis that may also affect the outcome of infection. Indeed, several groups have produced evidence that suggests that the ability of these cytokines to induce apoptosis may be critical for their pathogenic role in infections with *Listeria monocytogenes*. Lee et. al. have suggested that apoptosis of

macrophages may be an important virulence mechanism for *M. tuberculosis* (Lee, Remold et al. 2006). We have observed that macrophage apoptosis is completely dependent on the presence of a functional ESX-1 system, and partially dependent on the ability to respond to type I IFNs. It is possible that the mechanism by which type I IFNs promote virulence of *M. tuberculosis* may be through the promotion of apoptosis of infected macrophages, or of other cell types in the vicinity of infected macrophages *in vivo*.

M. tuberculosis is a highly sophisticated pathogen which has evolved many mechanisms for the evasion and manipulation of the host-immune system. The ESX-1 secretion system of *M. tuberculosis* is likely to be required for the secretion of virulence factors with important roles in the manipulation of the host. We propose that *M. tuberculosis* has evolved to elicit a type I IFN response as a pathogenic mechanism for the promotion of bacterial growth, and the that mechanism of this induction relies upon the ESX-1 mediated secretion of effectors into the cytosol of infected macrophages. In support of this hypothesis, we observed that the attenuation of Δ*esxA* mutant bacteria relative to wild-type is diminished in *IFNAR1*-/- mice. It has been conclusively demonstrated that type I IFNs play a significant role in the virulence of *L. monocytogenes*. We propose that the induction of IFN-β may be a strategy of many intracellular pathogenic bacteria for the promotion of virulence.

Materials and Methods.

Mice and Macrophages. C57BL/6 mice age 6-7 weeks were obtained from Charles River. HeJ/HeN mice were obtained from the National Cancer Institute. TBK1-/- and RIP2-/- macrophages were kind gifts from Genhong Cheng. TLR2-/- and TRIF-/- macrophages were obtained from Daniel Portnoy. Bone Marrow-Derived Macrophages were isolated by culturing in media containing 30% L-cell supernatant for six days.

Bacteria. The wild type strain of *M. tuberculosis* used in these studies was the Erdman strain. Previously described *M. tuberculosis* strains used were the following: the Δ*esxA* mutant SSM6, the *snm4* transposon mutant SSM3, and the *snm4* complemented strain SSM5 (Stanley, Raghavan et al. 2003). The *esxA* complemented strain was generated using pMH406 obtained from David Sherman. All strains were cultured in 7H9 medium containing 0.05% Tween-80 as described. Bacteria were prepared for mouse and macrophage infections as described previously (Stanley, Raghavan et al. 2003).

Mouse and macrophage infections. For microarray analysis of infected tissues, mice were inoculated with 10^7 CFU *M. tuberculosis* in PBS+0.05% Tween-80. Organs were harvested and immediately placed in RNAlater (Ambion, Inc, Austin, TX) for stabilization of RNA. RNA was prepared using an RNeasy kit (Ambion, Inc, Austin, TX) following rotor-stator homogenization of tissues. For enumeration of CFUs during infection, mice were infected with 10^6 CFU *M. tuberculosis*, organs were harvested at various timepoints after infection, and were processed as described (Stanley, Raghavan et al. 2003). For macrophage infections, $5x10^6$ macrophages were infected in a 10cm dish

in medium containing 5% horse serum and 5% fetal calf serum for 2h after which time the cells were washed and fresh medium added. RNA was prepared at defined timepoints using the RNeasy kit.

Microarray and quantitative PCR analysis. For array analysis RNAs from four individual mice were pooled, and 500ng total RNA was amplified using MessageAmp II (Ambion, Inc, Austin, TX) reactions in which amino-allyl dUTP is incorporated during transcription. 4ug amplified RNA from each sample were labeled with the fluorophore Cy5 (GE Healthcare, Piscataway, NJ) by coupling to the aa-dUTP as previously described (DeRisi, Iyer et al. 1997), and hybridized against 4ug of a pooled sample consisting of a pool of the experimental RNA samples labeled with Cy3 (GE Healthcare, Piscataway, NJ) on a MEEBO oligonucleotide array (Illumina INC, San Diego California) Hybridizations were carried out for 24h at 65C. Arrays were washed for one minute each in the following wash buffers: 2X SSC+0.03%SDS at 60C, 1X SSC at RT, 0.2X SSX at RT. Arrays were scanned using a GenePix 4000B scanner and GenePix PRO version 4.1 (Axon Instruments/Molecular Devices, Union City, CA). Arrays were analyzed using the MEEBO client for NOMAD (http://ucsf-nomad.sourceforge.net/), CLUSTER (Eisen, Spellman et al. 1998), and Java Treeview 1.0.8 (available at http://sourceforge.net/project/showfiles.php?group_id=84593). Each array experiment using RNA from three separate infection experiments was repeated at least twice; shown is a representative array for each of three infection experiments. For quantitative PCR 2μg of total RNA from each individual mouse sample were reverse transcribed in a 40μL reaction. 2μL were used in a quantitative real-time PCR reaction using SYBR green as a

label and the following primers: *ifnb*-F: 5'-ctggagcagctgaatggaaag; *ifnb*-R: 5'-cttgaagtccgccctgtaggt; β actin-F: 5'-aggtgtgatggtgggaatgg; β actin-R: 5'-gcctcgtcacccacatagga; TRAIL-F: 5'-acctcagcttcagtcagcacttc; TRAIL-R: 5'-tgtaagtcacagccacagacacag; PKR-F: 5'-ggagcacgaagtacaagcgc; PKR-R: 5'-gcaccgggttttgtatcga; daxx-F: 5'-ttcgggaaaatcgaaccttg; daxx-R: 5'-cctcagtcttgtcttgcatcattg. Results shown are representative of three separate infection experiments, with each PCR performed in triplicate. All values reported were in the linear range of the experiment and were normalized to actin values. Standard curves were generated by linear dilution of a cDNA sample generated from LPS stimulated macrophages.

ELISA and TUNEL assays. Macrophages were infected as described above. Macrophage culture supernatants were assayed by sandwich ELISA for IFN-β using a monoclonal anti-mouse IFN-β antibody (Seikagaku America, Falmouth, MA) for coating and polyclonal anti-mouse IFN-β (R&D Systems, Minneapolis, MN) followed by anti-rabbit-HRP (Promega, Madison, WI) for detection. For IL-12 and TNF-α ELISAs cytokines were measured using ELISA kits (BD Biosciences, Palo Alto, CA). For TUNEL staining, macrophages were removed from plates by incubation for 10min in 4mg/mL lidocaine at 37C, fixed with 4% para-formaldehyde, and stained using In Situ Cell Death Detection Kit, Fluorescein (Roche Applies Science, Indianapolis, IN).

Figure 1. Genes regulated in response to infection with wild-type and *esxA* mutant *M. tuberculosis* in tissues of infected mice.

Shown are each of three biological replicates where wild-type and mutant infected spleen (A) and lung (B) samples were normalized to uninfected tissue samples. For each experiment yellow boxes indicate up-regulation, blue boxes indicate down-regulation, black boxes indicate no change, and gray boxes indicate missing data. Genes depicted are regulated at least 3-fold during infection relative to levels in uninfected samples.

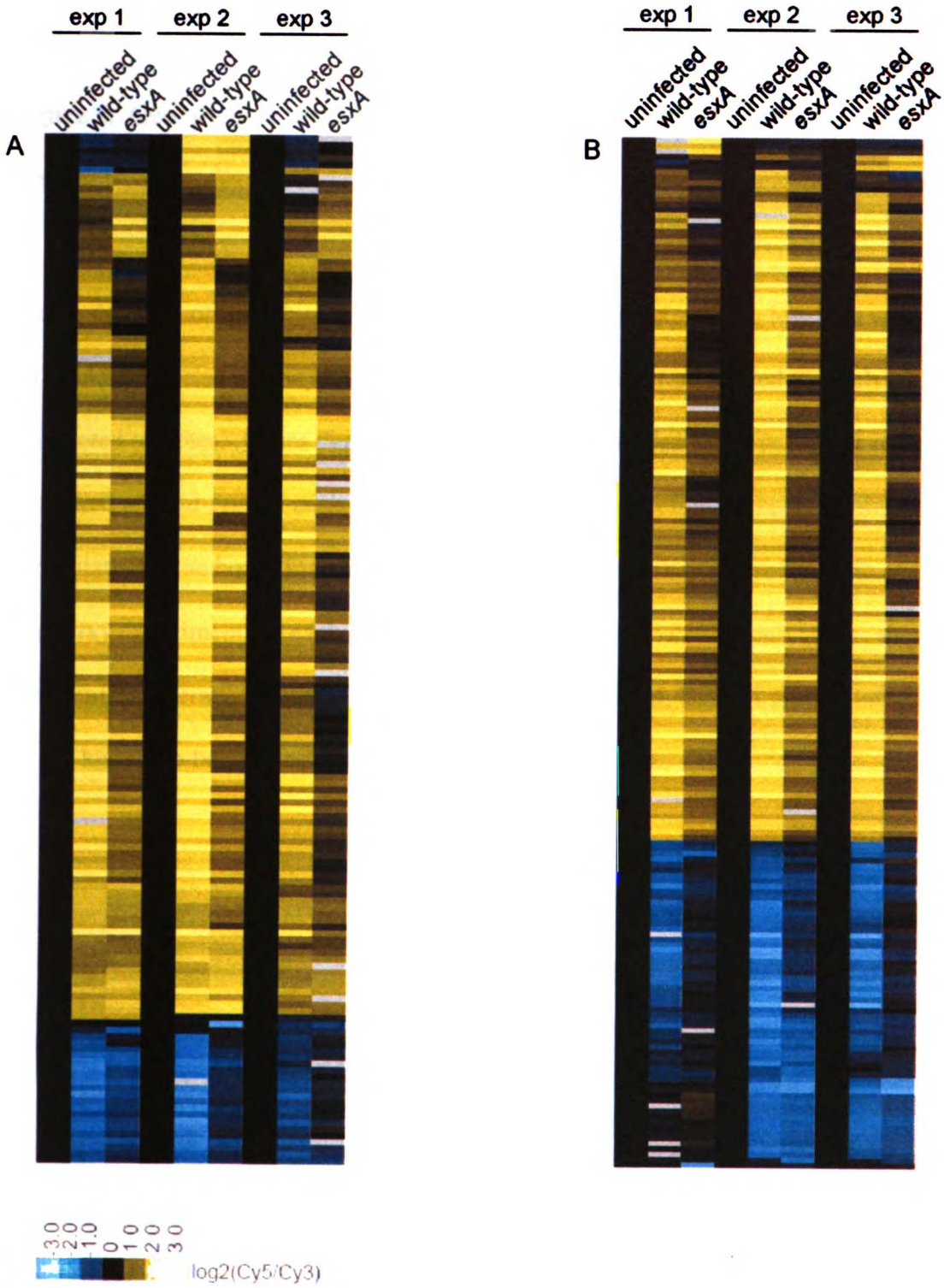
exp 1
exp 2
exp 3
uninfected
wild-type
esxA
A
B
-3.0
-2.0
-1.0
0
1.0
2.0
3.0
log2(Cy5/Cy3)

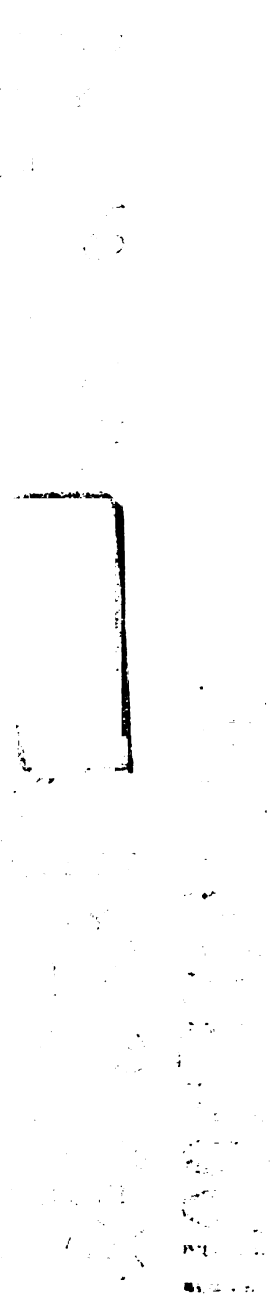

Figure 2. Genes whose induction is dependent on *esxA* in infected spleen and lung tissues.

Shown are each of three biological replicates where gene expression levels in wild-type and mutant infected spleen (A) and lung (B) samples were normalized to levels in uninfected samples. Genes depicted are at least two-fold decreased in mutant infection as compared to wild-type in each of the three experiments. Yellow boxes indicate upregulation, blue boxes indicate down-regulation and black boxes indicate no change. The array experiment for each biological replicate was repeated at least twice; shown are representative arrays. U=uninfected, W=wild-type infected, E=*esxA* mutant infected. Genes known to be IFN inducible are depicted by blue text.

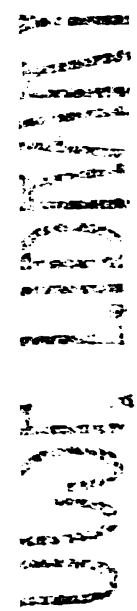

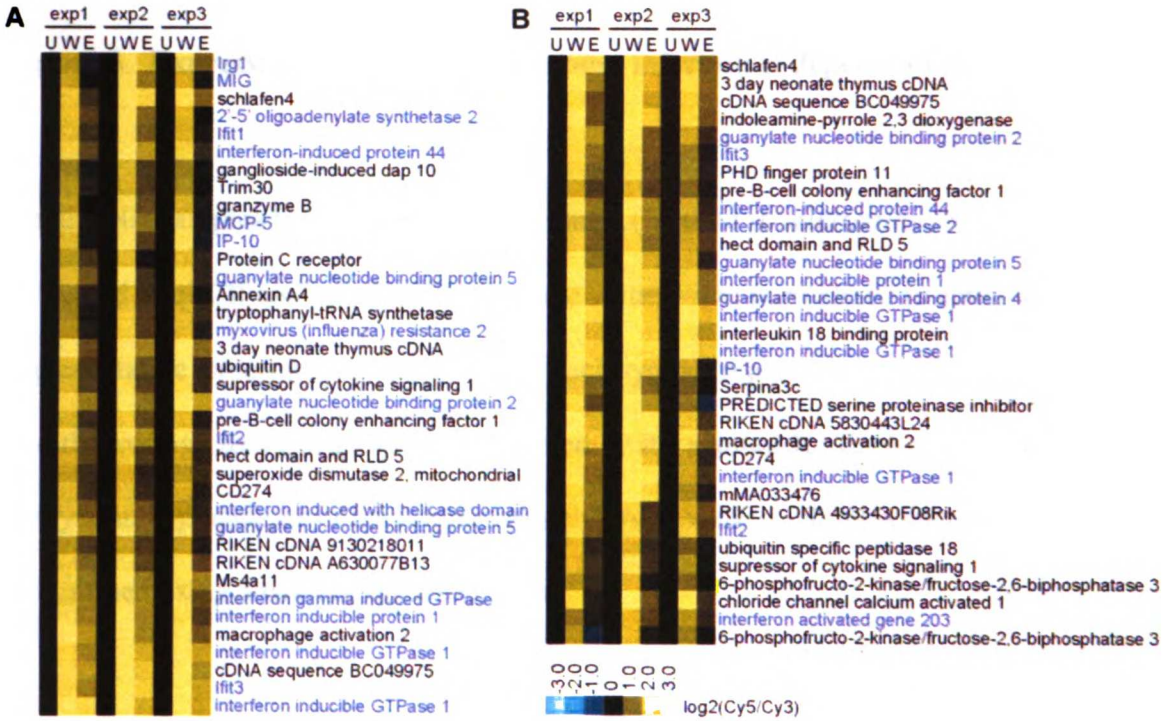
A
exp1 exp2 exp3
U W E U W E U W E
Irg1
MIG
schlafen4
2'-5' oligoadenylate synthetase 2
Ifit1
interferon-induced protein 44
ganglioside-induced dap 10
Trim30
granzyme B
MCP-5
IP-10
Protein C receptor
guanylate nucleotide binding protein 5
Annexin A4
tryptophanyl-tRNA synthetase
myxovirus (influenza) resistance 2
3 day neonate thymus cDNA
ubiquitin D
supressor of cytokine signaling 1
guanylate nucleotide binding protein 2
pre-B-cell colony enhancing factor 1
Ifit2
hect domain and RLD 5
superoxide dismutase 2, mitochondrial
CD274
interferon induced with helicase domain
guanylate nucleotide binding protein 5
RIKEN cDNA 9130218011
RIKEN cDNA A630077B13
Ms4a11
interferon gamma induced GTPase
interferon inducible protein 1
macrophage activation 2
interferon inducible GTPase 1
cDNA sequence BC049975
Ifit3
interferon inducible GTPase 1
B
exp1 exp2 exp3
U W E U W E U W E
schlafen4
3 day neonate thymus cDNA
cDNA sequence BC049975
indoleamine-pyrrole 2,3 dioxygenase
guanylate nucleotide binding protein 2
Ifit3
PHD finger protein 11
pre-B-cell colony enhancing factor 1
interferon-induced protein 44
interferon inducible GTPase 2
hect domain and RLD 5
guanylate nucleotide binding protein 5
interferon inducible protein 1
guanylate nucleotide binding protein 4
interferon inducible GTPase 1
interleukin 18 binding protein
interferon inducible GTPase 1
IP-10
Serpina3c
PREDICTED serine proteinase inhibitor
RIKEN cDNA 5830443L24
macrophage activation 2
CD274
interferon inducible GTPase 1
mMA033476
RIKEN cDNA 4933430F08Rik
Ifit2
ubiquitin specific peptidase 18
supressor of cytokine signaling 1
6-phosphofructo-2-kinase/fructose-2,6-biphosphatase 3
chloride channel calcium activated 1
interferon activated gene 203
6-phosphofructo-2-kinase/fructose-2,6-biphosphatase 3
-3 -2 -1 0 1 2 3
log2(Cy5/Cy3)

Figure 3. Expression of IFN-β during mouse infection is dependent on *esxA*.

Total RNA samples from spleens (A) and lungs (B) used in microarray experiments were subjected to qPCR analysis for IFN-β where values were normalized to actin. Shown is a representative experiment of three, where each symbol represents an individual mouse, and the average for each group is represented by the symbol X. Each sample was assayed in triplicate; error bars represent standard deviation. Significance was determined using a two tail unpaired t-test.

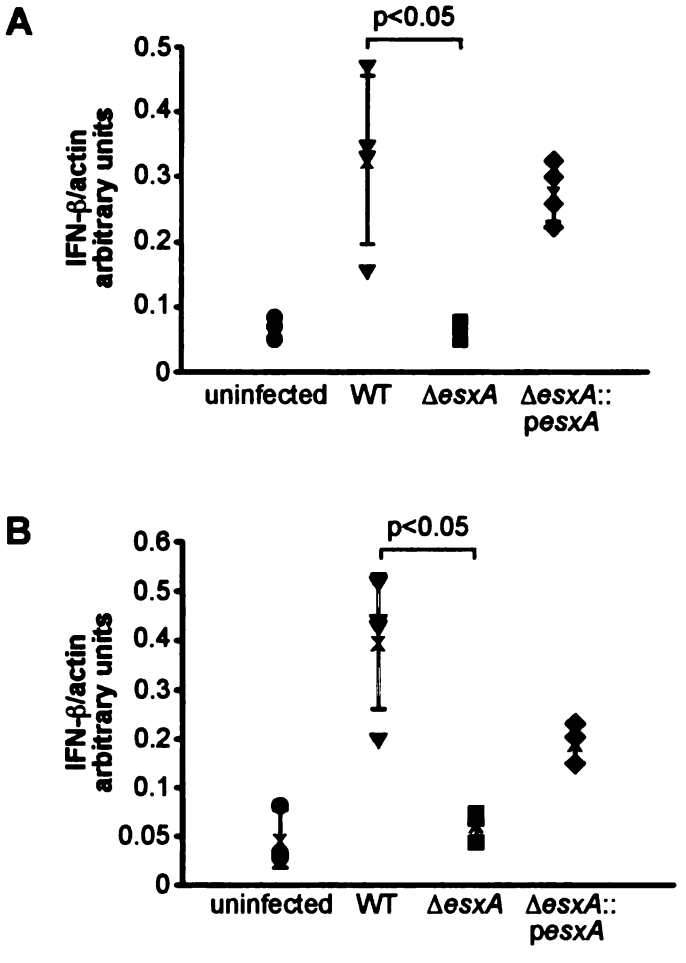
A
p<0.05
IFN-β/actin arbitrary units
0.5
0.4
0.3
0.2
0.1
0
uninfected
WT
ΔesxA
ΔesxA:: pesxA
B
p<0.05
IFN-β/actin arbitrary units
0.6
0.5
0.4
0.3
0.2
0.1
0.05
0
uninfected
WT
ΔesxA
ΔesxA:: pesxA

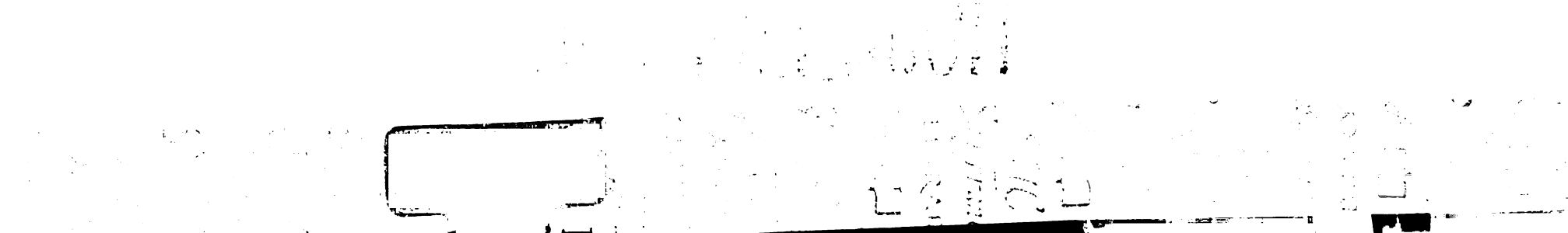

Figure 4. Induction of IFN-β in bone marrow-derived macrophages is dependent on the ESX-1 secretion system and the lipid virulence factor PDIM.

Bone marrow-derived macrophages were infected at a multiplicity of infection of 10, or were treated with 10ng/mL LPS. RNA was harvested at 0, 2, 4 and 8 hours after infection. IFN-β levels were determined by qPCR, and values were normalized to actin (A), (B), (D). Supernatants were collected from identical infections at 24 hours, and were subjected to ELISA for analysis of IFN-β protein concentration. Samples were assayed in triplicate; error bars represent standard deviations. Shown is a representative experiment of at least three.

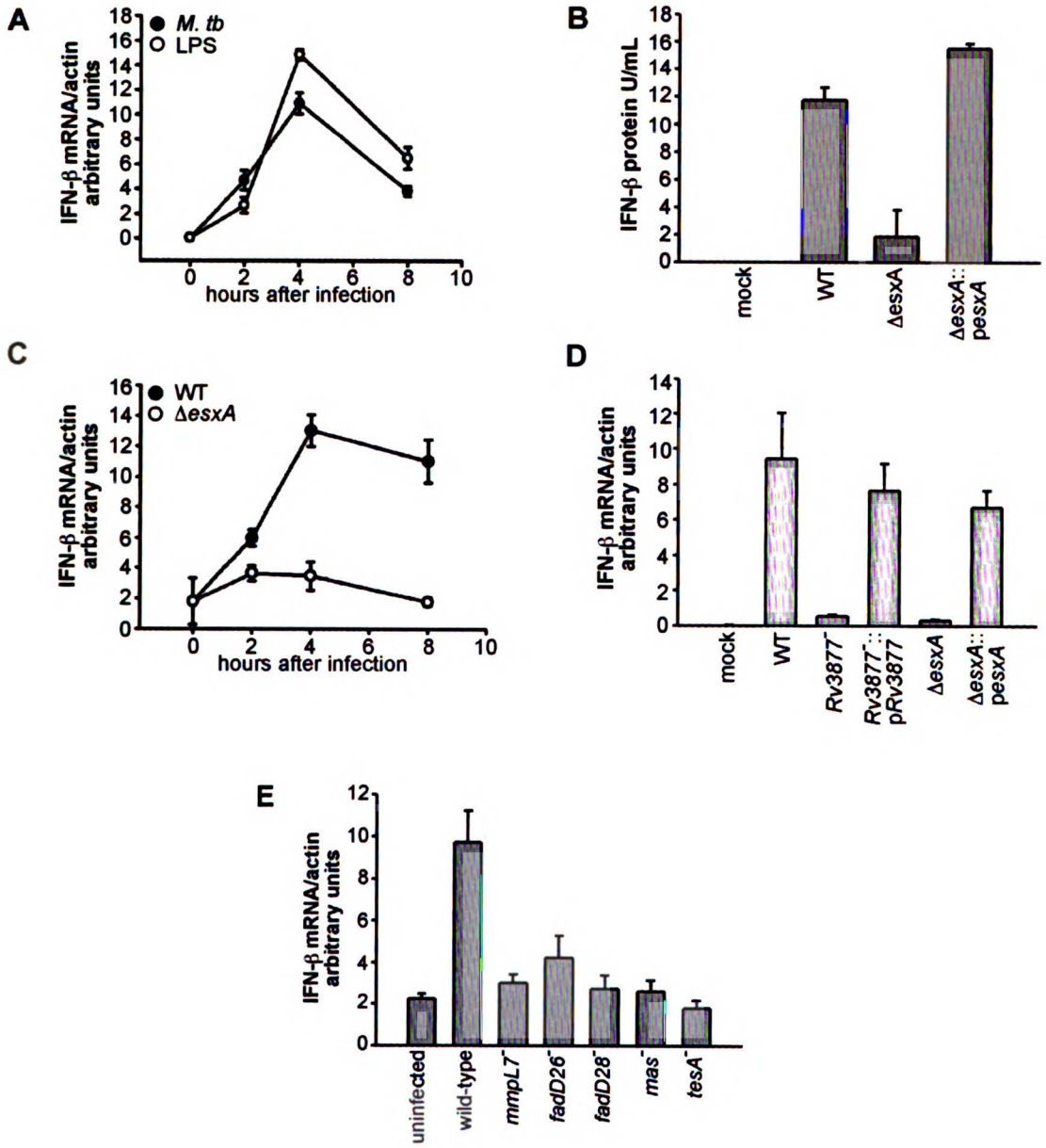
A
M. tb
LPS
IFN-β mRNA/actin arbitrary units
hours after infection
B
IFN-β protein U/mL
mock
WT
ΔesxA
ΔesxA::pesxA
C
WT
ΔesxA
IFN-β mRNA/actin arbitrary units
hours after infection
D
IFN-β mRNA/actin arbitrary units
mock
WT
Rv3877⁻
Rv3877⁻::pRv3877
ΔesxA
ΔesxA::pesxA
E
IFN-β mRNA/actin arbitrary units
uninfected
wild-type
mmpL7⁻
fadD26⁻
fadD28⁻
mas⁻
tesA⁻

Figure 5. IL-12 suppression mediated by the ESX-1 secretion system does not require type I IFN.

Bone marrow-derived macrophages were infected at a multiplicity of infection of 10, and supernatants were harvested at 24 hours after infection for analysis of IL-12 concentration by ELISA. Samples were assayed in triplicate; error bars represent standard deviations. Shown is a representative experiment of three.

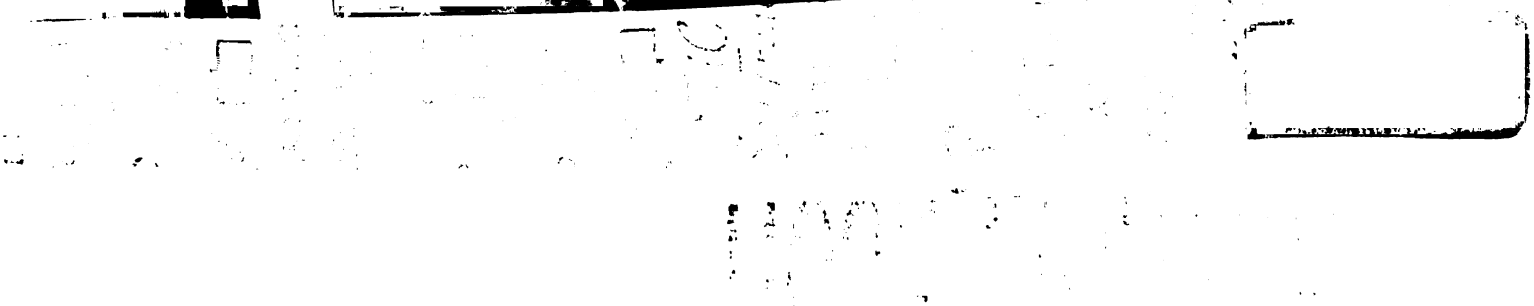

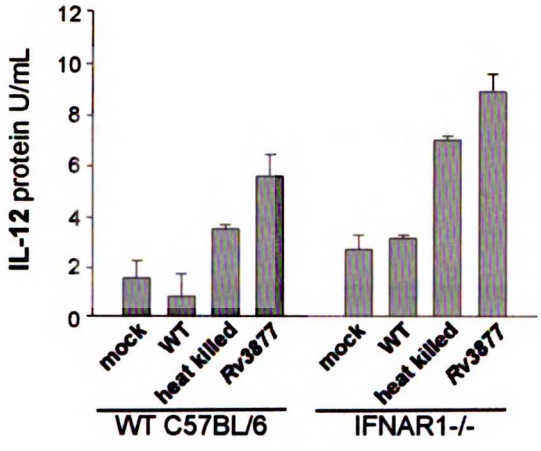
IL-12 protein U/mL
12
10
8
6
4
2
0
mock
WT
heat killed
Rv3877
mock
WT
heat killed
Rv3877
WT C57BL/6
IFNAR1-/-

Figure 6. Induction of IFN-β by bone marrow-derived macrophages is independent of TLR signaling and RIP2 and is dependent on TBK-1.

Wild-type C57BL/6 and knockout bone marrow-derived macrophages were infected at a multiplicity of infection of 10 and RNA was harvested at 4 hours after infection. IFN-β levels were determined by qPCR, and values were normalized to actin. Samples were assayed in triplicate; error bars represent standard deviations. Shown is a representative experiment of at least three.

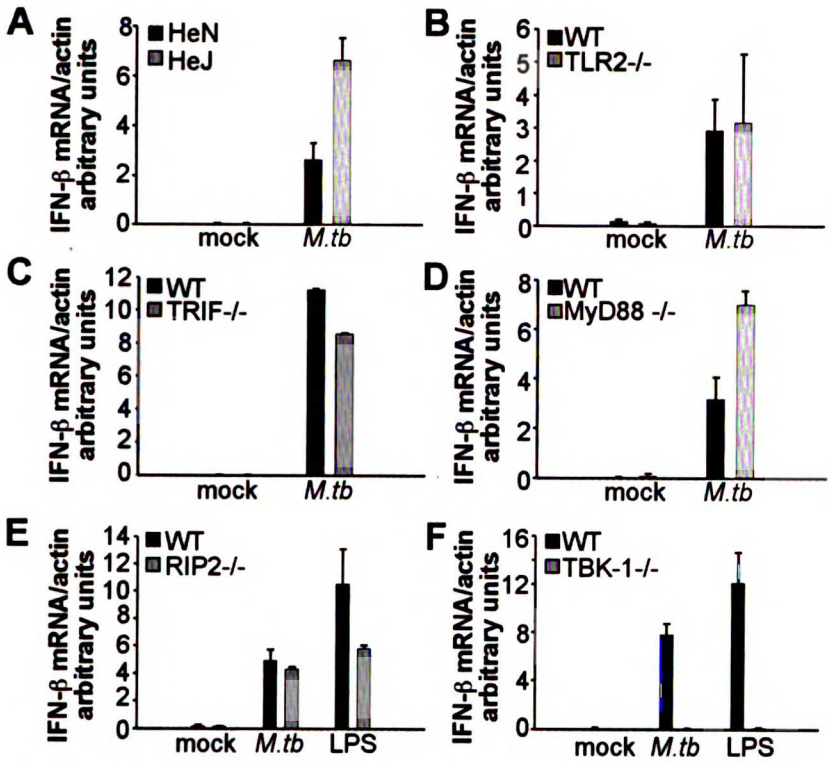
A
IFN-β mRNA/actin arbitrary units
HeN
HeJ
mock
M.tb
B
WT
TLR2-/-
C
WT
TRIF-/-
D
WT
MyD88 -/-
E
WT
RIP2-/-
LPS
F
WT
TBK-1-/-

Figure 7. Type I IFN receptor deficient mice show increased splenic resistance to infection with *M. tuberculosis.*

C57BL/6 mice were injected with $1x10^6$ CFU of the erdman wild-type strain of *M. tuberculosis*, and CFU were enumerated at 1, 10, and 21d after infection in the lungs (A) and spleens (C) of infected mice. Shown are two combined experiments with three mice per group. Significance was determined by the Mann-Whitney U non-parametric test. Spleens were removed and photographed at 1 and 10 days after infection (B), +/+ = C57BL/6, -/- = *IFNAR1*-/-. (D) C57BL/6 or *IFNAR1*-/- mice were infected as above with erdman or Δ*esx* mutant *M. tuberculosis*, and organs were harvested 1 and 10d after infection for enumeration of CFUs. Shown is one experiment with three mice per group.

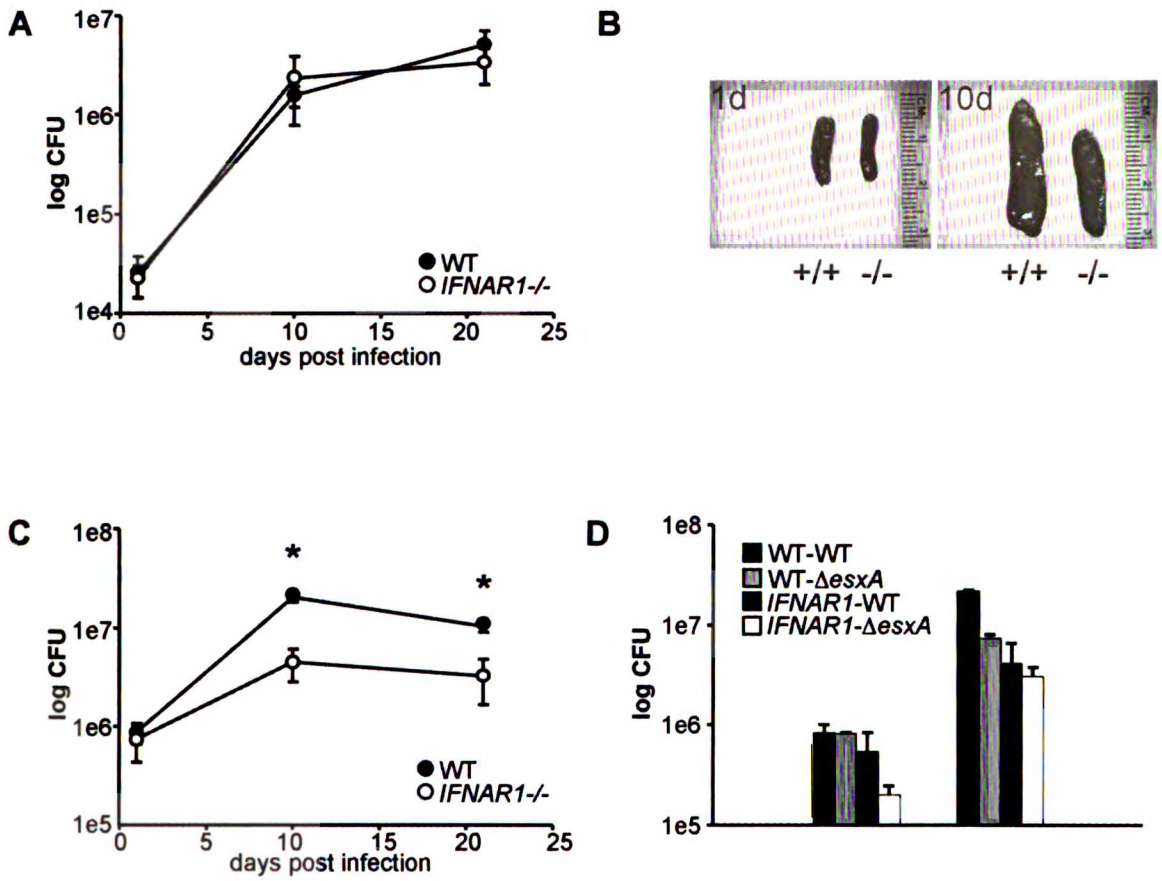
A
1e7
1e6
1e5
1e4
log CFU
0
5
10
15
20
25
days post infection
WT
IFNAR1-/-
B
1d
10d
+/+
-/-
+/+
-/-
C
1e8
1e7
1e6
1e5
log CFU
*
*
0
5
10
15
20
25
days post infection
WT
IFNAR1-/-
D
1e8
1e7
1e6
1e5
log CFU
WT-WT
WT-ΔesxA
IFNAR1-WT
IFNAR1-ΔesxA

Figure 8. Apoptosis of infected macrophages requires ESX-1 mediated secretion and is partially mediated by type I IFNs.

Wild-type C57BL/6 and *IFNAR1*-/- macrophages were infected with wild-type or *esxA* *M. tuberculosis* at an MOI=10. After 24h of infection, cells were washed and treated with lidocaine for removal from tissue culture dishes. Cells were fixed, permeabilized, and subjected to TUNEL staining using fluorescein conjugated dUTP. TUNEL positive cells were quantified using flow cytometry (A). Wild-type macrophages were infected with wild-type, *Rv3877* mutant, or Δ*esxA* mutant *M. tuberculosis* at an MOI=10, and RNA was made from infected monolayers at indicated timepoints after infection. mRNA levels of PKR (B) and daxx (C) were determined by qRT-PCR.

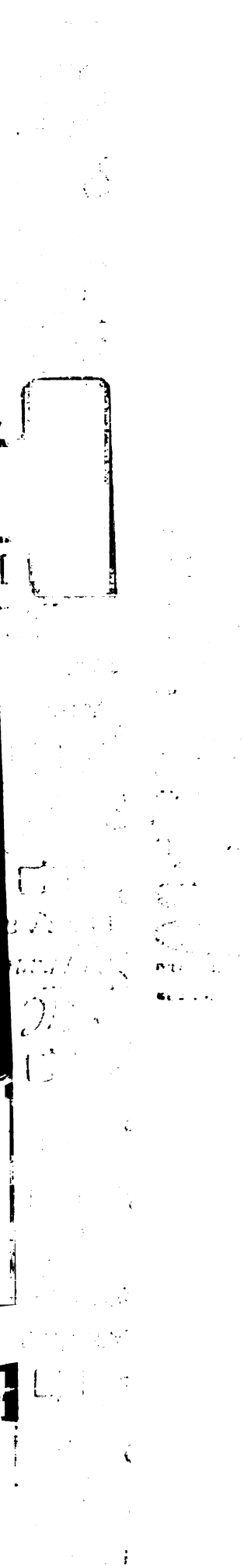

A

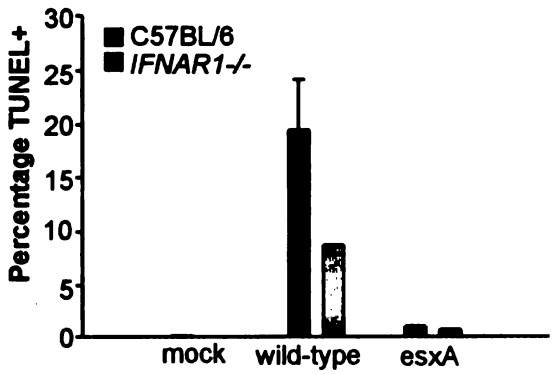
C57BL/6
IFNAR1-/-
Percentage TUNEL+
30
25
20
15
10
5
0
mock
wild-type
esxA

B

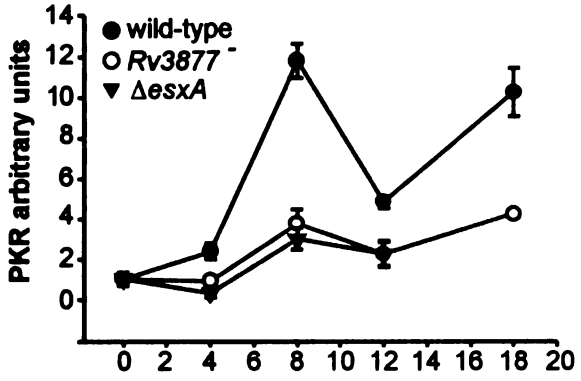
wild-type
Rv3877⁻
ΔesxA
PKR arbitrary units
14
12
10
8
6
4
2
0
0 2 4 6 8 10 12 14 16 18 20

C

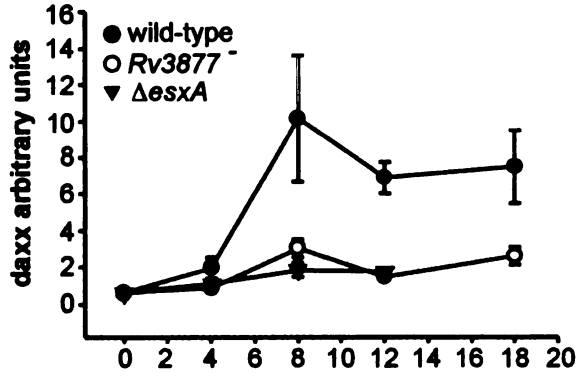
wild-type
Rv3877⁻
ΔesxA
daxx arbitrary units
16
14
12
10
8
6
4
2
0
0 2 4 6 8 10 12 14 16 18 20

Chapter 4

Restoration of the ESX-1 secretion system to BCG results in enhanced virulence and immunogenicity

Abstract.

M. tuberculosis infects an estimated 2 billion individuals world wide. Efforts to control the scope of infection are hampered by the failure of the widely used live vaccine strain Mycobacterium Bacille Calmette-Guerin (BCG) to prevent adult pulmonary infection. Genomic analysis has revealed that BCG has a acquired a deletion in the region of the genome encoding ESAT-6 and CFP-10, proteins that function as immunodominant antigens and virulence factors during infection with *M. tuberculosis*. We restored ESAT-6/CFP-10 production and secretion to BCG, and observed a slight increase in virulence coupled with an enhanced T-cell response in mice infected with this strain. We hypothesize that a recombinant BCG strain secreting ESAT-6 and CFP-10 could be more effective than BCG in protecting against infection with *M. tuberculosis*, however modifications which abrogate the enhanced virulence of the recombinant strain will be necessary for purposes of safety.

Introduction.

M. tuberculosis infection represents a significant burden on global public health, particularly in the developing world. The most widely used vaccine, Bacille Calmette-Guerin (BCG), was derived from *Mycobacterium bovis,* a pathogen of humans and other mammals that is closely related to *M. tuberculosis* at the genome level and is equally virulent in laboratory animals (Sreevatsan, Pan et al. 1997), (Dunn and North 1995). BCG was developed by passaging *M. bovis in vitro* 230 times over a period of 13 years, after which time a marked decrease in virulence was observed. Since that time, BCG has been passaged at numerous different laboratories, resulting in a proliferation of daughter

strains collectively known as BCG. It was believed that BCG, while significantly decreased in virulence, had retained potent immunogenicity, and it has been used widely as a live-attenuated vaccine. The efficacy of BCG, however, particularly in regions of the world where tuberculosis is endemic, is under question. It has been relatively well established that BCG is effective in protecting children against the early manifestations of disease (Colditz GA 1995), however estimates of protection against adult pulmonary tuberculosis range from 0-80% based on large well-controlled field trials. It is possible that the ineffectiveness of BCG in preventing adult disease results from a loss of immunogenicity that accompanied the original attenuation of virulence.

Comparitive genomics of BCG with the parent *M. bovis* has been used to identify genetic differences between the two strains (Behr, Wilson et al. 1999). Five genomic regions were identified to be present in *M. bovis* but absent in BCG strains. Of these deletions, one region designated RD1 (Region of Difference 1) was the only deletion found to be common to all known strains of BCG. It is therefore believed that the loss of RD1 was the primary attenuating mutation leading to the development of BCG. RD1 encompasses the genes Rv3871-Rv3879c, and deletes numerous genes of the ESX-1 secretion system, including *esxA* and *esxB* encoding ESAT-6 and CFP-10 respectively. The ESX-1 secretion system and its substrates ESAT-6/CFP-10 were recently identified as major determinants of virulence for *M. tuberculosis* (Stanley, Raghavan et al. 2003). Deletion of genes in this region from *M. tuberculosis* has been shown to result in dramatic attenuation of the bacterium. It is not surprising, therefore, that loss of this region from *M. bovis* could have contributed to the attenuation of BCG.

ESAT-6 and CFP-10 were originally identified as major T-cell antigens during infection with *M. tuberculosis* (Skjot, Oettinger et al. 2000). Loss of these antigens could have a detrimental effect on the immunogenicity of BCG as compared to the parental *M. bovis* strain. That ESAT-6 is capable of generating a protective immune response has been demonstrated in mouse models of vaccination. Delivery of ESAT-6 both as a DNA vaccine (Kamath, Feng et al. 1999) and as a protein subunit vaccine (Kamath, Feng et al. 1999) results in high levels of protection against subsequent challenge with *M. tuberculosis*.

We hypothesized that restoration of ESX-1 secretion to BCG would lead to an increase in immunogenicity of this strain, which could make BCG more useful as a vaccine. To this end we created a strain of BCG where the RD1 locus was restored, and found that this restored the secretion of ESAT-6 and CFP-10. The ESAT-6/CFP-10 secreting recombinant strain had a slight growth advantage over BCG in both the spleen and lungs of infected mice, suggesting a partial restoration of virulence. Importantly, we observed a significant increase in the numbers of CD4+ T-cells generated during infection with the recombinant strain as compared to wild-type BCG, as well as an increase in the proportion of activated T-cells in both the CD4 and CD8 lineages. The increased number and proportion of activated T-cells elicited by infection with the ESX-1 recombinant BCG suggests that restoration of ESAT-6/CFP-10 secretion to this strain did result in enhanced immunogenicity.

Results.

The RD1 deletion in BCG removes most of the genes identified as being required for the ESX-1 alternative secretion system. We hypothesized that loss of the RD1 locus from BCG is responsible for the attenuation of this strain, and possibly also for a decrease in immunogenicity. To test our hypothesis, we sought to restore ESX-1 mediated secretion to BCG. To this end, we screened an *M. tuberculosis* genomic library and identified a cosmid, *cesx*, that contained the 17.7kb *esx-1* locus as well as 19.7kb of flanking sequence. Introduction of this cosmid into BCG resulted in a recombinant strain (BCG::*cesx*) with *in vitro* growth kinetics identical to BCG (data not shown). Intersetingly, colonies formed by the recombinant strain had a morphology that more closely resembled colonies of *M. tuberculosis* rather than those formed by BCG (data not shown). To test whether introduction of *cesx* to BCG restored ESX-1 mediated secretion, we analyzed cell pellets and cell culture supernatants for the presence of ESAT-6 and CFP-10. We found that the recombinant strain was able to produce (Figure 1, lane 3) and secrete (lane 4) ESAT-6 and CFP-10 at levels comparable to wild-type *M. tuberculosis*.

To determine whether ESX-1 mediated secretion increases the ability of this strain to replicate in mice, we compared the growth of wild-type BCG and the recombinant ESAT-6/CFP-10 secreting strain in mouse infections. C57BL/6 were infected with 10^6 CFU BCG or BCG::*cesx* strain via the IV route, and bacterial numbers were monitored at various timepoints after infections. BCG replicates marginally in the lungs and spleens of infected animals (Figure 2A). The recombinant strain exhibits slightly enhanced bacterial growth at 7 and 14 days post infection in the lung (Figure 2A), and at seven

days in the spleen (Figure 2B), the only time-point examined for this organ. The modest increase in growth does not restore virulence to levels comparable to wild-type *M. bovis* or *M. tuberculosis*, however, both of which are capable replicating in numbers by several logs under these conditions.

To determine whether ESX-1 mediated secretion resulted in enhanced immunogenicity of BCG, we examined the cellular immune response in spleens of infected animals. Spleens were removed 10d post infection, and the cellular composition was analyzed by flow cytometry. The number of cells isolated from mice infected with BCG::*cesx* was two-fold greater than those from mice infected with wild-type BCG (Figure 3A), reflecting the difference in spleen size observed in the two infections (data not shown). The increase in cell number was observed in the Thy 1.2+ T-cell population of the spleen, which was increased two-fold in infections with BCG::*cesx* (Figure 3A). This increase was specific to the CD4 lineage, as no increase in number was observed in CD8+ cells (Figure 3A). We next characterized the nature of the T-cell populations present in both infections by staining isolated splenocytes for cell surface markers indicative of T-cell activation. In the CD4 subset of T-cells we observed a dramatic shift in the activation status of cells isolated from BCG::*cesx* infected mice. Naïve T-cells express high levels of L-selectin, a molecule required for homing to lymph nodes, and low levels of CD44, a cell surface glycoprotein also involved in adhesion that is expressed on the surface upon T-cell activation. T-cells populations from mice infected with BCG displayed high levels of L-selectin, and low levels of CD44, a pattern consistent with a population of T-cells where many of the cells remain naïve (Figure 3B, C). Splenocytes from BCG::*cesx* infected

expressed significantly lower levels of L-selectin, and higher levels of CD44 on their surface, a pattern consistent with activated T-cells. There also appeared to be slight shift towards activation in the CD8+ population of T-cells (Figure 3B, C).

Discussion.

In this study we restored ESX-1 mediated secretion of ESAT-6 and CFP-10 to the mycobacterial vaccine strain BCG. Infection with the resulting recombinant strain elicited increased numbers of CD4 T-cells in infected mice, and shifted both the CD4 and CD8 populations of T-cells towards a more activated state. We hypothesized that this increase in immunogenicity would translate into increased efficacy in protection against subsequent challenge with *M. tuberculosis*. This hypothesis was confirmed by the work of Pym et al who demonstrated that a BCG ESX-1 recombinant vaccine strain conferred enhanced protection against *M. tuberculosis* challenge when compared with wild-type BCG (Pym, Brodin et al. 2002; Pym, Brodin et al. 2003). BCG complemented with the ESX-1 locus is therefore a promising vaccine candidate.

The ESX-1 secretion system is a major determinant of virulence for *M. tuberculosis*, and this was reflected in the slight increase in virulence that we observed in infections with the ESX-1 recombinant strain of BCG. As virulence was not restored to the level of wild-type *M. bovis* or *M. tuberculosis*, it is likely that other attenuating mutations have accumulated in the BCG genome since the original attenuating mutation. Any increase in virulence, however raises safety issues when considering the use of this strain as a vaccine. The introduction of balancing attenuating mutations could decrease the

virulence of the ESX-1 recombinant BCG to levels resembling wild-type BCG. For example, the complex secreted lipid PDIM has been shown to be required for full virulence of *M. tuberculosis* during mouse infection (Cox, Chen et al. 1999). Genes encoding PDIM synthesis and secretion are therefore good candidates for attenuating mutations.

Current efforts to understand the role of ESAT-6 and CFP-10 in virulence could also lead to vaccine strains that produce ESAT-6 and CFP-10 that are functionally ablated, yet retain immunogenicity and therefore engender greater protection against subsequent *M. tuberculosis* infection. ESAT-6 and CFP-10 have been used with good success as subunit vaccines, but better efficacy of protection than that engendered by BCG has not been observed (Brandt, Elhay et al. 2000; Olsen, Hansen et al. 2000). It is possible that the expression and secretion of ESAT-6 and CFP-10 by BCG may be optimal for delivery of these potent T-cell antigens. The BCG::c*ESX* strain is there for a promising candidate for further development as a live attenuated vaccine for tuberculosis.

Materials and Methods.

Bacterial strains. The wild-type strains used in this study were the Pasteur strain of bacillus Calmette-Guerin and the Erdman strain of *M. tuberculosis*. The recombinant BCG strain BCG::*cesx:* was generated by introduction of the cosmid cjsc49 into BCG. cjsc49 was isolated from a cosmid library of Erdman genomic DNA constructed in the integrating vector pYUB412 using *esxA* as a probe. Sequencing of both ends of the insert

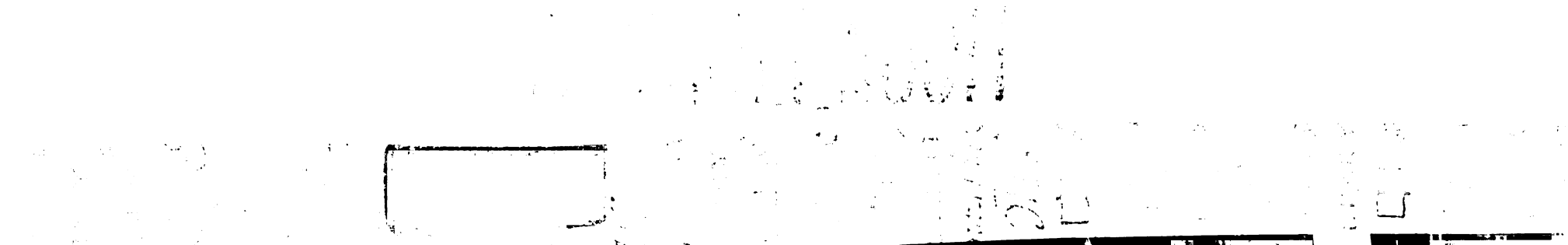

revealed an insert size of 37kb spanning nucleotides 4325031 to 4362407 with respect to the sequence of the H37Rv *M. tuberculosis* strain.

Protein preparation and anaylsis. Concentrated culture supernatants were prepared by growing *M. tuberculosis* or BCG as previously described (Stanley, Raghavan et al. 2003). Cell lysates and supernatants were separated by SDS-PAGE using 10-20% acrylamide gels. Proteins were visualized by immunoblotting by using antibodies against ESAT-6 (Hyb 76-8), CFP-10 (K8493) or GroEL (HAT5), all kind gifts of P. Andersen (Statens Serum institute, Copenhagen, Denmark).

Mouse Infections and flow cytometry. C57BL/6 mice were infected i.v., and organs were harvested at various timepoints after infection. For enumeration of CFUs, samples were processed exactly as described (Cox, Chen et al. 1999). For flow cytometry of splenocytes, spleens were crushed in a tissue culture dish using the plunger of a 10mL syringe for generation of a single cell suspension. Cells were washed, and subjected to hypotonic treatment for the lysis of red blood cells. 10^6 splenocytes were stained on ice with antibodies against CD4, CD8, CD62L (L-selectin), and CD44. Samples were fixed with 4% para-formaldehyde and analyzed using a FACStar flow cytometer.

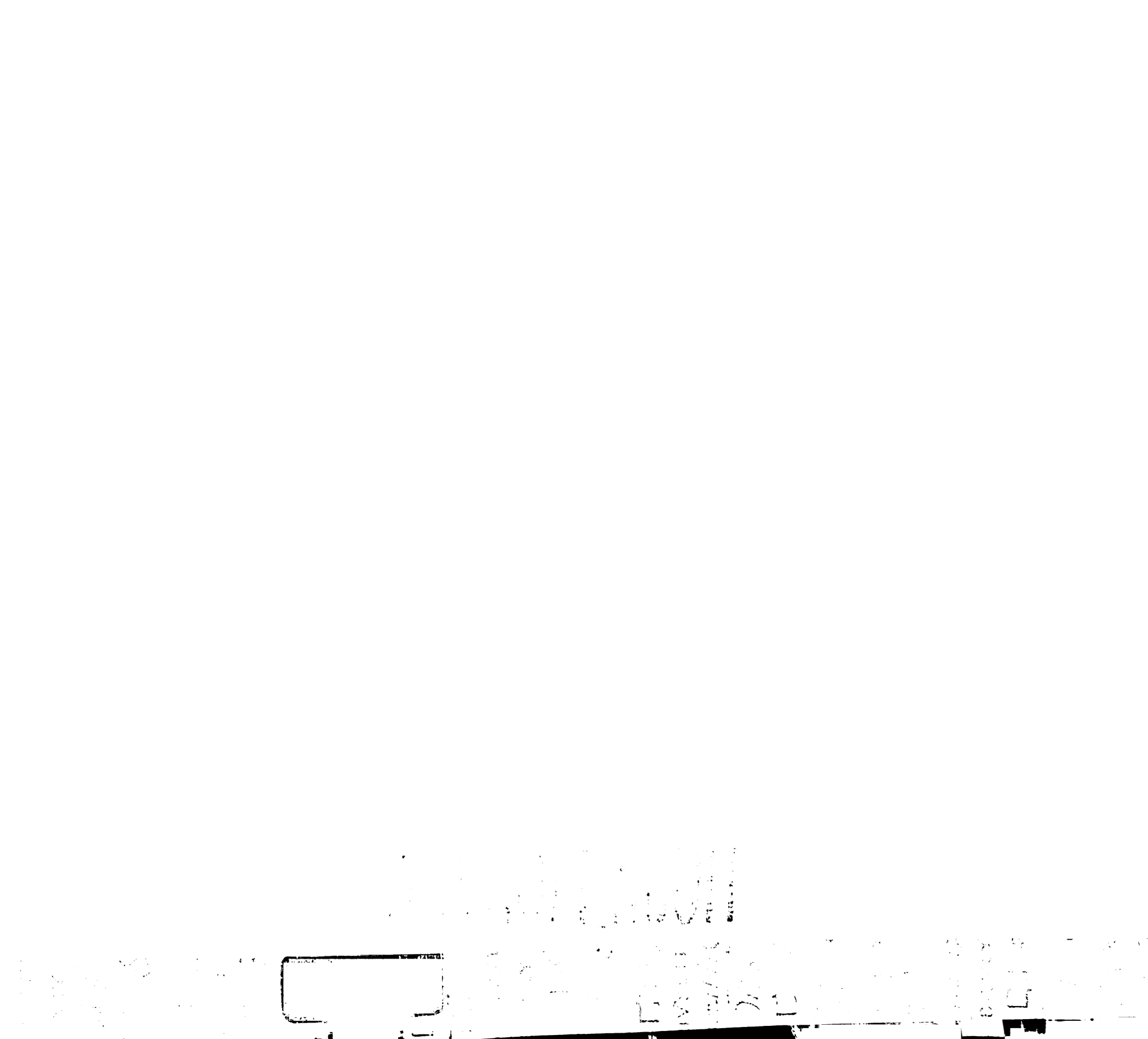

Figure 1. Complementation of BCG with the ESX-1 locus restores ESAT-6 and CFP-10 secretion.

Western blot detection of ESAT-6, CFP-10 and GroEL from cell pellet (P) and supernatant (S) fractions from BCG (Pasteur strain), BCG transformed with an integrating cosmid containing the ESX-1 locus (BCG+cESX) and from WT *M. tuberculosis*.

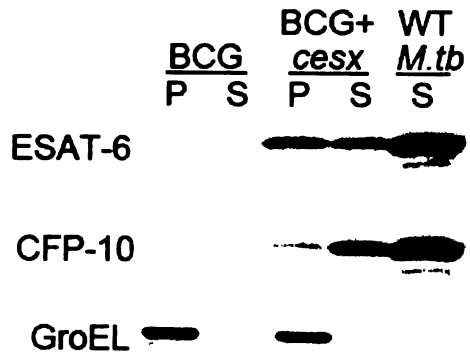
BCG+ WT
BCG cesx M.tb
P S P S S
ESAT-6
CFP-10
GroEL

Figure 2. Complementation of BCG with the ESX-1 locus results in an increase in virulence.

C57BL/6 mice were injected i.v. with $1x10^6$ cfu of each strain, and organs were harvested at 1, 7, and 14 days after infection. Bacteria from lungs (A) and spleens (B) were plated for enumeration of CFUs. The results are representative of two separate experiments using five mice per timepoint, and the error bars represent standard deviation.

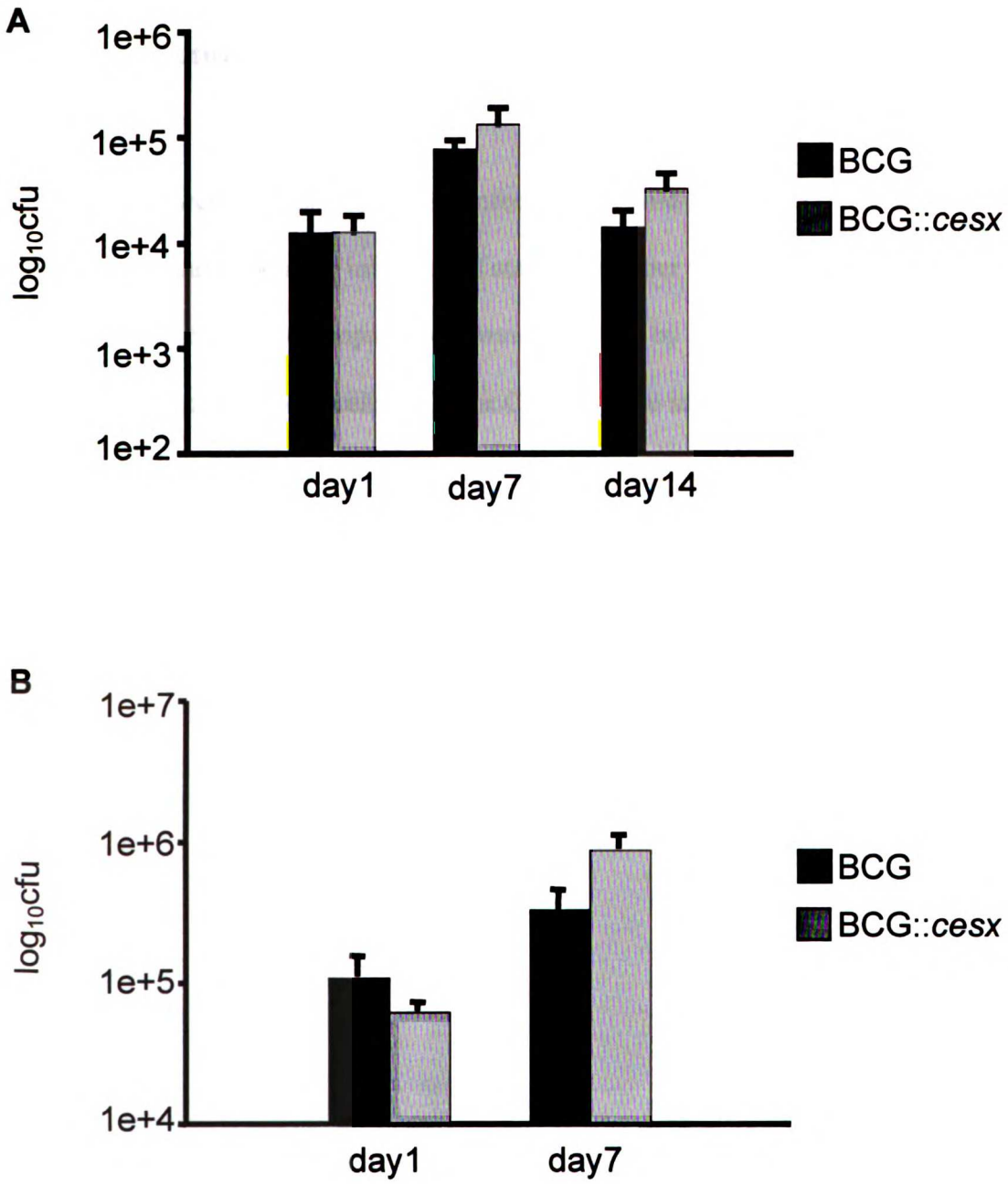
A
1e+6
1e+5
1e+4
1e+3
1e+2
log10cfu
day1
day7
day14
BCG
BCG::cesx
B
1e+7
1e+6
1e+5
1e+4
log10cfu
day1
day7
BCG
BCG::cesx

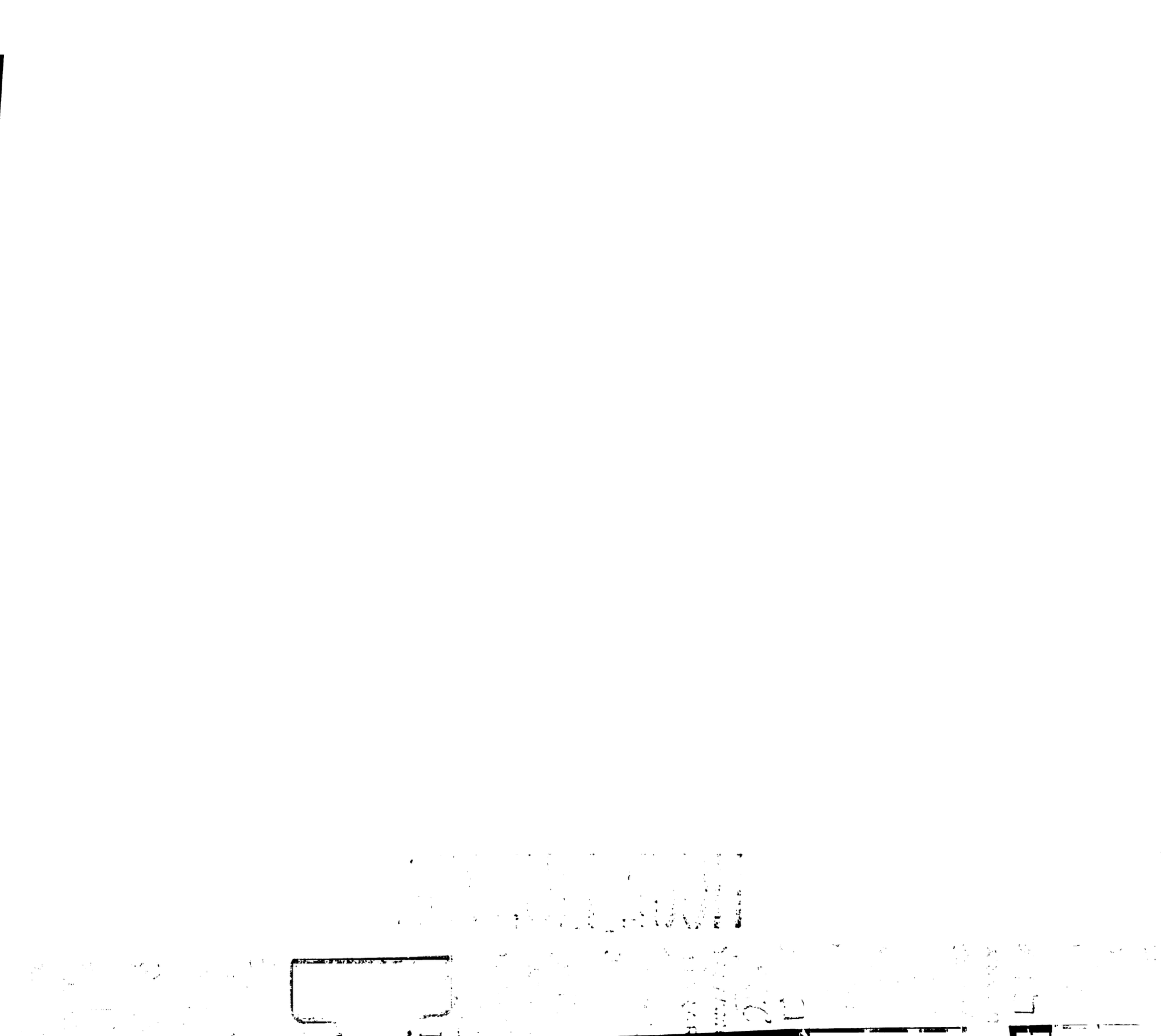

Figure 3. BCG::cESX infection of mice results in an increase in T-cell number and activation status.

Splenocytes were isolated from mice infected with wild-type BCG or the recombinant BCG::*cesx* strain 10d after infection. Total cell number was determined by counting on a hemocytometer, and cell populations were identified by staining with antibodies against Thy1.2 to identify total T-cells, CD4, or CD8 (A). To identify activation status of T-cells, splenocytes were stained with CD4, CD8, and either CD62L, which is more highly expressed on naïve T-cells (B), or CD44, which is more highly expressed on activated T-cells.

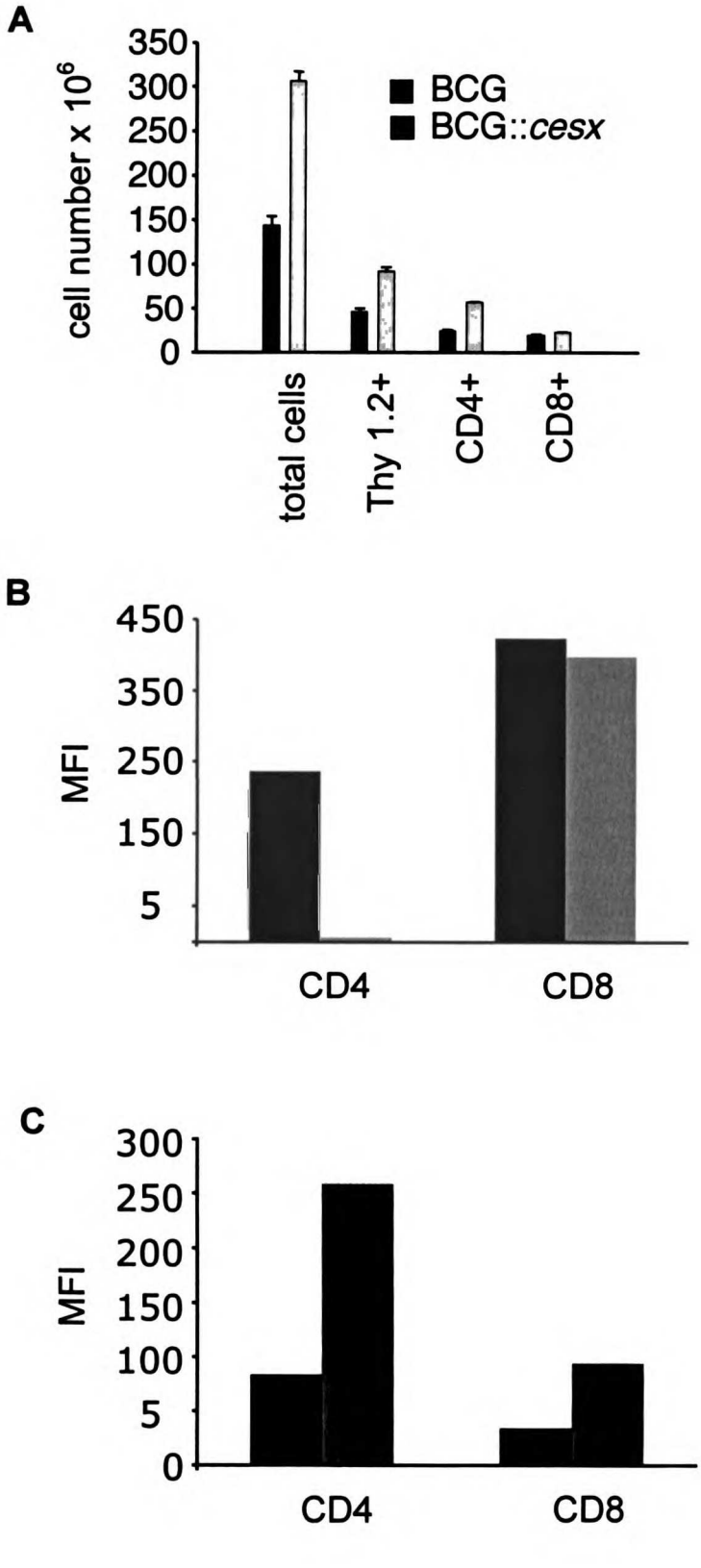
A
cell number x 10^6
350
300
250
200
150
100
50
0
BCG
BCG::cesx
total cells
Thy 1.2+
CD4+
CD8+
B
MFI
450
350
250
150
5
CD4
CD8
C
MFI
300
250
200
150
100
5
0
CD4
CD8

Chapter 5

Conclusions and Perspectives

The ESX-1 secretion system is a fundamental determinant of virulence.

In this study we have identified the first alternative secretion system in *Mycobacterium tuberculosis*, and have demonstrated its fundamental importance for virulence. The primary measurements of virulence in the mouse model of *M. tuberculosis* infection are the measurement of bacterial replication *in vivo*, and the determination of the time to death resulting from infection with a particular strain. We have found that *M. tuberculosis* mutants lacking components (*Rv3870, Rv3871,Rv 3877*) or substrates (*esxA, esxB*) of the ESX-1 secretion system are defective for growth in the lungs and spleens of C57BL/6 mice, replicating more slowly than wild-type bacteria, particularly during the first week after i.v. infection. Although in our studies the growth defect is most pronounced during early stages of infection, a difference in bacterial numbers is maintained through at least three weeks after infection. Perhaps more indicative of the requirement for ESX-1 secretion during infection is our finding that BALB/C mice infected with these mutants do not succumb to infection in time to death experiments for at least one year after infection. Interestingly, at time-points taken just before wild-type mice succumb to infection, there is no difference in the number of bacteria in the lungs of mice infected with wild-type or ESX-1 mutant bacteria. Although virulence in a time to death experiment is usually tightly linked to bacterial number in *M. tuberculosis* infection, a small number of mutants that unlink these phenotypes have been identified. It is possible that mutants of this class, including the ESX-1 mutants, are attenuated due to alterations in the immune response to infection that do not affect bacterial numbers. A more careful analysis of the differences in pathology of mice infected with wild-type vs ESX-1 mutant *M. tuberculosis* at late time-points will help to reveal the basis for

attenuation of these mutants, and could help advance our understanding of the mechanisms that lead to death during infection with wild-type *M. tuberculosis.*

Growth defects of ESX-1 mutants have been described in several studies using different variations on the mouse models of infection. Pronounced growth defects were identified in the lungs of C57BL/6 mice four weeks after aerosol infection with ESX-1 (Guinn, Hickey et al. 2004), and up to 20 weeks after i.v. infection of BALB/C mice (Hsu, Hingley-Wilson et al. 2003). Comparison of these and our data with infection data from other avirulent mutants of *M. tuberculosis* reveal that ESX-1 mutants are among the most attenuated mutants identified to date, underscoring the fundamental importance of this secretion system for *M. tuberculosis* virulence.

The importance of the ESX-1 secretion system for virulence extends beyond its role in *M. tuberculosis.* Genes encoding ESX-1 homologs are found in all virulent mycobacteria, including *M.bovis, M. marinum, M. avium,* and *M. leprae*, and have been shown to be required for virulence of *Mycobacterium marinum* (Gao, Guo et al. 2004) and *Mycobacterium bovis* (Wards, de Lisle et al. 2000). Homologs of individual ESX-1 genes are also found in other gram-positive organisms, including *Corynebacterium diphtheriae, Bacillus subtilis, Bacillus anthracis, Staphylococcus aureus*, and *Clostridium acetybutylicum* (Pallen 2002), (Gey Van Pittius, Gamieldien et al. 2001). It has been shown that homologs of *esxA, esxB,* and *Rv3870/Rv3871* are required for pathogenesis of *Staphylococcus aureus* in murine abcesses (Burts, Williams et al. 2005). The ESX-1 mediated secretion of virulence factors may therefore be a generalized virulence strategy

for the pathogenesis of human bacterial infection for gram-positive organisms. This is a particularly attractive hypothesis as the identification of conserved secretion systems required for virulence, such as the type III and type IV systems of gram negative bacteria, have been lacking in gram positive organisms.

The function of the ESX-1 secretion system.

Although it is clear that the ESX-1 secretion system is required for virulence, the specific function(s) of virulence factors secreted by this system have not been clearly defined, and will remain a topic of immense interest in the field of *M. tuberculosis* for years to come. It was proposed initially that ESAT-6 and CFP-10 might act as pore forming proteins, inducing cytolysis of infected cells for the purpose of cell-to-cell spread. Jacobs et. al. reported a decrease in cell lysis in lung epithelial cells and bone marrow derived macrophages infected *in vitro* with ESX-1 mutant bacteria when compared to wild-type. Additionally, these mutants appeared to be defective for tissue invasiveness in the lungs of infected mice (Hsu, Hingley-Wilson et al. 2003). Similarly, Guinn et. al. reported a defect in cytotoxity of ESX-1 mutants, coupled with what appeared to be a defect in cell-to-cell spreading in macrophage monolayers infected *in vitro* (Guinn, Hickey et al. 2004). As the sequence of ESAT-6 dimer is similar to those of viral cationic pore-forming peptides, it was proposed that ESAT-6 could intercalate into membranes to form pores, resulting in lysis of infected cells. Several lines of evidence refute this hypothesis, however. First, although we also observed a significant decrease in cell lysis during infection of bone-marrow derived macrophages by ESX-1 mutants when compared to wild-type bacteria, we were unable to replicate the cell-to-cell spreading defect of ESX-1

mutants observed in the Guinn et. al. study. We believe that the cell lysis defect is a direct consequence of the failure of ESX-1 mutants to replicate in macrophages rather than a loss of an active pore-forming activity. Most importantly, the recently published solution structure of the ESAT-6/CFP-10 dimer is inconsistent with that of a membrane spanning pore-forming complex. The surface of the dimer has a uniform distribution of positive and negative charge, with no significant hydrophobic patches (Renshaw, Lightbody et al. 2005). Indeed, the surface features of the ESAT-6/CFP-10 complex are most consistent with a function based on specific binding to one or more target proteins (Renshaw, Lightbody et al. 2005).

Bacteria such as *M. tuberculosis* are recognized as pathogens by macrophages because of distinct and invariant components of their outer walls or membranes, the recognition of which leads to the activation of anti-microbial responses by the host. We propose that the ESX-1 system functions to direct virulence factors to the host-pathogen interface to influence the subsequent response to infection such that an environment permissible for bacterial growth is created and maintained. ESX-1 mutants are attenuated for growth in macrophages, and our analysis of infected macrophages has revealed that the ESX-1 secretion system is important for regulating many aspects of macrophage infection. Macrophage production of IL-12 and TNF-α is suppressed by a functional ESX-1 secretion system. The suppression of IL-12 and/or TNF-α could have effects on infection that would extend beyond the macrophage during infection of an animal, influencing the nature and the scope of the resulting immune response. It is unlikely that the attenuation of ESX-1 mutants during infection of bone marrow macrophages is a

result of increased levels of IL-12 and TNF-α, indicating other roles for ESX-1 mediated secretion. We reported that ESX-1 mediated secretion also has a suppressive effect on iNOS, an observation which could account for the growth defects of ESX-1 mutants, however this result was later determined to be an artifact. Jason Macgurn, a fellow graduate student in the Cox lab has shown that ESX-1 secretion system components are required for phagosome maturation arrest (J. MacGurn, unpublished data). It is possible that delivery of ESX-1 mutants to a lysosomal compartment contributes to their attenuation both *in vitro* and *in vivo*. Another possibility, suggested by preliminary data, is that ESX-1 mediated secretion induces apoptotic pathways in infected macrophages, an activity which could lead to reduced growth and spreading of *M. tuberculosis* during macrophage infection. We have also shown that ESX-1 is required for induction of type I IFNs, cytokines that can benefit bacterial growth and virulence, potentially through the induction of apoptosis.

To understand whether ESX-1 control of cytokine production might be a critical determinant of pathogenesis, we sought to identify whether phenotypes observed in macrophages infected *ex vivo* occurred in the context of mouse infection. To this end, we performed qRT-PCR on specific transcripts in spleen and lung tissue from mice infected with ESX-1 mutant or wild-type *M. tuberculosis* from one to five days after infection. We did not observe higher levels of either IL-12 or TNF-α in tissues infected with ESX-1 mutants, a finding which directly contradicts the results obtained from infection of bone marrow-derived macrophages (S. Raghavan and S. Stanley, unpublished observations). As were unable to discriminate between cytokines produced by different cell types within

the tissues, it is possible that production of IL-12 and TNF-α by dendritic and other cell types may have masked a difference in levels produced by tissue macrophages. Analysis of IL-12 production in specific cell types isolated from infected lungs will be required to determine levels of IL-12 production by infected macrophages *in vivo*. Interestingly, we observed lower levels of iNOS in tissues infected with ESX-1 mutants, even at time-points at which bacterial numbers were equivalent to wild-type (S. Stanley, unpublished results). The finding that an attenuated mutant induces lower levels of iNOS than wild-type might indicate that the host is able to use a measure other than bacterial number and replication to sense the virulence of a particular strain, and limits the immune response accordingly. Alternatively, *M. tuberculosis* may tune the production of species required by the host for to levels that are most favorable for bacterial growth.

To identify all the genes that are regulated by ESX-1 mediated secretion during mouse infection, we performed microarray analysis on RNAs from infected tissues using MEEBO arrays. MEEBO arrays provide greater coverage of the mouse genome than arrays used in any other studies to date, thus providing the opportunity to probe novel pathways induced during infection with *M. tuberculosis* as well as those already described to be important for infection. Interesting, we observed that the majority of genes whose induction was identified to be dependent on ESX-1 were previously characterized as interferon dependent, including genes that are understood as being part of an antiviral type I IFN response, such as 2',5' oligoadenylate synthase, and MxA, as well as genes that are known to be induced by infection with *M. tuberculosis*, including IP-10. Using qPCR we were able to determine that the type I IFN, IFN-β, is produced in

an ESX-1 dependent manner *in vivo*. The lack of type I IFN production during infection with ESX-1 mutants likely accounts for the observed defect in the induction of large numbers of IFN responsive genes. It is likely that the defect in IFN-β production observed *in vivo* occurs at the level of the infected macrophage, as we also found that components and substrates of the ESX-1 secretion system are required for generation of IFN-β by bone-marrow derived macrophages infected *ex vivo*.

The exact role of IFN-β during infection with *M. tuberculosis* has yet to be elucidated. Others have shown that type I IFNs are required for inducing iNOS, RANTES, IP-10 and other gene products that are thought to be important for controlling infection (Shi, Blumenthal et al. 2005). We have found that mice lacking the type I IFN receptor (*IFNAR1*-/-) are better able to control infection with *M. tuberculosis* in the spleen, indicating that type I IFNs may be detrimental to the host, a finding which makes sense with the fact that these cytokines are elicited by the ESX-1 mediated secretion of virulence factors. At no timepoint did we see that the knockout mice were more susceptible to infection, a finding that is hard to reconcile with the observed requirement for *IFNAR1* in iNOS production by bone marrow-derived macrophages. The *in vitro* experiments, however, were performed in the absence of IFN-γ. The production of IFN-γ *in vivo* likely overrides the need for type I IFN for the induction of iNOS. It is possible that type I IFNs can be both beneficial and detrimental to the host depending upon the timing of production, and the context of infection. The fact that ESX-1 mutants are less attenuated relative to wild-type in the *IFNAR1*-/- mice suggests, however, that the induction of IFN-β by the ESX-1 secretion system is a component of this systems

contribution to virulence. The induction of IFN-β is the first direct link we have found between ESX-1 mediated secretion and virulence during an animal infection. Time to death analysis of *M. tuberculosis* infections of *IFNAR1-/-* should help to clarify whether the production of type I IFNs is in the balance more productive for the host response, or for the pathogenesis of *M. tuberculosis.*

Mechanism of ESX-1 mediated secretion.

To date a total of seven genes have been identified that are required for the secretion of ESAT-6 and CFP-10 and presumably encode components of the ESX-1 secretion system in *M. tuberculosis.* Three of these genes, *Rv3870, Rv3871,* and *Rv3877* are located at the RD1 genomic locus in proximity to *esxA* (Hsu, Hingley-Wilson et al. 2003; Stanley, Raghavan et al. 2003; Guinn, Hickey et al. 2004). Interestingly, four genes, *Rv0151c, Rv3615, Rv3616c,* and *Rv3849* are found chromosomally unlinked from the RD1 locus (S. Raghavan, unpublished results, J. Macgurn, unpublished results, (Fortune, Jaeger et al. 2005). We have shown that physical interactions link Rv3871 to Rv3870, Rv3870 to CFP-10, and CFP-10 to ESAT-6, strengthening the hypothesis that Rv3870 and Rv3871 function together as part of a machine required for ESAT-6/CFP-10 export. It is likely that there are many components of the ESX-1 secretion system that have yet to be identified. *Mycobacterium smegmatis,* a non-pathogenic, fast-growing relative of *M. tuberculosis,* is used as a model organism for ESAT-6 secretion. Four genes with homologs at the *M. tuberculosis* RD1 locus were found to be required for ESAT-6 secretion in *M. smegmatis* (Converse and Cox 2005). These genes are likely to be required for ESX-1 mediated secretion in *M. tuberculosis.* Once the full set of proteins

that comprise the ESX-1 secretion machine are identified, physical interaction mapping can be used to construct a complete model for ESX-1 mediated secretion.

Four proteins required for ESAT-6/CFP-10 secretion, Rv0152c, Rv3615c, Rv3616c, and Rv3849, are themselves secreted into culture supernatants, and lack canonical sec signal sequences. Surprisingly, it was found that the secretion of all four of these proteins is dependent on the presence of ESAT-6/CFP-10 (S. Raghavan, unpublished results, J. Macgurn, unpublished results, (Fortune, Jaeger et al. 2005). It is possible that these proteins must associate, either directly or indirectly, to be recognized and/or transported by the ESX-1 secretion system. Alternatively, it is possible that Rv0152c, Rv3615c, Rv3616c, Rv3849, ESAT-6, and CFP-10 all encode components of the transport machinery such that loss of any of these proteins abrogates functioning of the apparatus, disrupting secretion of all six proteins. In this case the virulence factor substrates may not yet have been identified. Finally, it is possible that these proteins may have a role as both components of the secretion system, and virulence factors active during infection. An example of a protein with a role in secretion and virulence is the *Yersinia* protein effector LcrV, which is secreted by the type III secretion system yet is required for type III mediated secretion of other effector proteins (Sing, Rost et al. 2002). If all of the proteins associated with ESX-1 secretion identified to date are components of the secretion machine, it will be important to identify the actual secretion substrates. Potential substrates are not limited to proteins, but could also be nucleic acid or lipid species.

An interesting remaining question is the site of action of ESX-1 effectors during infection of macrophages. One possibility is that effector proteins are secreted into the phagosomal lumen and engage receptors located on the phagosomal membrane, thereby activating and/or repressing host signaling pathways. Another possibility is that the ESX-1 secretion system functions in the manner of a type III or type IV system for transport of effectors across the host cell membrane directly into the cytosol. This would provide *M. tuberculosis*, which remains confined within a membrane bound compartment, enhanced potential for accessing and directly altering signaling pathways for greater control of macrophage cell biology. Evidence that *M. tuberculosis* is capable of accessing cytosolic signaling pathways was provided by Ferwerda et. al. (Ferwerda, Girardin et al. 2005) who showed that NOD proteins, cytosolic pattern recognition receptors, are involved in the response to infection with *M. tuberculosis*. In support of this hypothesis, we have have found the induction of IFN-β to be independent of TLRs, the only known phagosomal receptors whose activation can lead to the induction of type I IFNs. Additionally, evidence is mounting which suggests that CFP-10 gains access to the cytosol during infection. First, ectopic expression of CFP-10 in J774 macrophages leads to decreased levels of B7 expression, iNOS production, and an altered pattern of tyrosine phosphorylation in macrophage lysates, phenotypes which suggest that CFP-10 can interact directly with macrophage signaling pathways (Singh, Singh et al. 2003). CFP-10 and ESAT-6 are presented on MHC I molecules. Although MHC I usually presents antigens present in the cytosol, cross presentation of phagosomal antigens can lead to presentation of non-cytosolic antigens on MHC I. Recently it was shown that CFP-10 presentation by MHC I requires components which are specific to the cytosolic antigen

processing pathway, evidence which demonstrates that CFP-10 gains access to the cytosol during infection (Lewinsohn 2006). Thus far, the evidence that CFP-10 and/or ESAT-6 access the cytosol is indirect. Direct localization of ESAT-6 and CFP-10 during infections will be essential for understanding where and how these proteins function.

Understanding the mechanism and function of the ESX-1 secretion system will be of significant interest for years to come. ESX-1 secretion represents a novel pathway for protein translocation across membranes, and as such it will be important to understand the specific mechanisms involved. The *esx* genes as well as those encoding the FtsK/SpoIII homologs are conserved across many bacterial species and may represent the minimal requirement for ESX-1 type secretion. It is possible that the gene amplifications and addition of new ESX-1 components in mycobacteria may be an adaptation to an intracellular lifestyle and/or virulence. In *M. tuberculosis* the ESX-1 secretion system is likely very complex, and modulates many aspects of virulence. It is my belief that work on this system thus far has only scratched the surface. For example, the *M. tuberculosis* genome encodes 22 homologs of ESAT-6. It is conceivable that all of these proteins are secreted and active during different phases of infection *in vivo*, and may contribute to virulence. To complicate matters, there are also four predicted homologs of the ESX-1 secretion system which could also be functional, each of which could secrete an array of different substrates, or could be specific to a particular phase of infection. In order to begin to understand the complexity of this family of proteins, a deeper insight into the function and role of ESAT-6 and CFP-10 will be necessary.

References

Andersen, P., A. B. Andersen, et al. (1995). "Recall of long-lived immunity to Mycobacterium tuberculosis infection in mice." J Immunol **154**(7): 3359-72.

Armstrong, J. A. and P. D. Hart (1975). "Phagosome-lysosome interactions in cultured macrophages infected with virulent tubercle bacilli. Reversal of the usual nonfusion pattern and observations on bacterial survival." Journal of Experimental Medicine **142**(1): 1-16.

Auerbuch, V., D. G. Brockstedt, et al. (2004). "Mice lacking the type I interferon receptor are resistant to Listeria monocytogenes." J Exp Med **200**(4): 527-33.

Banaiee, N., E. Z. Kincaid, et al. (2006). "Potent inhibition of macrophage responses to IFN-gamma by live virulent Mycobacterium tuberculosis is independent of mature mycobacterial lipoproteins but dependent on TLR2." J Immunol **176**(5): 3019-27.

Behr, M. A., M. A. Wilson, et al. (1999). "Comparative genomics of BCG vaccines by whole-genome DNA microarray." Science **284**(5419): 1520-3.

Beltan, E., L. Horgen, et al. (2000). "Secretion of cytokines by human macrophages upon infection by pathogenic and non-pathogenic mycobacteria." Microb Pathog **28**(5): 313-8.

Berthet, F. X., P. B. Rasmussen, et al. (1998). "A Mycobacterium tuberculosis operon encoding ESAT-6 and a novel low- molecular-mass culture filtrate protein (CFP-10)." Microbiology **144**(Pt 11): 3195-203.

Bouchonnet, F., N. Boechat, et al. (2002). "Alpha/beta interferon impairs the ability of human macrophages to control growth of Mycobacterium bovis BCG." Infect Immun **70**(6): 3020-5.

Brandt, L., M. Elhay, et al. (2000). "ESAT-6 subunit vaccination against Mycobacterium tuberculosis." Infect Immun **68**(2): 791-5.

Burts, M. L., W. A. Williams, et al. (2005). "EsxA and EsxB are secreted by an ESAT-6-like system that is required for the pathogenesis of Staphylococcus aureus infections." Proc Natl Acad Sci U S A **102**(4): 1169-74.

Carrero, J. A., B. Calderon, et al. (2004). "Type I interferon sensitizes lymphocytes to apoptosis and reduces resistance to Listeria infection." J Exp Med **200**(4): 535-40.

Colditz GA, B. C., Mosteller F, Brewer TF, Wilson ME, Burdik E, Fineberg HV (1995). "The efficacy of bacillus Calmette-Buerin vaccination of newborns and infants in the prevention of tuberculosis: meta analyses of the published literature." Pediatrics(96): 29-35.

Cole, S. T., R. Brosch, et al. (1998). "Deciphering the biology of Mycobacterium tuberculosis from the complete genome sequence [see comments]." Nature **393**(6685): 537-44.

Converse, S. E. and J. S. Cox (2005). "A protein secretion pathway critical for Mycobacterium tuberculosis virulence is conserved and functional in Mycobacterium smegmatis." J Bacteriol **187**(4): 1238-45.

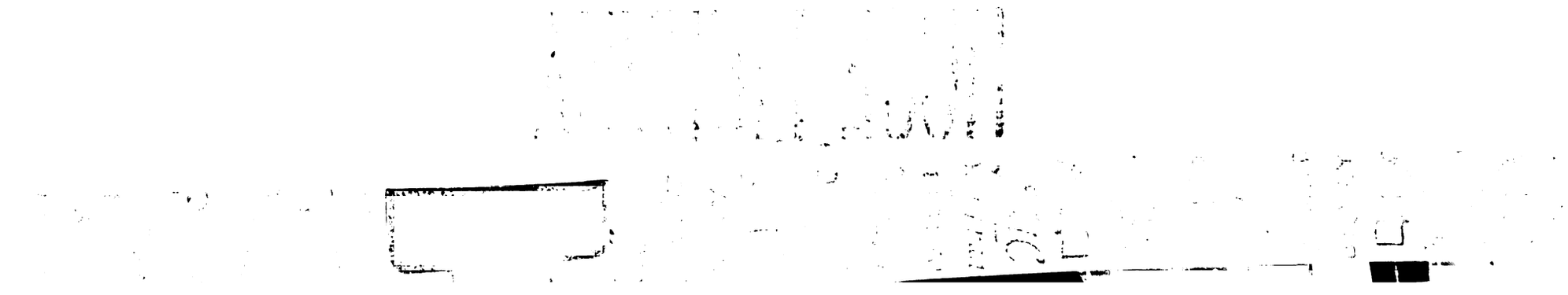

Coombes, B. K., Y. Valdez, et al. (2004). "Evasive maneuvers by secreted bacterial proteins to avoid innate immune responses." Curr Biol **14**(19): R856-67.

Cooper, A. M., J. Magram, et al. (1997). "Interleukin 12 (IL-12) is crucial to the development of protective immunity in mice intravenously infected with mycobacterium tuberculosis." Journal of Experimental Medicine **186**(1): 39-45.

Cooper, A. M., J. E. Pearl, et al. (2000). "Expression of the nitric oxide synthase 2 gene is not essential for early control of Mycobacterium tuberculosis in the murine lung." Infect Immun **68**(12): 6879-82.

Cooper, A. M., B. H. Segal, et al. (2000). "Transient loss of resistance to pulmonary tuberculosis in p47(phox-/-) mice." Infect Immun **68**(3): 1231-4.

Cox, J. S., B. Chen, et al. (1999). "Complex lipid determines tissue-specific replication of Mycobacterium tuberculosis in mice." Nature **402**(6757): 79-83.

DeRisi, J. L., V. R. Iyer, et al. (1997). "Exploring the metabolic and genetic control of gene expression on a genomic scale." Science **278**(5338): 680-6.

Dunn, P. L. and R. J. North (1995). "Virulence ranking of some Mycobacterium tuberculosis and Mycobacterium bovis strains according to their ability to multiply in the lungs, induce lung pathology, and cause mortality in mice." Infect Immun **63**(9): 3428-37.

Dye, C., S. Scheele, et al. (1999). "Global Burden of Tuberculosis." JAMA **282**(7): 677-686.

Economou, A. (1999). "Following the leader: bacterial protein export through the Sec pathway." Trends Microbiol **7**(8): 315-20.

Eisen, M. B., P. T. Spellman, et al. (1998). "Cluster analysis and display of genome-wide expression patterns." Proc Natl Acad Sci U S A **95**(25): 14863-8.

Falcone, V., E. B. Bassey, et al. (1994). "Differential release of tumor necrosis factor-alpha from murine peritoneal macrophages stimulated with virulent and avirulent species of mycobacteria." FEMS Immunol Med Microbiol **8**(3): 225-32.

Ferwerda, G., S. E. Girardin, et al. (2005). "NOD2 and toll-like receptors are nonredundant recognition systems of Mycobacterium tuberculosis." PLoS Pathog **1**(3): 279-85.

Finlay, B. B. and S. Falkow (1997). "Common themes in microbial pathogenicity revisited." Microbiology and Molecular Biology Reviews **61**(2): 136-69.

Fitzgerald, K. A., S. M. McWhirter, et al. (2003). "IKKepsilon and TBK1 are essential components of the IRF3 signaling pathway." Nat Immunol **4**(5): 491-6.

Flynn, J. L., J. Chan, et al. (1993). "An essential role for interferon gamma in resistance to Mycobacterium tuberculosis infection." Journal of Experimental Medicine **178**(6): 2249-54.

Flynn, J. L., M. M. Goldstein, et al. (1995). "Tumor necrosis factor-alpha is required in the protective immune response against Mycobacterium tuberculosis in mice." Immunity **2**(6): 561-72.

Fortune, S. M., A. Jaeger, et al. (2005). "Mutually dependent secretion of proteins required for mycobacterial virulence." Proc Natl Acad Sci U S A **102**(30): 10676-81.

Fortune, S. M., A. Solache, et al. (2004). "Mycobacterium tuberculosis inhibits macrophage responses to IFN-gamma through myeloid differentiation factor 88-dependent and -independent mechanisms." J Immunol **172**(10): 6272-80.

Gao, J. J., Q. Xue, et al. (2001). "Bacterial DNA and lipopolysaccharide induce synergistic production of TNF-alpha through a post-transcriptional mechanism." J Immunol **166**(11): 6855-60.

Gao, L. Y., S. Guo, et al. (2004). "A mycobacterial virulence gene cluster extending RD1 is required for cytolysis, bacterial spreading and ESAT-6 secretion." Mol Microbiol **53**(6): 1677-93.

Gey Van Pittius, N. C., J. Gamieldien, et al. (2001). "The ESAT-6 gene cluster of Mycobacterium tuberculosis and other high G+C Gram-positive bacteria." Genome Biol **2**(10).

Giacomini, E., E. Iona, et al. (2001). "Infection of human macrophages and dendritic cells with Mycobacterium tuberculosis induces a differential cytokine gene expression that modulates T cell response." J Immunol **166**(12): 7033-41.

Giacomini, E., E. Iona, et al. (2001). "Infection of human macrophages and dendritic cells with Mycobacterium tuberculosis induces a differential cytokine gene expression that modulates T cell response." J Immunol **166**(12): 7033-41.

Golemis, E., I. Serebriiskii, et al. (1999). Interaction trap/two-hybrid system to identify interacting proteins. Current Protocols in Molecular Biology. F. M. Ausubel, R. Brent, R. E. Kingstonet al. New York, John Wiley & Sons.

Guinn, K. M., M. J. Hickey, et al. (2004). "Individual RD1-region genes are required for export of ESAT-6/CFP-10 and for virulence of Mycobacterium tuberculosis." Mol Microbiol **51**(2): 359-70.

Hemmi, H., T. Kaisho, et al. (2003). "The roles of Toll-like receptor 9, MyD88, and DNA-dependent protein kinase catalytic subunit in the effects of two distinct CpG DNAs on dendritic cell subsets." J Immunol **170**(6): 3059-64.

Hsu, T., S. M. Hingley-Wilson, et al. (2003). "The primary mechanism of attenuation of bacillus Calmette-Guerin is a loss of secreted lytic function required for invasion of lung interstitial tissue." Proc Natl Acad Sci U S A **100**(21): 12420-5.

Inohara, N. and G. Nunez (2003). "NODs: intracellular proteins involved in inflammation and apoptosis." Nat Rev Immunol **3**(5): 371-82.

Kamath, A. T., C. G. Feng, et al. (1999). "Differential protective efficacy of DNA vaccines expressing secreted proteins of Mycobacterium tuberculosis." Infect Immun **67**(4): 1702-7.

Kaushal, D., B. G. Schroeder, et al. (2002). "Reduced immunopathology and mortality despite tissue persistence in a Mycobacterium tuberculosis mutant lacking alternative sigma factor, SigH." Proc Natl Acad Sci U S A **99**(12): 8330-5.

Kawai, T., O. Takeuchi, et al. (2001). "Lipopolysaccharide stimulates the MyD88-independent pathway and results in activation of IFN-regulatory factor 3 and the expression of a subset of lipopolysaccharide-inducible genes." J Immunol **167**(10): 5887-94.

Keenan, R. J., D. M. Freymann, et al. (2001). "The signal recognition particle." Annu Rev Biochem **70**: 755-75.

Kobayashi, K., N. Inohara, et al. (2002). "RICK/Rip2/CARDIAK mediates signalling for receptors of the innate and adaptive immune systems." Nature **416**(6877): 194-9.

Lee, J., H. G. Remold, et al. (2006). "Macrophage apoptosis in response to high intracellular burden of Mycobacterium tuberculosis is mediated by a novel caspase-independent pathway." J Immunol **176**(7): 4267-74.

Lee, V. T. and O. Schneewind (2001). "Protein secretion and the pathogenesis of bacterial infections." Genes Dev **15**(14): 1725-52.

Lewinsohn, D. M., Grotzke, J.E., Heinzel, A.S., Zhu, L., Ovendale, P.J., Johnson, M., Alderson, M.R. (2006). "Secreted Porteins from *Mycobacterium tuberculosis* Gain Access to the Cytosolic MHC Class-I Antigen-Processing Pathway." The Journal of Immunology **177**: 437-442.

Lewis, K. N., R. Liao, et al. (2003). "Deletion of RD1 from Mycobacterium tuberculosis mimics bacille Calmette- Guerin attenuation." J Infect Dis **187**(1): 117-23.

MacMicking, J. D., R. J. North, et al. (1997). "Identification of nitric oxide synthase as a protective locus against tuberculosis." Proc Natl Acad Sci U S A **94**(10): 5243-8.

Mahairas, G. G., P. J. Sabo, et al. (1996). "Molecular analysis of genetic differences between Mycobacterium bovis BCG and virulent M. bovis." J Bacteriol **178**(5): 1274-82.

Manca, C., L. Tsenova, et al. (2001). "Virulence of a Mycobacterium tuberculosis clinical isolate in mice is determined by failure to induce Th1 type immunity and is associated with induction of IFN-alpha /beta." Proc Natl Acad Sci U S A **98**(10): 5752-7.

McKinney, J. D., K. Honer zu Bentrup, et al. (2000). "Persistence of Mycobacterium tuberculosis in macrophages and mice requires the glyoxylate shunt enzyme isocitrate lyase [see comments]." Nature **406**(6797): 735-8.

McKinney, J. D., J. Jacobs, W.R., et al. (1998). Persisting Problems in Tuberculosis. Emerging Infections. A. Fauci and R. Krause. London, Academic Press: 51-146.

Means, T. K., S. Wang, et al. (1999). "Human toll-like receptors mediate cellular activation by Mycobacterium tuberculosis." J Immunol **163**(7): 3920-7.

Nagai, T., O. Devergne, et al. (2003). "Timing of IFN-beta exposure during human dendritic cell maturation and naive Th cell stimulation has contrasting effects on Th1 subset generation: a role for IFN-beta-mediated regulation of IL-12 family cytokines and IL-18 in naive Th cell differentiation." J Immunol **171**(10): 5233-43.

Nathan, C. and M. U. Shiloh (2000). "Reactive oxygen and nitrogen intermediates in the relationship between mammalian hosts and microbial pathogens." Proc Natl Acad Sci U S A **97**(16): 8841-8.

Nau, G. J., J. F. Richmond, et al. (2002). "Human macrophage activation programs induced by bacterial pathogens." Proc Natl Acad Sci U S A **99**(3): 1503-8.

North, R. J., L. Ryan, et al. (1999). "Growth rate of mycobacteria in mice as an unreliable indicator of mycobacterial virulence." Infect Immun **67**(10): 5483-5.

O'Connell, R. M., S. K. Saha, et al. (2004). "Type I interferon production enhances susceptibility to Listeria monocytogenes infection." J Exp Med **200**(4): 437-45.

O'Connell, R. M., S. A. Vaidya, et al. (2005). "Immune activation of type I IFNs by Listeria monocytogenes occurs independently of TLR4, TLR2, and receptor interacting protein 2 but involves TNFR-associated NF kappa B kinase-binding kinase 1." J Immunol **174**(3): 1602-7.

O'Riordan, M., C. H. Yi, et al. (2002). "Innate recognition of bacteria by a macrophage cytosolic surveillance pathway." Proc Natl Acad Sci U S A **99**(21): 13861-6.

Olsen, A. W., P. R. Hansen, et al. (2000). "Efficient protection against Mycobacterium tuberculosis by vaccination with a single subdominant epitope from the ESAT-6 antigen." Eur J Immunol **30**(6): 1724-32.

Overbergh, L., D. Valckx, et al. (1999). "Quantification of murine cytokine mRNAs using real time quantitative reverse transcriptase PCR." Cytokine **11**(4): 305-12.

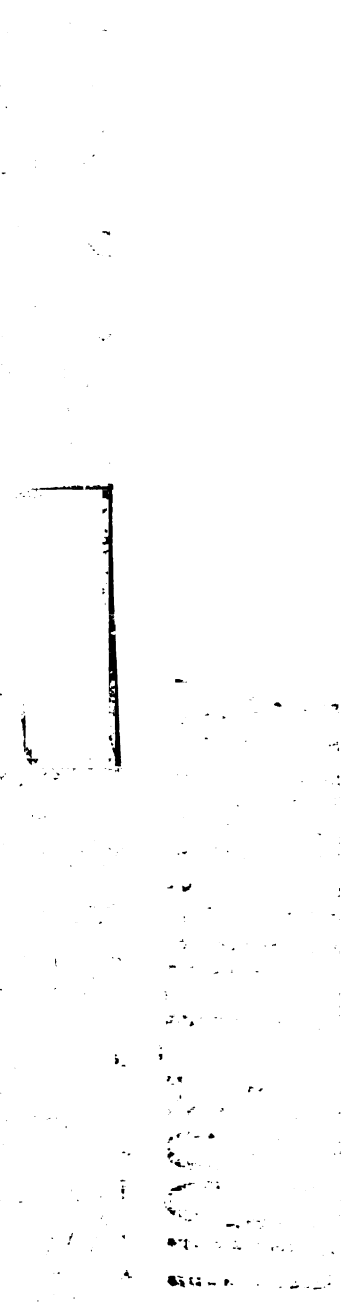

Pallen, M. J. (2002). "The ESAT-6/WXG100 superfamily - and a new Gram-positive secretion system?" Trends Microbiol **10**(5): 209-12.

Perry, A. K., G. Chen, et al. (2005). "The host type I interferon response to viral and bacterial infections." Cell Res **15**(6): 407-22.

Perry, A. K., E. K. Chow, et al. (2004). "Differential requirement for TANK-binding kinase-1 in type I interferon responses to toll-like receptor activation and viral infection." J Exp Med **199**(12): 1651-8.

Pomerantz, J. L. and D. Baltimore (1999). "NF-kappaB activation by a signaling complex containing TRAF2, TANK and TBK1, a novel IKK-related kinase." Embo J **18**(23): 6694-704.

Prabhakar, S., Y. Qiao, et al. (2003). "Inhibition of response to alpha interferon by Mycobacterium tuberculosis." Infect Immun **71**(5): 2487-97.

Pym, A. S., P. Brodin, et al. (2002). "Loss of RD1 contributed to the attenuation of the live tuberculosis vaccines Mycobacterium bovis BCG and Mycobacterium microti." Mol Microbiol **46**(3): 709-17.

Pym, A. S., P. Brodin, et al. (2003). "Recombinant BCG exporting ESAT-6 confers enhanced protection against tuberculosis." Nat Med **9**(5): 533-9.

Renshaw, P. S., K. L. Lightbody, et al. (2005). "Structure and function of the complex formed by the tuberculosis virulence factors CFP-10 and ESAT-6." Embo J **24**(14): 2491-8.

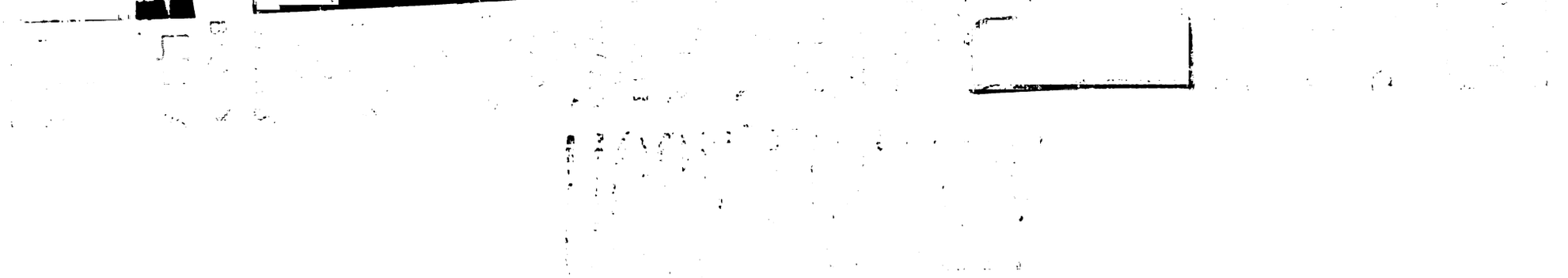

Renshaw, P. S., P. Panagiotidou, et al. (2002). "Conclusive evidence that the major T-cell antigens of the M. tuberculosis complex ESAT-6 and CFP-10 form a tight, 1:1 complex and characterisation of the structural properties of ESAT-6, CFP-10 and the ESAT-6-CFP-10 complex: implications for pathogenesis and virulence." J Biol Chem **8**: 8.

Russell, D. G. (1998). "What does 'inhibition of phagosome-lysosome fusion' really mean?" Trends Microbiol **6**(6): 212-4.

Sharma, S., B. R. tenOever, et al. (2003). "Triggering the interferon antiviral response through an IKK-related pathway." Science **300**(5622): 1148-51.

Shi, S., A. Blumenthal, et al. (2005). "Expression of many immunologically important genes in Mycobacterium tuberculosis-infected macrophages is independent of both TLR2 and TLR4 but dependent on IFN-alphabeta receptor and STAT1." J Immunol **175**(5): 3318-28.

Sieling, P. A. and R. L. Modlin (2001). "Activation of toll-like receptors by microbial lipoproteins." Scand J Infect Dis **33**(2): 97-100.

Sing, A., D. Rost, et al. (2002). "Yersinia V-antigen exploits toll-like receptor 2 and CD14 for interleukin 10-mediated immunosuppression." J Exp Med **196**(8): 1017-24.

Singh, B., G. Singh, et al. (2003). "Intracellular expression of Mycobacterium tuberculosis-specific 10-kDa antigen down-regulates macrophage B7.1 expression and nitric oxide release." Clin Exp Immunol **134**(1): 70-7.

Skjot, R. L., T. Oettinger, et al. (2000). "Comparative evaluation of low-molecular-mass proteins from Mycobacterium tuberculosis identifies members of the ESAT-6 family as immunodominant T-cell antigens." Infect Immun **68**(1): 214-20.

Sonnenberg, M. G. and J. T. Belisle (1997). "Definition of Mycobacterium tuberculosis culture filtrate proteins by two-dimensional polyacrylamide gel electrophoresis, N-terminal amino acid sequencing, and electrospray mass spectrometry." Infect Immun **65**(11): 4515-24.

Sreevatsan, S., X. Pan, et al. (1997). "Restricted structural gene polymorphism in the Mycobacterium tuberculosis complex indicates evolutionarily recent global dissemination." Proc Natl Acad Sci U S A **94**(18): 9869-74.

Stanley, S. A., S. Raghavan, et al. (2003). "Acute infection and macrophage subversion by Mycobacterium tuberculosis requires a novel specialized secretion system." Proc. Natl. Acad. Sci. USA **100**: 13001-13006.

Stark, G. R., I. M. Kerr, et al. (1998). "How cells respond to interferons." Annu Rev Biochem **67**: 227-64.

Stenger, S. and R. L. Modlin (2002). "Control of Mycobacterium tuberculosis through mammalian Toll-like receptors." Curr Opin Immunol **14**(4): 452-7.

Steyn, A. J., D. M. Collins, et al. (2002). "Mycobacterium tuberculosis WhiB3 interacts with RpoV to affect host survival but is dispensable for in vivo growth." Proc Natl Acad Sci U S A **99**(5): 3147-52.

Stockinger, S., T. Materna, et al. (2002). "Production of type I IFN sensitizes macrophages to cell death induced by Listeria monocytogenes." J Immunol **169**(11): 6522-9.

Sturgill-Koszycki, S., U. E. Schaible, et al. (1996). "Mycobacterium-containing phagosomes are accessible to early endosomes and reflect a transitional state in normal phagosome biogenesis." EMBO Journal **15**(24): 6960-8.

Taki, S. (2002). "Type I interferons and autoimmunity: lessons from the clinic and from IRF-2-deficient mice." Cytokine Growth Factor Rev **13**(4-5): 379-91.

Tekaia, F., S. V. Gordon, et al. (1999). "Analysis of the proteome of Mycobacterium tuberculosis in silico." Tuber Lung Dis **79**(6): 329-42.

Thoma-Uszynski, S., S. Stenger, et al. (2001). "Induction of direct antimicrobial activity through mammalian toll-like receptors." Science **291**(5508): 1544-7.

Ting, L. M., A. C. Kim, et al. (1999). "Mycobacterium tuberculosis inhibits IFN-gamma transcriptional responses without inhibiting activation of STAT1." J Immunol **163**(7): 3898-906.

Tullius, M. V., G. Harth, et al. (2001). "High extracellular levels of Mycobacterium tuberculosis glutamine synthetase and superoxide dismutase in actively growing cultures are due to high expression and extracellular stability rather than to a protein-specific export mechanism." Infect Immun **69**(10): 6348-63.

Vale, R. D. (2000). "AAA proteins. Lords of the ring." J Cell Biol **150**(1): F13-9.

Verdugo, R. A. and J. F. Medrano (2006). "Comparison of gene coverage of mouse oligonucleotide microarray platforms." BMC Genomics **7**: 58.

Via, L. E., R. A. Fratti, et al. (1998). "Effects of cytokines on mycobacterial phagosome maturation." J Cell Sci **111**: 897-905.

Wards, B. J., G. W. de Lisle, et al. (2000). "An esat6 knockout mutant of Mycobacterium bovis produced by homologous recombination will contribute to the development of a live tuberculosis vaccine." Tuber Lung Dis **80**(4-5): 185-9.

Weiden, M., N. Tanaka, et al. (2000). "Differentiation of monocytes to macrophages switches the Mycobacterium tuberculosis effect on HIV-1 replication from stimulation to inhibition: modulation of interferon response and CCAAT/enhancer binding protein beta expression." J Immunol **165**(4): 2028-39.

Yamamoto, M., S. Sato, et al. (2002). "Cutting edge: a novel Toll/IL-1 receptor domain-containing adapter that preferentially activates the IFN-beta promoter in the Toll-like receptor signaling." J Immunol **169**(12): 6668-72.

Appendix A

Characterization of the *M. tuberculosis* secretion proteome and identification of ESX-1 secretion substrates.

Introduction.

The ESX-1 secretion machine is a major virulence determinant of *M. tuberculosis*, and has been shown to regulate many key aspects of pathogenicity. We hypothesize that the ESX-1 secretion system is responsible for the secretion of multiple virulence factors, each of which could have a different function during infection. As all of the substrates of ESX-1 secretion identified to date, including ESAT-6 and CFP-10, are secreted into supernatants of cells grown during log phase growth *in vitro* we reasoned that by comparing supernatants of wild-type and ESX-1 mutant cells we could identify novel ESX-1 secretion substrates.

Esx family proteins are good candidates for ESX-1 secretion substrates. ESAT-6 and CFP-10, encoded by *esxA* and *esxB,* are members of a 22 member gene family in *M. tuberculosis* consisting of the genes *esxA-esxW*, all of which encode small (~100AA) proteins. These proteins are characterized by their size and a central WXG motif, and have widely varying levels of similarity. With the exception of ESAT-6 and CFP-10, nothing is known about the function of the Esx family members. EsxG, ExsJ, EsxH, EsxK, and EsxM have been found to be secreted from *M. tuberculosis* cells, however the mechanism of secretion remains unknown. Like *esxA* and *esxB,* the *esx* family genes are usually found encoded in pairs in a shared operon. Interestingly, four of these operons are flanked by homologues of genes at the *esxA/B* locus that have been identified as components of the ESX-1 secretion machine.

Results.

To begin our studies of protein secretion in *M. tuberculosis*, we the defined the conditions we would use for analysis of secreted proteins during log phase growth *in vitro*, as previous studies of proteins secreted from *M. tuberculosis* were performed using conditions where the bacteria were clearly undergoing lysis. To this end we used GroEL as a marker for lysis, and determined growth conditions in which we observed the maximal number of proteins in cell supernatants (ST-CF) without observation of GroEL. These conditions were used in our initial analysis of ESX-1 mutants (see chapter 2 figure 1 and chapter 2 materials and methods), and for all subsequent analyses. We reasoned that production of ST-CF under these conditions would allow us to rigorously define the secreted protein profile, without the complication of cell lysis, and by comparison of ST-CF profiles, to identify proteins whose secretion is dependent on ESX-1. Three major bands are present in the low molecular weight region of the protein profile of wild-type ST-CF separated by one-dimensional SDS-PAGE (Fig. 1) and silver stained for visualization of proteins. Interestingly, although it is known that ESX-1 mutants fail to secrete multiple substrates, only one of these bands (band 3, see Fig. 1) is missing in ESX-1 mutants, indicating that each band on the gel might contain multiple protein species. To determine the protein composition of each band, we excised each of the bands from the gel, performed in gel trypsin digestion of proteins, isolated the resultant peptides, and subjected them to MALDI-TOF mass spectrometry. We were able to identify peptides mapping to multiple proteins in each of the three bands. Interestingly, most of the proteins identified were Esx family members (Fig. 1). Band 3 was found to contain ESAT-6 and CFP-10, as expected, as well as seven other Esx family members.

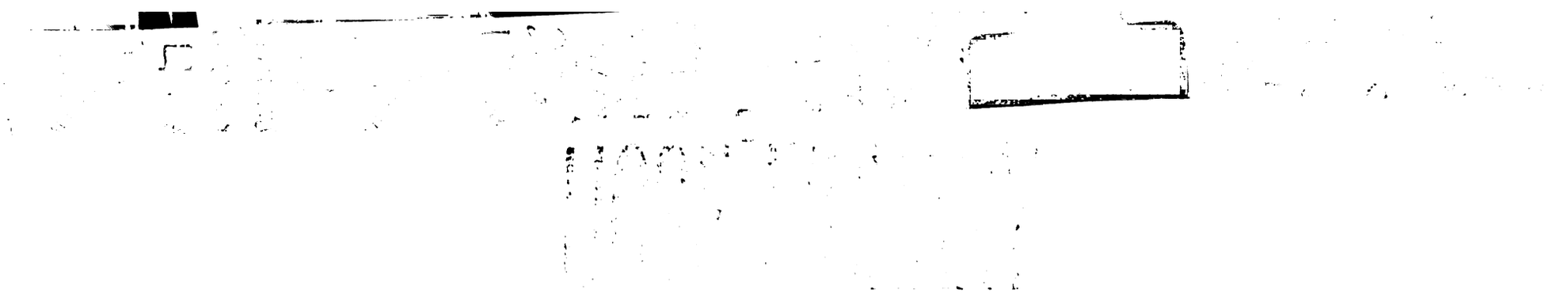

None of these family members were unique to band 3, indicating that these Esx proteins are not dependent on ESX-1 for secretion. The fact that most proteins identified by mass spectrometry were not unique one of the three bands could result from each protein containing modifications that cause it to run in multiple bands on SDS-PAGE. Alternatively, 1-D SDS-PAGE could be insufficient for resolution of the multiple protein species contained within this molecular weight region.

To obtain higher resolution of low molecular weight proteins in ST-CF (5-13.5kD) we turned to 2-D gel electrophoresis in which proteins were separated in the first dimension by isoelectric point (pI), and in the second dimension by size using standard SDS-PAGE. Initially we used a wide gradient of pIs for separation in the first dimenstion, but found that the majority of the proteins in the low molecular weight region have isoelectric points between 4 and 5 (data not shown). We therefore used a pI gradient of 3.9-5.1 for the first dimension of separation, and ran the second dimension such that low molecular weight proteins were retained on the gel. Under these conditions we observed >20 separate proteins on a Coomassie stained gel, four of which were missing in the ST-CFs from ESX-1 mutants (Fig. 2A). Spot 1 contained peptides of mass 1901.22D corresponding to AA 58-74 of ESAT-6, and 3428.38D corresponding to AA 2-33 of ESAT-6 with the addition of an acetyl group. Although the expected peptide obtained from trypsin digest contains AA 1-33, it is not uncommon for bacterial proteins to have the N-terminal methionine removed. Spot 2 contains the same peptide sequences, without the acetyl group on the N-terminal peptide. Spot 3 contains peptides of mass 2004.88D, corresponding to AA 27-44 of CFP-10, 1595.26D corresponding to AA 6-20

of CFP-10, 1318.03D corresponding to AA 66-77 of CFP-10, 1143.34D corresponding to AA 45-67, and 909.61D corresponding to AA75-85 of CFP-10. The composition of spot four is identical to that of spot 3.

To determine the identity of protein spots in the low molecular region whose secretion is independent of ESX-1, we excised these spots from wild-type and mutant gels, and analyzed their composition by mass spec. Although we did not complete our identification of all protein spots, we were able to identify, esxO esxW, esxL, mpt64, and MT2420 (data not shown).

To identify differences in high molecular weight proteins, we separated in the first dimension using pI ranges of 3.9-5.1, and 4-7. Under both conditions a grouping of spots was observed on silver stained gels at approximately 40kDa and at the midpoint of the pI range, in wild-type but not ESX-1 samples (Fig. 2B). These spots were of too low abundance to observe by Coomassie staining. Although we attempted to identify the composition of these spots by mass spectrometry, we were unable to obtain sufficient amounts of protein from the silver stained gels for identification.

Discussion.

In this study we analyzed the composition of supernatants containing proteins secreted by wild-type and ESX-1 mutant *M. tuberculosis* strains during growth *in vitro*. We found that in addition to esxA/esxB (ESAT-6/CFP-10) a subset of Esx family members are secreted into ST-CFs, including EsxG, EsxJ, EsxK, EsxL, EsxN, EsxO, EsxP, and EsxW.

This is the first report that EsxL, EsxN, EsxO, EsxP, and EsxW are secreted. We did not find EsxH and EsxM to be secreted, which is not surprising given that our analysis of spots is incomplete. It is possible that some of the spots whose composition we have not yet analyzed may contain EsxH and/or EsxM. Alternatively, it is possible that these proteins are not actively secreted and were only found in supernatants in previous studies due to high levels of cell lysis.

Of these Esx family proteins we identified only ESAT-6 and CFP-10 as being dependent on ESX-1 for secretion. This analysis agrees with results obtained by iTRAC mass spectrometry (Champion et. al., manuscript in press) in which the same Esx proteins identified as secreted in this study were found in supernatants from both wild-type and ESX-1 mutants. An interesting possibility is that these Esx proteins are dependent on one of the four paralogs of the ESX-1 secretion machine encoded at separate loci. We did, however, identify a group of spots that is consistently present in wild-type but not ESX-1 mutant supernatants. Determination of the identity of these spots may result in identification of novel ESX-1 secretion substrates.

Materials and Methods.

Preparation of culture supernatants. Bacteria were started from 1mL frozen aliquots in 7H9 medium, and grown to OD_{600}= 0.6-0.8. This culture was used to start a culture in Sautons medium + 0.05% Tween-80 at OD_{600}= 0.05; cells were pelleted prior to transfer to Sauton's for removal of 7H9. Cultures were grown to OD_{600}= 0.6-0.8, and cells from this culture were inoculated into 150mL Sautons + 0.005% Tween-80 at OD_{600}= 0.05 as

described above. Cultures were grown for 5 days at which time cells were pelleted, and supernatants were filtered twice through a 0.22μM filter prior to removal from BSL3. Supernatants were concentrated using Amicon Ultra Centrifugal Filter Devices with a MW cutoff of 5000D (Millipore Corporation, Billerica, MA).

2D protein gels. For analysis of low molecular weight proteins, 75μg protein were used. Bio-Rad ReadyPrep 2-D cleanup kit (Biorad, Hercules, CA) was used to remove salts, detergents, lipids, and phenolic compounds. Samples were then resuspended in 8M Urea, 2% CHAPS, 0.2% ampholytes, and 10mM DTT. A 11cm pH 3.9-5.1 IPG strip was rehydrated with sample overnight, focused for 25000 V hours and equilibrated to SDS buffer according to manufacturer's protocol (Bio-Rad, Hercules, CA). IPG strips were embedded in a 4-20% gradient Bio-Rad Criterion Gel, and gels were run for 95 min at 75V. Gels were stained with either Coomassie or silver. For high molecular weight proteins, 11cm 3.9-5.1 or 4-7 IPG strips were used as above, with second dimension run for 115 min. For mass spectrometry, spots were excised, destained in 200 mM ammonium bicarbonate with 40% acetonitrile, and subject to overnight digestion with trypsin (Sigma). The digest was concentrated on reversed-phase ZipTips (Millipore) and crystallized in CHCA matrix. MALDI-TOF was performed on a VoyagerPro workstation. Spot m/z profiles were analysed by ProFound (http://prowl.rockefeller.edu/profound_bin/WebProFound.exe) to identify spots.

Figure 1. Esx Family members are abundant components of ST-CF.

Proteins in ST-CF were separated by 10-20% SDS-PAGE and visualized by silver staining. Three prominent bands (labeled 1,2,3) were excised from the gel and protein identities were determined by MALDI-TOF mass spectrometry analysis.

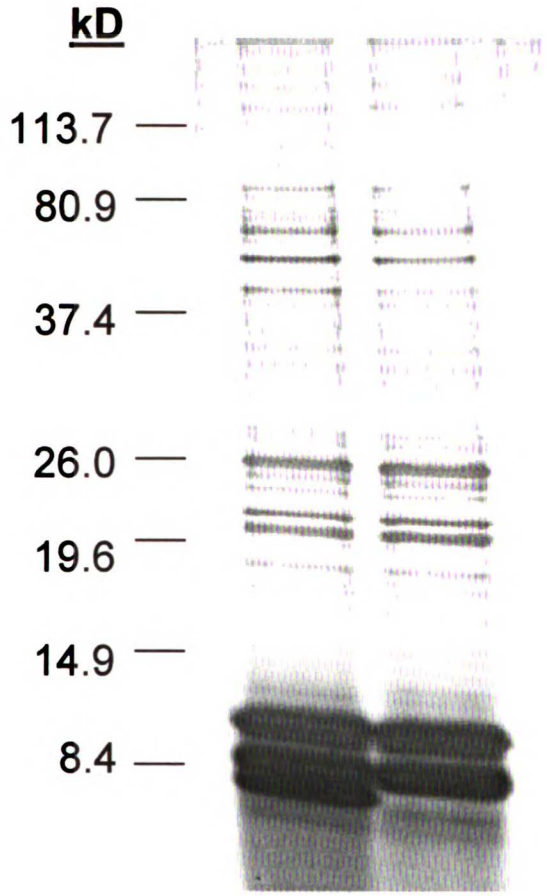

Band1	Band 2	Band3
esxA		esxA
esxB	esxB	esxB
esxG		
esxJ	esxJ	esxJ
esxK	esxK	esxK
	esxL	esxL
	esxN	esxN
esxO	esxO	esxO
esxP		esxP
esxW	esxW	esxW
Rv3195		
PPE		
	PE	

Figure 2. Proteins dependent on ESX-1 for secretion are identified in ST-CFs

Short-term culture filtrate (STCF) was collected from wild-type and mutant cultures and analyzed by 2-D electrophoresis. For low molecular weight proteins (A), 75 μg of protein were hydrated onto 3.9–5.1 IPG strips and focused, followed by separation on 10-20% gradient SDS-PAGE. Proteins were stained with Coomassie brilliant blue. For high molecular weight proteins, 150μg of protein were hydrated onto 4-7 IPG strips, folloed by separation by 10-20% gradient SDS-PAGE. Proteins were stained with silver. In all cases, spots were excised and identified by MALDI-TOF mass spectrometry analysis. Differences between wild-type and mutant are marked by arrows.

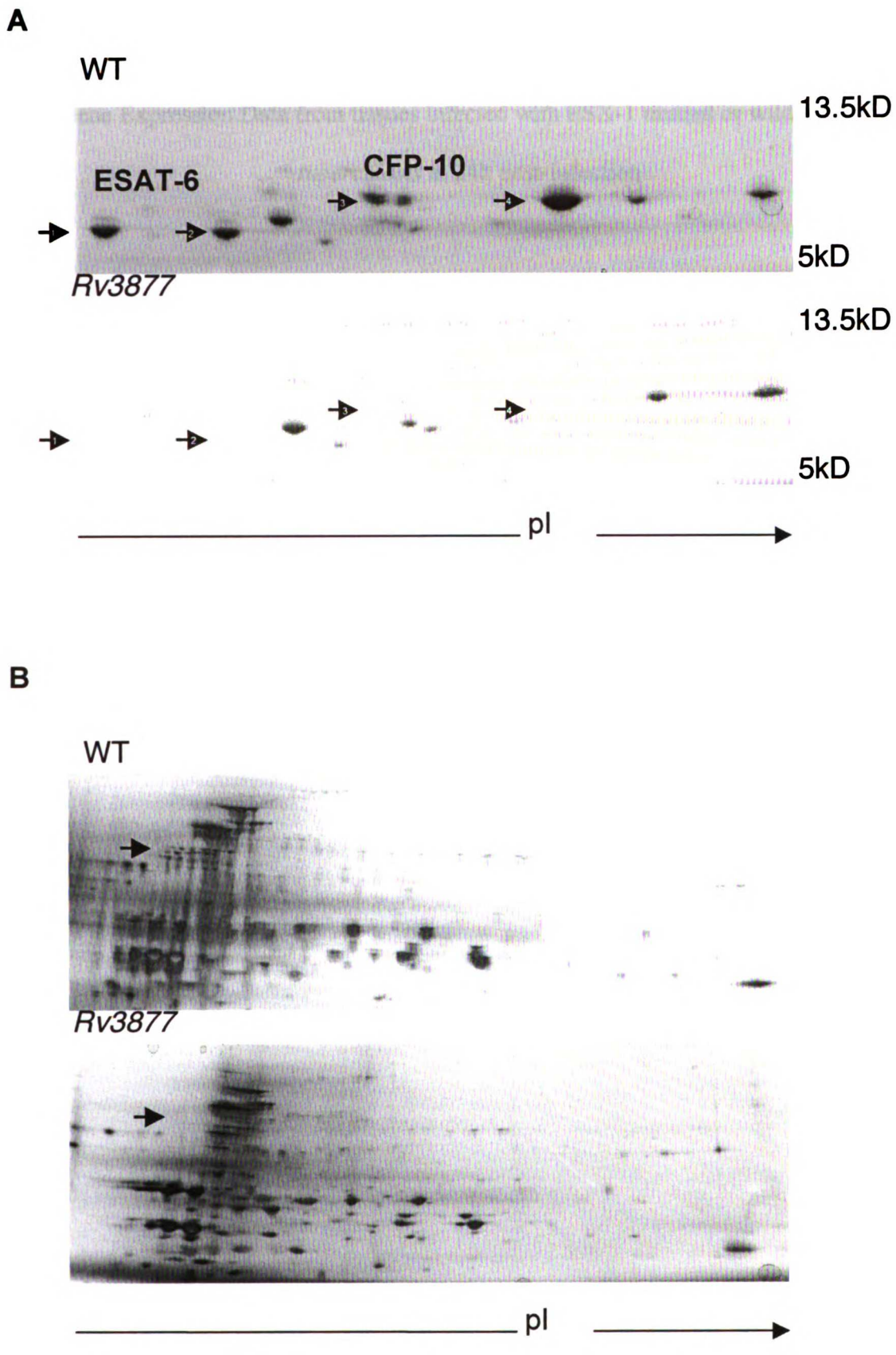
A
WT
13.5kD
ESAT-6
CFP-10
5kD
Rv3877
13.5kD
5kD
pI
B
WT
Rv3877
pI

Appendix B

Gene Expression Data from tissues infected with ESX-1 mutant or wild-type *M. tuberculosis* at 24h post-infection

Table 1. Genes regulated >3 fold in the spleen; log_2(Cy5/Cy3) normalized to uninfected

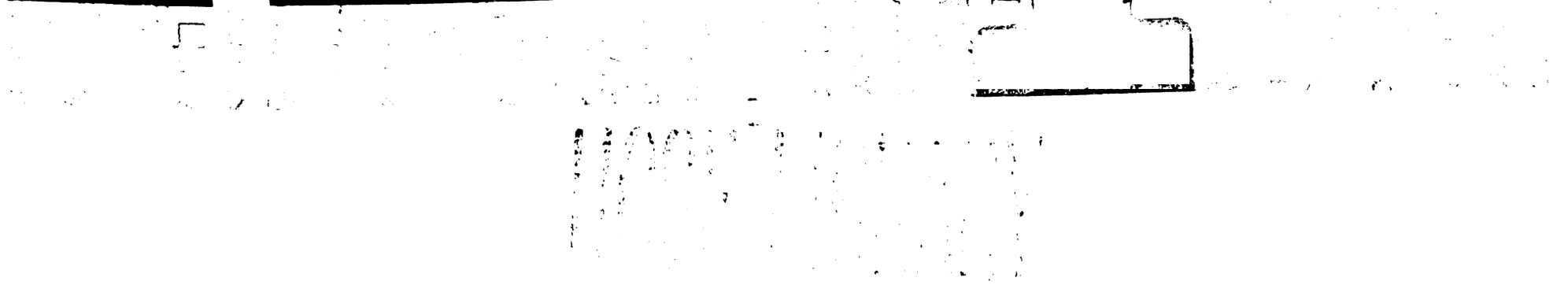

GENE NAME	WT	esxA	WT	esxA	WT	esxA
phospholipid transfer protein (Pltp)	4.424437	-0.149342	-0.431776	-0.446058	-0.556555	
RIKEN cDNA 4930402E16 gene (4930402E16Rik)	1.924495	1.85599	-0.488144	-0.092506	-0.371341	-0.1548
pleckstrin homology domain containing, family F (with FYVE domain) member 2 (Plekhf2)	2.401717	0.403199	0.276043	0.351125	0.395506	
myeloperoxidase (Mpo)	-0.087445	0.61673	1.124889	0.561169	1.68816	2.077766
cathelicidin antimicrobial peptide (Camp)	-0.872401	-0.088049	0.042371	-0.35554	1.15848	1.609486
Mus musculus eukaryotic translation initiation factor 2C, 2,	0.128575	-0.253635	0.243775	-0.119959	1.891694	2.005665
radical S-adenosyl methionine domain containing 2 (Rsad2)	0.899093	0.101846	2.12434	0.623265	0.312131	-0.841725
interferon-stimulated protein (Isg20)	0.714553	0.283119	1.738449	0.57703	0.43056	-0.466358
carbonic anhydrase 1 (Car1)	0.744355	0.778787	1.862044	1.317905	0.285537	0.279904
sphingosine kinase 1 (Sphk1), transcript variant 1	0.55993	0.252256	1.678929	1.333759	0.01409	0.058471
complement component 3 (C3)	1.059159	0.533636	0.934554	0.203362	1.766163	0.727363
transglutaminase 2, C polypeptide (Tgm2)	0.725657	0.428883	1.153221	0.018885	1.797382	0.728131
suppressor of cytokine signaling 1 (Socs1)	0.426115	-0.267441	2.216342	0.895638	1.63743	-0.186187
interferon regulatory factor 7 (Irf7)	0.232617	-0.009709	2.450769	0.966027	1.639106	0.000357
serine (or cysteine) peptidase inhibitor, clade A, member 3C (Serpina3c)	1.710921	0.200083		1.677713	2.817443	1.098524
membrane-spanning 4-domains, subfamily A, member 11 (Ms4a11)	1.143462		2.477914	1.098381	2.061619	0.96719
PREDICTED: immunoresponsive gene 1 (Irg1)	1.714258	-0.253635	5.218857	2.070724	3.338186	0.994776
guanine nucleotide binding protein (G protein), gamma 12 (Gng12)	0.724928	-0.289259	1.670641	0.618212	1.286995	0.448494
Fc fragment of IgG, low affinity IIIa, receptor (Fcgr3a)	0.664628	0.220296	2.053145	1.111366	1.771457	0.377633
PREDICTED: serine (or cysteine) proteinase inhibitor, clade A, member 3G (Serpina3g)	1.328879	0.418311	3.071872	1.596793	2.961179	0.923438
solute carrier organic anion transporter family, member 3a1 (Slco3a1)	0.794688	0.126969	1.675087	0.687396	1.592133	0.260237
PHD finger protein 11 (Phf11)	0.499817	0.068293	2.134041	0.933221	1.911213	0.217169
metallothionein 2 (Mt2)	0.88702	0.295258	2.266859	1.318162	1.176039	0.731742
lymphocyte antigen 6 complex, locus I (Ly6i)	1.24959	0.926937	3.606139	2.251296	2.819274	1.864867
mMA033476	0.873574	0.523973	2.637254	1.580196	2.307182	1.032744
tumor necrosis factor, alpha-induced protein 2 (Tnfaip2)	1.021562	0.557331	1.657415	0.434687	0.813469	-0.320488
HRAS like suppressor 3 (Hrasls3)	0.841932	0.505357	1.799905	0.623265	0.907519	-0.115407
interferon, alpha-inducible protein (G1p2)	1.443601	0.794728	2.96983	1.051359	1.69508	0.14122
interferon induced transmembrane protein 1 (Ifitm1)	0.781811	0.505357	1.961968	0.606777	0.958114	0.364726
2'-5' oligoadenylate synthetase 2 (Oas2)	2.198606	0.684965	3.011052	1.102433	1.975616	-0.045866
Mus musculus interferon-induced protein with tetratricopeptide repeats 1, mRNA	2.130602	0.490526	3.110182	1.01183	1.921874	0.129706
interferon-induced protein 44 (Ifi44)	2.514293	0.746365	3.627081	1.681682	2.399489	0.401593
poly (ADP-ribose) polymerase family, member 12 (Parp12)	1.477001	0.598267	2.235589	0.925674	1.566854	0.070327
thymidylate kinase family LPS-inducible member (Tyki)	1.830638	0.003523	2.50601		1.466603	-0.005223
Mus musculus mRNA for ganglioside-induced differentiation associated protein 10	1.4167	0.142294	1.968495	0.653639	1.335358	0.051159
tripartite motif protein 30 (Trim30)	1.578213	0.226991	1.916772	0.660569	1.438588	-0.060365
chemokine (C-C motif) ligand 12 (Ccl12)	2.520892	0.097837	4.64004	1.234223	3.285238	0.110253
granzyme B (Gzmb)	1.722178	0.02054	2.702607	0.826799	1.903666	0.168259
chemokine (C-X-C motif) ligand 10 (Cxcl10)	2.047097	0.081968	3.763681	0.718422	2.816248	-0.21893
chemokine (C-X-C motif) ligand 9 (Cxcl9)	1.778086	-0.057715	3.250065	1.300206	1.936088	0.096875
xanthine dehydrogenase (Xdh)	1.121006	0.15299	1.889211	0.918721	1.466603	0.217169

glycoprotein 49 A (Gp49a)	1.089513	0.185897	1.73167	0.677713	1.233289	0.352098
lectin, galactose binding, soluble 9 (Lgals9)	1.087839	0.161403	2.132768	1.021815	1.250599	0.37471
schlafen 4 (Slfn4)	2.28238	0.473347	4.600073	2.485762	2.688995	0.954134
interferon regulatory factor 1 (Irf1)	1.058705	-0.063303	1.793433	1.163834	1.275574	0.46044
protein C receptor, endothelial (Procr)	1.673846	0.569487	2.060978	0.141114	2.020977	0.3427
guanylate nucleotide binding protein 5 (Gbp5), transcript variant 2	1.994333	0.911951	3.064653	0.556151	2.543771	0.348413
chemokine (C-C motif) ligand 4 (Ccl4)	1.351128	0.629008	1.820811	0.234223	1.326878	0.065166
pre-B-cell colony-enhancing factor 1 (Pbef1)	1.957409	0.5119	2.279158	0.819185	1.972614	0.271617
interferon-induced protein with tetratricopeptide repeats 2 (Ifit2)	2.893446	0.790759	3.838585	1.519314	3.289725	0.539097
schlafen 5 (Slfn5)	1.796333		2.387716	0.658598	1.955197	0.380668
hect domain and RLD 5 (Herc5)	1.915589	0.746365	2.343821	0.652581	1.895446	0.332646
RIKEN cDNA 9130218O11 gene (9130218O11Rik)	1.654286	0.617082	1.801748	0.661333	1.738149	0.217169
guanylate nucleotide binding protein 5 (Gbp5), transcript variant 1	3.424364	1.534861	3.363427	1.111366	3.175554	0.439561
superoxide dismutase 2, mitochondrial (Sod2)	1.703102	0.491108	1.941032	0.376827	1.61416	0.439561
CD274 antigen (Cd274)	1.978044	0.516883	2.107581	0.434687	1.860139	0.217169
Mus musculus 0 day neonate lung cDNA, RIKEN full-length enriched library	1.560792	0.843227	1.985427	0.718422	1.488629	0.264474
schlafen 1 (Slfn1)	1.367646	0.746365	1.826411	0.63096	1.329099	0.126971
interferon induced with helicase C domain 1 (Ifih1)	2.056945	0.91629	2.170782	0.878079	1.618606	0.320262
purine-nucleoside phosphorylase (Pnp)	1.410582	0.570794	1.672776	0.628502	1.24729	0.217169
RIKEN cDNA 5830443L24 gene (5830443L24Rik)	1.93593	0.842581	1.796765	0.909951	1.573518	0.354672
GTPase, very large interferon inducible 1 (Gvin1)	2.021113	1.005752	2.170505	1.253588	1.617405	0.217169
Mus musculus 3 days neonate thymus cDNA, RIKEN full-length enriched library, clone	3.206001	0.845901	4.059136	1.392652	4.320752	1.091638
sarcoglycan, beta (dystrophin-associated glycoprotein) (Sgcb)	1.283537	0.308244	1.799057	0.605432	1.853626	0.802131
tryptophanyl-tRNA synthetase (Wars)	1.419515	0.138683	2.201155	0.641881	2.008238	0.42362
torsin family 3, member A (Tor3a)	1.131754	0.140029	1.899586	0.55135	1.829173	0.316704
lymphocyte antigen 6 complex, locus F	1.322346	0.331328	2.006983	0.623265	1.638702	0.299631
annexin A4 (Anxa4)	1.389768	0.30158	2.05113	0.533067	1.815073	0.114075
myxovirus (influenza virus) resistance 2 (Mx2)	1.555003		2.353158	0.681682	2.037017	0.217169
ubiquitin D (Ubd)	2.035465	0.643272	3.035518	0.926334	3.01409	0.397741
suppressor of cytokine signaling 1 (Socs1)	1.994548	0.663903	2.778464	0.722801	2.599053	0.418803
torsin family 3, member A (Tor3a)	0.991438	0.238762	1.744926	0.596793	1.294542	0.01923
ubiquitin specific peptidase 18 (Usp18)	1.736777	0.782891	3.306508	1.096719	2.643907	0.287558
pre-B-cell colony-enhancing factor 1 (Pbef1)	1.322522	0.341975	2.721546	0.833685	2.175554	0.332646
lectin, galactose binding, soluble 3 (Lgals3)	1.155876	0.542007	2.111401	0.573709	1.966785	0.548374
secretin (Sct)	1.362358	0.674215	2.070759	0.637765	2.206736	0.409814
transglutaminase 2, C polypeptide (Tgm2)	0.970731	0.594362	1.598915	0.298993	1.723935	0.253695
lymphocyte antigen 6 complex, locus A (Ly6a)	1.390453	0.928568	2.262556	0.717087	2.265396	0.802131
bone marrow stromal cell antigen 2 (Bst2)	1.193322	0.837996	1.946342	0.526404	1.906644	0.873214
guanylate nucleotide binding protein 2 (Gbp2)	2.522608	1.31405	3.407606	1.218281	3.61647	1.604192
leukocyte immunoglobulin-like receptor, subfamily B, member 4 (Lilrb4)	1.24959	0.868356	1.626609	0.529015	1.766163	0.819833
interferon induced transmembrane protein 2 (Ifitm2)	0.868641	0.671403	1.60412	0.333759	1.248556	0.754197
Mus musculus premature mRNA for mKIAA1554 protein	1.774252	0.974171	2.562612	1.141113	2.382152	0.217169
DNA segment, Chr 11, Lothar Hennighausen 2, expressed (D11Lgp2e)	1.450123	0.668363	1.899586	1.036777	1.60986	0.267795
pyrophosphatase (Pyp)	1.261272	0.710741	2.370032	0.946735	1.860139	0.646012
interferon-induced protein with tetratricopeptide repeats 3 (Ifit3)	1.908082	0.925689	3.418254	1.370285	2.673054	0.613097

2'-5' oligoadenylate synthetase-like 2 (Oasl2)	1.977218	1.235112	3.4137	1.748796	2.567443	0.589137
guanylate nucleotide binding protein 1 (Gbp1)	2.631461	1.436681	5.146708	2.509609	3.85892	
poly (ADP-ribose) polymerase family, member 9 (Parp9)	1.030756	0.558293	1.741724	0.828523	1.411667	0.087886
histocompatibility 2, complement component factor B (H2-Bf)	1.616372	0.78384	2.306865	1.070724	2.41824	1.182403
interferon inducible GTPase 1 (Iigp1)	2.553924	1.353023	3.554792	1.872179	3.592133	1.664628
PREDICTED: mixed lineage kinase domain-like (Mlkl)	1.783272	0.902484	2.746073	1.269628	2.128733	0.912314
cDNA sequence BC049975 (BC049975)	2.635869	1.585901	4.138146	2.092751	3.688995	1.369172
PREDICTED: cDNA sequence BC013672 (BC013672)	1.376502	0.588824	1.868959	0.935674	1.638007	0.527509
T-cell specific GTPase (Tgtp)	2.623986	1.726187	3.608659	1.878079	3.195475	1.3427
membrane-spanning 4-domains, subfamily A, member 11 (Ms4a11)	2.507902	1.302759	3.110182	1.333759	2.779969	1.324084
interferon regulatory factor 1 (Irf1)	1.046773	0.516067	1.739768	0.834188	1.778547	0.488471
tubulin, beta 6 (Tubb6)	1.448899	0.55372	1.724253	1.03173	1.25491	0.847935
formyl peptide receptor, related sequence 2 (Fpr-rs2)	1.780105	0.871896	2.549959	1.092751	1.849931	1.217169
2'-5' oligoadenylate synthetase 1G (Oas1g)	1.112086	0.519594	1.984436	0.988623	1.351126	0.790354
interferon-induced protein with tetratricopeptide repeats 3 (Ifit3)	2.571518	1.304361	3.854353	2.218281	2.994982	1.632206
lectin, galactose binding, soluble 9 (Lgals9)	1.342699	0.709839	2.183233	1.208228	1.836552	0.930864
interleukin 18 binding protein (Il18bp)	1.740978	1.200083	2.173249	0.821553	2.033935	0.876132
membrane-spanning 4-domains, subfamily A, member 4C (Ms4a4c)	1.358524	1.068293	1.616193	0.704402	1.753224	0.579739
Mus musculus brain cDNA, clone MNCb-1429, similar to Mus musculus peroxiredoxin V (PrxV)	1.312326	1.100002	1.709302	0.699887	1.721963	0.913777
SLAM family member 8 (Slamf8)	2.230225	1.442359	2.635558	1.183199	2.312651	0.669681
RIKEN cDNA 9830147J24 gene (9830147J24Rik)	2.138559	1.530636	2.626609	1.083215	2.301085	0.711934
interferon activated gene 204 (Ifi204)	2.442235	1.796991	2.994705	1.547883	2.573518	0.854599
guanylate nucleotide binding protein 4 (Gbp4)	1.866261	1.272434	1.96983	1.051359	1.836552	0.527509
interferon inducible GTPase 2 (Iigp2)	1.797894	1.218434	1.929351	0.854149	1.836552	0.558206
interferon activated gene 205 (Ifi205)	2.296896	1.574184	2.304249	1.176658	2.273123	0.876132
interferon inducible GTPase 1 (Iigp1)	3.74263	2.642529	3.828243	1.819185	4.001379	1.632206
GTPase, very large interferon inducible 1 (Gvin1)	1.974483	1.18377	2.146708	1.021815	2.024897	0.824851
mMA035547	2.130291	1.308244	2.284446	1.253269	2.029197	1.024524
RIKEN cDNA A630077B13 gene (A630077B13Rik)	2.308484	1.068293	2.645222	0.800635	2.690975	0.6766
hypothetical protein E430029F06 (E430029F06)	1.793911	0.889323	1.838585	0.476717	1.936088	0.579739
protein kinase, interferon-inducible double stranded RNA dependent (Prkr)	1.813019	0.816755	2.230903	0.977615	1.766163	0.632206
interferon inducible protein 1 (Ifi1)	2.75209	1.331328	3.085097	1.374981	2.640632	0.570806
macrophage activation 2 (Mpa2)	3.319979	1.567395	3.790222	1.405908	3.380873	0.880134
SAM domain and HD domain, 1 (Samhd1)	1.56905	0.782891	2.128092	0.768696	1.936088	0.573312
SAM domain and HD domain, 1 (Samhd1)	1.686323	0.810495	2.121116	0.828967	2.075491	0.600497
PHD finger protein 11 (Phf11)	1.664628	1.09835	2.260049	0.918721	2.11666	0.617707
interferon gamma induced GTPase (Igtp)	2.528125	1.383795	3.168734	1.456615	2.919968	0.76971
deltex 3-like (Drosophila) (Dtx3l)	0.781989	1.739768	0.850676	1.796925	0.403582	
SAM domain and HD domain, 1 (Samhd1)	1.649831	0.832095	1.789524	0.77917	1.878372	0.487258
leucine aminopeptidase 3 (Lap3)	1.765714	0.921452	1.87672		1.804843	0.979009
signal transducer and activator of transcription 1 (Stat1)	1.447529	0.90683	1.650958	1.159429	1.526975	0.819833
signal transducer and activator of transcription 1 (Stat1)	2.156481	1.290686	2.253623	1.567556	1.957783	0.88702
interferon regulatory factor 1 (Irf1)	2.059487	1.635334	2.186509	1.485762	2.135397	1.217169
chemokine (C-X-C motif) ligand 5 (Cxcl5)	2.33089	0.977691	1.754521	0.735121	1.638007	0.858715
chemokine (C-C motif) receptor 5 (Ccr5)	1.686995	0.55372	1.402068	0.429974	1.1812	0.217169

RIKEN cDNA C730029A08 gene (C730029A08Rik)	-1.264289	-0.673538	-0.626664	-0.134165	-1.699501	-0.553349
killer cell lectin-like receptor, subfamily A, member 18 (Klra18)	-1.288067	-0.912598	-1.024913	-0.529739	-1.604931	-0.452007
elastase 1, pancreatic (Ela1)	-1.415296	-1.706602	-1.090076	-0.22812	-1.469054	-1.018048
sprouty homolog 1 (Drosophila) (Spry1)	-1.723643	-0.481441	-1.428201	-0.903281	-0.705458	0.324084
glutathione S-transferase, alpha 3 (Gsta3)	-0.994336	0.124877	-1.383807	-0.251204	-1.798622	-0.37799
insulin-like growth factor binding protein 5 (Igfbp5)	-0.70621	0.175758	-1.409342	-0.691776	-1.79023	-0.488088
selenoprotein P, plasma, 1 (Sepp1)	-1.518236	-0.417134	-1.577579	-1.137547	-1.629766	-0.31121
expressed sequence AI481750 (AI481750)	-1.388812	-0.575563	-1.290698	-0.988169	-1.615708	-0.079813
thrombomodulin (Thbd)	-1.960977	-0.72312	-1.805271	-1.087705	-2.128868	-0.925789
Mus musculus Ly49H mRNA, /cds=p(197,997)	-1.24395	-0.7097	-1.314544	-0.77255	-1.833299	-0.782831
killer cell lectin-like receptor subfamily A, member 10 (Klra10)	-1.009602	-0.416364	-1.435088	-0.89936	-1.690695	-0.664187
RIKEN cDNA E130203B14 gene (E130203B14Rik)	-1.639153	-0.235488	-2.084247	-0.366681	-1.719264	0.122532
DNA segment, human D4S114 (D0H4S114)	-1.400961	-0.269754	-1.96877	-0.765777	-1.58378	0.148997
Mus musculus adult male colon cDNA, RIKEN full-length enriched library	-1.335372	-0.168746	-1.925701	-0.97367	-1.400947	-0.168122
transcription factor 21 (Tcf21)	-1.315194	-0.063532	-1.76395	-0.776295	-1.281143	-0.036588
Mus musculus 10 days neonate skin cDNA, RIKEN full-length enriched library	-1.313999	-0.2112	-1.691236	-0.595158	-0.932668	0.05367
guanylate cyclase 1, soluble, alpha 3 (Gucy1a3)	-1.646574	-0.190441	-1.656826	-0.585623	-1.108306	0.243164
BB357349 RIKEN full-length enriched, adult male corpus striatum Mus musculus cDNA	-0.84517	-2.851413	-0.741529	-2.665177	-0.45121	
ADAM-like, decysin 1 (Adamdec1)	-1.215533	-0.447904	-2.037482	-0.401344	-1.594427	-0.216484
Mus musculus mRNA for mKIAA0237 protein /cds=p(1,792)	-1.620775	-0.50929	-1.894769	-0.479232	-1.397336	-0.244411
mannose receptor, C type 1 (Mrc1)	-2.056218	-0.269937	-2.714197	-0.674703	-2.267784	-0.56524
expressed sequence AW046396 (AW046396)	-1.674174	-0.509975	-2.50049	-0.798691	-2.216559	-0.731606
transcription factor 21 (Tcf21)	-1.601266	-0.519529	-1.691236	-0.741009	-1.631597	-0.135503
RIKEN cDNA 2610001E17 gene (2610001E17Rik)	-1.514696	-0.162869	-1.659085	-0.728526	-1.509472	-0.2475
mMR030084	-1.598407	-0.48496	-1.669209	-0.492212	-1.926859	-0.295281
chemokine (C-X-C motif) ligand 12 (Cxcl12), transcript variant 1	-1.611704	-0.546086	-2.033725	-1.154696	-1.732291	-0.703976
endothelial cell-specific molecule 1 (Esm1)	-1.64853	-0.201796	-2.553732	-1.203898	-2.11836	-0.493325
sushi, nidogen and EGF-like domains 1 (Sned1)	-1.207048	-0.287582	-1.94605	-1.058559	-1.751236	-0.580338
EGF-like module containing, mucin-like, hormone receptor-like sequence 4 (Emr4)	-1.216728	-0.06099	-2.27911	-0.37251	-2.13826	-0.357946
transferrin (Trf)	-1.275251	-0.121723	-2.269939	-0.604841	-1.590772	-0.244735
protein tyrosine phosphatase 4a2 (Ptp4a2)	-1.176675	0.088285	-4.002193		-2.838699	-0.165301
Fc receptor, IgE, low affinity II, alpha polypeptide (Fcer2a)	-0.645057	0.041821	-1.705735	-0.39256	-0.84152	-0.027944
RIKEN cDNA 6430529G09 gene (6430529G09Rik)	-0.897251	-0.417754	-2.033725	-1.040525	-1.112822	-0.712442
Mus musculus 8 days embryo whole body cDNA, RIKEN full-length enriched library	-1.106748	-0.407258	-2.354828	-1.424269	-1.204393	-0.768034
chemokine (C-C motif) ligand 21b (Ccl21b)	-1.497124	-0.427664	-2.25034	-1.690315	-1.401782	-0.590186
phospholipase A2, group IID (Pla2g2d)	-0.815365		-1.656826	-1.372219	-0.970803	-0.619333
chemokine (C-C motif) ligand 21b (Ccl21b)	-0.826761	0.146452	-1.788949	-1.456673	-1.344868	-0.537719
chemokine (C-C motif) ligand 21b (Ccl21b)	-0.477817	-0.253635	-2.219731	-1.591433	-1.403762	-0.478825
RIKEN cDNA 8030402F09 gene (8030402F09Rik)	-1.072338	-0.025366	-1.921772	-1.319684	-1.209589	0.062446
PREDICTED: immunoglobulin kappa chain variable 38(V38) (Igk-V38)	-0.318694	-0.253635	-1.853292	-1.607348	-0.604481	-0.290978
PREDICTED: immunoglobulin kappa chain variable 38(V38) (Igk-V38)	-0.5844	-0.271337	-1.657683	-1.531312	-0.523344	-0.335372
PREDICTED: similar to anti-PRSV coat protein monoclonal antibody PRSV-L 3-8	-0.366069	0.022	-2.117996	-1.276441	-0.196362	-0.507197
Mus musculus adult male aorta and vein cDNA, RIKEN full-length enriched library	-0.794804	-0.298029	-1.290698	-1.743057	-0.063912	-0.460903
mMO036346	-0.713884	-0.731682	-1.168909	-1.653836	-0.435881	-0.541823
Immunoglobulin heavy chain (gamma polypeptide) (Ighg)	-0.72714	-0.363259	-1.449896	-1.971518	-1.366731	-2.289184
PREDICTED: immunoglobulin heavy chain 1a (serum IgG2a) (Igh-1a)	-0.097509	-0.098912	-2.173128	-2.394162	-1.599965	-2.392885

PREDICTED: immunoglobulin heavy chain 1a (serum IgG2a) (Igh-1a)	-0.236969	0.13139	-2.149835	-2.366681	-1.957627	-2.743661
PREDICTED: gene model 189, (NCBI) (Gm189)	-0.028191	0.418311	-1.673031	-1.421129	-1.36257	-1.095989
Mus musculus IgVk km4 gene,	-0.1548	0.298906	-1.768471	-1.615968	-1.474845	-1.068233
PREDICTED: gene model 189, (NCBI) (Gm189)	0.323674	-1.648369	-1.421129	-1.534704	-1.062939	
PREDICTED: gene model 189, (NCBI) (Gm189)	-0.231537	0.280189	-1.676589	-1.490874	-1.587474	-1.136468
PREDICTED: gene model 1524, (NCBI) (Gm1524)	0.043139	0.265739	-1.740145	-1.651742	-1.713005	-1.352197
PREDICTED: gene model 189, (NCBI) (Gm189)	-0.231537	0.020126	-1.786931	-1.509938	-1.804153	-1.397541
PREDICTED: gene model 189, (NCBI) (Gm189)	-0.072338	0.099037	-1.783467	-1.515704	-1.697238	-1.203163
PREDICTED: gene model 189, (NCBI) (Gm189)	-0.17711	0.113574	-1.718119	-1.483495	-1.710275	-1.238511
PREDICTED: gene model 189, (NCBI) (Gm189)	-0.219895	0.146296	-1.657683	-1.388707	-1.601046	-1.129282
PREDICTED: gene model 189, (NCBI) (Gm189)	0.2516	-1.633021	-1.371834	-1.615708	-1.164702	
PREDICTED: gene model 1502, (NCBI) (Gm1502)	-0.013444	0.086215	-1.924826	-1.70137	-1.421464	-1.186187
PREDICTED: gene model 189, (NCBI) (Gm189)	0.054487	-1.646841	-1.426775	-1.36257	-0.970458	
Mus musculus IgVk 23-39 gene,	-0.171874	0.072135	-0.34549	-1.881681	-0.233837	-0.937159
protein kinase C, eu (Prkcn)	0.046498	-2.490674	-0.225928	-0.406482	0.058344	0.126021

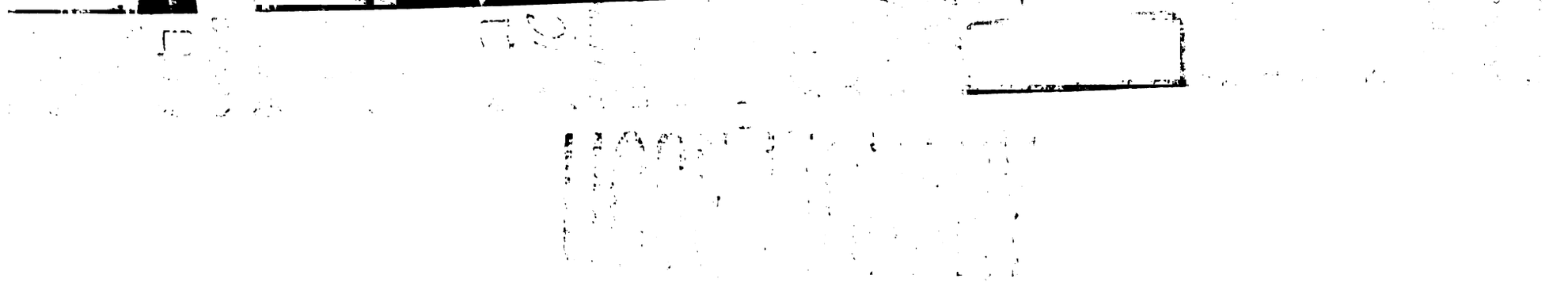

GENE NAME	WT	esxA	WT	esxA	WT	esxA
cytochrome P450, family 1, subfamily a, polypeptide 1 (Cyp1a1)	-1.401902	-0.588106	1.609225	-0.715804	-1.018194	-0.97990
thrombomodulin (Thbd)	-1.306622	-0.676537	-1.610786	-0.56042	-1.341158	-0.68808
RIKEN cDNA 1110018M03 gene (1110018M03Rik)	-1.620881	-0.98015	-2.030689	-1.019698	-0.914806	-0.59559
Mus musculus Mit1/Lb9 mRNA, partial sequence	-1.687712	-1.401677	-2.123798	-1.244052	-1.462936	
protocadherin 12 (Pcdh12)	-1.504472	-0.798073	-1.934764	-0.307245	-0.634184	0.012445
Mus musculus adult male hippocampus cDNA	-1.898136	-1.122475	-2.200614	-0.460519	-0.890959	0.180322
endothelin receptor type B (Ednrb)	-1.845852	-1.033665	-2.606191	-0.636369	-1.427012	-0.56565
sema domain, immunoglobulin domain (Ig), short basic domain, secreted, (semaphorin) 3C (Sema3c)	-1.387226	-0.761257	-1.687927	-0.603948	-0.949853	-0.11185
hairy/enhancer-of-split related with YRPW motif 1 (Hey1)	-1.908862	-0.963276	-2.320196	-0.866982	-1.209567	-0.07690
sodium channel, voltage-gated, type VII, alpha (Scn7a)	-1.61979	-0.949015	-1.659851	-0.365067	-1.012423	-0.14684
protocadherin alpha subfamily C, 1 (Pcdhac1)	-2.368988	-1.237451	-2.301337	-0.626909	-1.646784	-0.39646
protocadherin alpha subfamily C, 1 (Pcdhac1)	-1.738937	-1.095914	-2.151995	-0.590565	-1.159155	-0.23096
RIKEN cDNA E230020D15 gene (E230020D15Rik)	-2.091453	-1.408902		-0.617753	-1.297776	-0.36024
ephrin B2 (Efnb2)	-2.038498	-1.149495	-1.894711	-0.696312	-1.03673	0.042819
protocadherin alpha subfamily C, 1 (Pcdhac1)	-2.283258	-1.126775	-2.089583	-0.695263	-0.93278	-0.42736
endothelial cell-specific molecule 1 (Esm1)	-2.193113	-1.651917	-2.15027	-1.262911	-0.405533	
solute carrier family 6 (neurotransmitter transporter, noradrenalin), member 2 (Slc6a2)	-1.8264	-1.613333	-1.712241	-0.78259	-0.872344	-0.31332
flavin containing monooxygenase 1 (Fmo1)	-1.397149	-1.255165	-1.818536	-0.643529	-0.691119	-0.42736
angiotensin I converting enzyme (peptidyl-dipeptidase A) 1 (Ace)	-1.479694	-0.187089	-1.746593	-0.290872	-0.748587	-0.13298
hydroxyprostaglandin dehydrogenase 15 (NAD) (Hpgd)	-1.233702	-0.362883	-1.810138	-0.214905	-0.931148	-0.25567
insulin-like growth factor binding protein 5 (Igfbp5)	-0.385827	-1.678185	-0.129253	0.15141	-0.57992	-0.59593
DEAD (Asp-Glu-Ala-Asp) box polypeptide 6 (Ddx6)	-0.05381	-0.065846	-0.160324	-3.729478	-0.770464	-1.04794
regenerating islet-derived 3 gamma (Reg3g)	1.6147	1.581045	-0.133782	0.090613	-0.372439	0.207243
placenta-specific 8 (Plac8)	1.717441	1.921072	2.27674	2.459555	1.260107	0.937636
sphingomyelin phosphodiesterase, acid-like 3B (Smpdl3b)	1.701635	2.13626	2.0397	2.517436	0.817386	1.041409
cholesterol 25-hydroxylase (Ch25h)	1.415391	1.554203	1.84973	1.347143	1.116946	
chemokine (C-C motif) ligand 4 (Ccl4)	1.939135	1.844079	2.579809	2.270521	1.600344	1.366189
solute carrier family 2 (facilitated glucose transporter), member 6 (Slc2a6)	1.483455	2.081118	1.773951	1.986068	1.221067	1.318538
phospholipase A2, group VII (platelet-activating factor acetylhydrolase, plasma) (Pla2g7)	1.459002	1.778984	1.703137	1.867975	1.065972	1.29743
lymphocyte cytosolic protein 2 (Lcp2)	1.053258	1.61581	1.416076	1.674419	1.056573	1.165215
interleukin 1 beta (Il1b)	0.957057	1.089835	1.531553	1.806575	1.394443	
histocompatibility 2, complement component factor B (H2-Bf)	0.976086	1.169891	2.121089	1.836119	1.190429	1.087213
allograft inflammatory factor 1 (Aif1)	1.003265	0.96961	1.778646	1.476972	0.886648	0.703884
formyl peptide receptor, related sequence 2 (Fpr-rs2)	1.072029	0.952027	1.651135	1.568745	0.430969	0.546644
S100 calcium binding protein A9 (calgranulin B) (S100a9)	1.248784	0.902274	1.876202	1.793619	0.943232	0.572639
schlafen 4 (Slfn4)	4.517403	3.233121	3.745894	2.217082	2.443042	0.99975
2'-5' oligoadenylate synthetase 1G (Oasl1g)	1.666047	1.247621	1.379063	0.416372	0.940088	0.266183
PC Details: [Mismatch Controls; Anchored]Mus musculus beta-2 microglobulin (B2m), mRNA.	1.786154	1.210554	1.394493	0.925135	1.492369	0.786043
PC Details: [Mismatch Controls; Anchored]Mus musculus beta-2 microglobulin (B2m), mRNA.	1.783016	1.377031	1.387163	0.855484	1.429175	0.760048

schlafen 1 (Slfn1)	1.846025	1.340036	1.394493	1.060486	1.354797	0.970399
chemokine (C-C motif) receptor 5 (Ccr5)	1.8601	1.400472	1.855443	1.163606	1.356134	0.824178
Fc fragment of IgG, low affinity IIIa, receptor (Fcgr3a)	1.882551	1.465567	1.860082	1.441633	0.64564	0.356399
lymphocyte antigen 6 complex, locus I (Ly6i)	1.846025	1.943615	2.3007	1.829949	0.758641	0.515797
sorting nexin 10 (Snx10)	1.353321	0.675126	2.018382	0.896126	1.161271	0.220479
guanylate nucleotide binding protein 5 (Gbp5), transcript variant 2	2.846025	1.206649	3.151209	1.79659	1.912183	0.249484
2'-5' oligoadenylate synthetase 2 (Oas2)	1.819058	0.889167	2.203366	0.81109	1.379688	0.104915
pre-B-cell colony-enhancing factor 1 (Pbef1)	1.547367	0.83399	1.967756	0.763038	1.386219	0.136122
Mus musculus premature mRNA for mKIAA1554 protein	1.958793	0.808455	2.139236	0.916885	1.372075	0.395335
interferon-induced protein 44 (Ifi44)	2.730548	1.212801	3.098594	1.393378	1.859681	0.301952
tripartite motif protein 30 (Trim30)	1.749001	0.907991	1.932785	0.849058	1.2442	0.257138
interferon inducible GTPase 2 (Iigp2)	2.097564	1.053798	2.604359	1.257922	1.649609	0.480224
hect domain and RLD 5 (Herc5)	2.126133	0.977562	2.399103	1.092983	1.793539	0.606587
uridine phosphorylase 1 (Upp1)		1.08735	2.171658	0.81109	1.317988	0.315837
guanylate nucleotide binding protein 2 (Gbp2)	2.629038	1.506751	3.356467	0.948594	1.810412	0.368984
mMC024858	3.774132	1.861153	4.894124	1.714128	2.694003	0.765285
interferon, alpha-inducible protein (G1p2)	1.855611	1.000198	2.01793	0.57936	1.196504	0.456447
Mus musculus 3 days neonate thymus cDNA, RIKEN full-length enriched library, clone:A630095J17 produc	3.752916	1.297252	5.237268	1.948593	2.694003	1.049738
interferon-induced protein with tetratricopeptide repeats 3 (Ifit3)	2.091138	0.594719	2.499983	0.881479	1.26516	0.465724
cDNA sequence BC049975 (BC049975)	2.582991	0.844079	4.034054	1.703481	2.384148	0.938349
indoleamine-pyrrole 2,3 dioxygenase (Indo)	3.419492	0.873225	4.850731	2.211628	2.530504	0.859802
DNA segment, Chr 14, ERATO Doi 668, expressed (D14Ertd668e)	2.152356	0.863887	2.049969	0.552665	1.012179	0.065186
interferon regulatory factor 7 (Irf7)	1.737212	0.581045	1.630222	0.546495	0.799937	0.038303
interferon-induced protein with tetratricopeptide repeats 3 (Ifit3)	2.544856	1.157018	2.68113	0.948594	1.334107	0.101712
PHD finger protein 11 (Phf11)	2.326018	0.993368	2.528278	0.841678	1.408601	0.216848
pre-B-cell colony-enhancing factor 1 (Pbef1)	1.752916	0.631671	1.931794	0.695827	1.114059	-0.100414
chemokine (C-X-C motif) ligand 10 (Cxcl10)	3.760909	2.241295	5.030007	2.170986	1.836022	0.167831
serine (or cysteine) peptidase inhibitor, clade A, member 3C (Serpina3c)	2.15036	1.069146	2.745894	1.074124	0.986184	-0.038318
interferon-induced protein with tetratricopeptide repeats 3 (Ifit3)	2.318094	1.104896	2.641737	1.048129	1.032499	0.097408
interferon regulatory factor 1 (Irf1)	1.620144	0.81237	2.139236	0.674419	0.995583	0.019649
interferon activated gene 205 (Ifi205)	1.527343	0.849639	2.270481	0.913828	0.980976	-0.152614
pyrophosphatase (Pyp)	1.491843	0.698139	1.930649	0.862864	0.659238	-0.275357
histocompatibility 2, T region locus 22 (H2-T22)	1.521299	0.886584	1.865061	1.029514	0.666867	-0.266424
PREDICTED: serine (or cysteine) proteinase inhibitor, clade A, member 3G (Serpina3g)	2.552294	0.754581	3.668489	1.489162	1.214974	-0.49775
lymphocyte antigen 6 complex, locus F	1.486623	0.584212	1.795282	1.379933	0.46551	0.117333
PC Details: [Mismatch Controls; Distributed]|Mus musculus beta-2 microglobulin (B2m), mRNA.	1.184101	0.59966	1.703137	0.867975	0.837066	0.358886
T-cell specific GTPase (Tgtp)	2.879973	1.489897	3.90742	1.90279	1.858634	
interferon inducible protein 1 (Ifi1)	3.138807	1.560286	3.935095	2.2381	2.251221	1.087213
SAM domain and HD domain, 1 (Samhd1)	1.441635	1.056624	1.963665	1.036056	1.024152	0.327164
2'-5' oligoadenylate synthetase-like 2 (Oasl2)	1.846025	1.103395	2.356467	1.241375	1.184329	0.517201

SAM domain and HD domain, 1 (Samhd1)	1.822942	1.010729	2.037356	1.133018	1.25438	0.570422
tryptophanyl-tRNA synthetase (Wars)	2.335063	1.155119	2.78949	2.007487	1.336451	0.373517
RIKEN cDNA 5830443L24 gene (5830443L24Rik)	3.420934	1.850505	4.50847	2.887193	2.109041	0.536198
signal transducer and activator of transcription 1 (Stat1)	2.380802	1.243175	3.125297	1.802743	1.381413	
interferon gamma induced GTPase (Igtp)	3.113506	1.77369	4.021879	2.563303	1.943232	1.028319
macrophage activation 2 (Mpa2)	3.65338	2.195154	4.724199	3.408025	2.644675	1.029497
granzyme B (Gzmb)	2.729832	1.721222	2.773952	1.829949	1.262515	0.239216
histocompatibility 2, T region locus 23 (H2-T23)	1.440386	1.026077	1.761673	1.110057	0.886648	0.239216
proteosome (prosome, macropain) subunit, beta type 8 (large multifunctional peptidase 7) (Psmb8)	1.436505	0.892989	1.606362	1.109058	0.791789	0.305853
GTPase, very large interferon inducible 1 (Gvin1)	2.6021	1.975324	3.139236	2.416742	1.457397	0.523312
class II transactivator (C2ta)	1.906146	0.611418	2.489733	1.408025	1.208576	0.50225
PREDICTED: mixed lineage kinase domain-like (Mlkl)	1.82741	0.540855	2.376275	1.170986	0.977796	0.128435
CD274 antigen (Cd274)	2.780437	1.179682	3.851954	2.064071	1.747942	0.32328
interferon inducible GTPase 1 (Iigp1)	2.81126	1.105886	4.753946	2.855484	1.764392	0.555362
mMA033476	2.403357	1.229919	3.550169	2.371805	1.459834	0.210787
membrane-spanning 4-domains, subfamily A, member 11 (Ms4a11)	2.05857	1.920531	2.236098	1.801036	2.045847	1.661449
membrane-spanning 4-domains, subfamily A, member 11 (Ms4a11)	1.106088	0.925693	1.621105	1.090613	1.542694	1.158296
membrane-spanning 4-domains, subfamily A, member 4C (Ms4a4c)	1.988044	1.822599	2.443017	1.948593	2.641536	1.672175
membrane-spanning 4-domains, subfamily A, member 4B (Ms4a4b)	1.099782	1.05053	1.038307	0.826603	1.709771	1.261242
RIKEN cDNA 4933430F08 gene (4933430F08Rik)	2.322839	1.166007	2.439631	0.551258	1.850122	0.824178
interferon-induced protein with tetratricopeptide repeats 2 (Ifit2)	2.492389	0.922553	2.487159	0.618445	2.208576	0.654253
SLAM family member 8 (Slamf8)	1.918175	1.658212	3.34087	2.270522	2.121114	1.523312
Mus musculus proteosome (prosome, macropain) subunit, beta type 8 (large multifunctional protease 7)	1.299882	0.685817	1.962358	1.356678	1.311146	1.074502
RIKEN cDNA 9830147J24 gene (9830147J24Rik)	2.036848	1.543077	3.17486	1.769623	2.221067	
guanylate nucleotide binding protein 4 (Gbp4)	2.596666	1.581045	3.679804	2.012724	2.393608	1.136966
macrophage activation 2 like (Mpa2l)	2.900473	1.358652	4.032321	2.185633	2.554073	
SAM domain and HD domain, 1 (Samhd1)	1.092665	0.704828	2.013705	1.118519	1.099642	0.581977
RIKEN cDNA A630077B13 gene (A630077B13Rik)	3.038671	2.223723	4.059801	2.426641	2.455491	1.617727
schlafen 2 (Slfn2)	1.308369	1.152201	1.925111	0.973256	1.18363	
GTPase, very large interferon inducible 1 (Gvin1)	2.052476	1.658212	2.635662	1.974128	1.788468	1.00921
interleukin 18 binding protein (Il18bp)	3.28491	1.911193	3.683557	2.170986	2.825248	1.531998
signal transducer and activator of transcription 1 (Stat1)	2.50899	1.555049	2.861702	1.685559	1.986184	
interferon activated gene 204 (Ifi204)	3.10906	2.284652	3.750671	2.204933	3.041926	1.743258
interferon inducible GTPase 1 (Iigp1)	3.624811	2.315584	4.10271	2.086097	3.428021	1.923714
interferon inducible GTPase 1 (Iigp1)	3.777638	2.188727	4.348689	2.533556	3.744629	2.087213
hypothetical protein E430029F06 (E430029F06)	2.656364	1.389679	3.062068	1.887193	2.836608	1.850174
radical S-adenosyl methionine domain containing 2 (Rsad2)	1.372571	0.780116	2.620363	0.755948	2.097545	0.813452
asparagine synthetase (Asns)	0.904919	0.591313	1.814801	0.560028	1.275691	0.552876
caspase 11, apoptosis-related cysteine peptidase (Casp11)	1.379244	0.808455	2.376275	1.015708	1.93976	0.852747
interferon activated gene 205 (Ifi205)	1.606198	0.904086	2.752213	1.183059	2.301686	1.087213
protein kinase, interferon-inducible double stranded RNA dependent (Prkr)	1.304564	0.49883	1.724199	0.674419	1.360579	0.419788

leucine aminopeptidase 3 (Lap3)	1.318778	0.626585	1.759388	0.653138	1.26516	0.45334
poly (ADP-ribose) polymerase family, member 9 (Parp9)	1.451746	0.717733	2.212485	0.855484	1.61363	0.710358
poly (ADP-ribose) polymerase family, member 11 (Parp11)	1.011085	0.221149	1.802201	0.769623	1.278966	0.769037
proteosome (prosome, macropain) subunit, beta type 9 (large multifunctional peptidase 2) (Psmb9)	0.493582	1.791313	0.896126	1.64564	0.944768	
interferon regulatory factor 1 (Irf1)	1.720495	0.627141	2.013705	0.91822	1.54486	1.102163
PHD finger protein 11 (Phf11) 2.18998	1.646897	2.176073	0.923502	0.554073	-0.125781	
interferon regulatory factor 1 (Irf1)	1.616544	0.971629	1.614574	0.857828	0.167668	-0.255549
xanthine dehydrogenase (Xdh) 1.386594	-0.041886	2.180264	0.920579	1.138187	0.484972	
deltex 3-like (Drosophila) (Dtx3l)	0.757296	-0.041278	2.124736	0.79659	0.984259	0.443356
PREDICTED: EST AA175286 (AA175286)	1.144249	0.358652	1.653809	0.633092	1.129505	0.087213
interferon activated gene 203 (Ifi203)	1.145586	0.540855	1.925111	0.614174	1.321585	0.206794
chloride channel calcium activated 1 (Clca1)	2.360598	0.251737	3.461164	0.823063	2.825248	0.44085
interferon activated gene 203 (Ifi203)	1.223261	0.144527	1.930649	0.674419	1.532365	0.329414
ubiquitin specific peptidase 18 (Usp18)	1.918175	0.330638	1.931794	0.426641	1.002126	-0.128516
suppressor of cytokine signaling 1 (Socs1)	1.877734	0.481509	2.650198	0.484646	1.499625	0.058643
6-phosphofructo-2-kinase/fructose-2,6-biphosphatase 3 (Pfkfb3), transcript variant 1	1.514819	0.395178	1.954204	0.147902	1.079293	0.016823
6-phosphofructo-2-kinase/fructose-2,6-biphosphatase 3 (Pfkfb3), transcript variant 1	1.503138	-0.534433	1.946591	0.129166	1.277108	-0.063347
PREDICTED: poly (ADP-ribose) polymerase family, member 14 (Parp14)	0.86772	0.203001	1.6049	0.228701	1.484211	0.839285
vascular cell adhesion molecule 1 (Vcam1)	0.62606	0.221149	2.04256	0.619971	1.643377	0.710358
interferon induced transmembrane protein 6 (Ifitm6)	0.799929	1.438087	0.758146	1.680397	1.218492	1.399157
tissue inhibitor of metalloproteinase 1 (Timp1)	0.613365	1.891526	1.023759	1.771716	0.538725	1.243332
Mus musculus 3 days neonate thymus cDNA, RIKEN full-length enriched library, clone:A630029C13 produc	0.667055	1.621687	0.676893	1.502192	0.434136	1.244754
EGF-like module containing, mucin-like, hormone receptor-like sequence 4 (Emr4)	0.755828	2.68058	1.27674	2.861882	0.834181	2.36732
Mus musculus adult male thymus cDNA, RIKEN full-length enriched library, clone:5830403K23 product:si	0.533142	1.260088	0.419344	1.785095	0.594467	1.239216
serum amyloid A 3 (Saa3)	0.306866	2.51298	2.17486	3.43402	1.285198	1.9008
paired immunoglobin-like type 2 receptor beta (Pilrb)	0.496691	1.159344	1.246151	1.818009	0.542	1.087213
myosin IG (Myo1g)	0.494262	1.253683	0.708602	1.708643	0.229536	0.872619
S100 calcium binding protein A4 (S100a4)	0.607239	1.134221	0.409325	1.602598	-0.083604	0.645208
Mus musculus 13 days embryo head cDNA, RIKEN full-length enriched library, clone:3110037K17 product:	1.135532	1.668508	0.367505	1.419223	0.083685	0.912883
SAM domain, SH3 domain and nuclear localisation signals, 1 (Samsn1)	0.74649	1.832583	0.653809	1.419223		0.699287
resistin like alpha (Retnla)	1.417932	1.114983	0.902197	1.604639	-0.270077	0.414787
leukocyte specific transcript 1 (Lst1)	1.286154	1.396127	0.987233	1.626665	0.269118	
myosin, heavy polypeptide 2, skeletal muscle, adult (Myh2)	-1.546292	-0.095066	4.348689	2.91822	1.301686	1.515547
myosin, heavy polypeptide 8, skeletal muscle, perinatal (Myh8)	-0.407964	-0.494799	2.27674	2.196521	-0.705474	-0.047437
troponin I, skeletal, fast 2 (Tnni2)	-0.528518	-0.331392	3.139236	2.678986	-0.346551	0.378676
creatine kinase, muscle (Ckm)	-0.202505	-0.182918	1.762166	1.571524	-0.339233	-0.021312
troponin T3, skeletal, fast (Tnnt3)	-0.764174	-0.334509	2.739149	2.408025	-0.466023	0.034101
tropomyosin 2, beta (Tpm2)	-0.660463	-0.299839	2.54952	2.192519	-0.627925	

7542346
3 1378 00754 2346

For reference

Not to be taken from the room.